Developing an Injectable Glycosaminoglycan-Based Hydrogel Drug Delivery System for Neuroblastoma

A Major Qualifying Quarterly Project Report submitted to the faculty of

WORCESTER POLYTECHNIC INSTITUTE

in partial fulfillment of the Degree of Bachelor Science.

Submitted By:

Christina Avakian

Christina Avakian

Emelia Carleton

Emelia Carleton

Akhil Chilamkurthi

Akhil Chilamkurthi

Andrew Voronin

Andrew Voronin

April 27th, 2023

Professor Jeannine M. Coburn, Ph.D., Advisor

Department *of B*iomedical Engineering

Table of Contents

Table of Contents i

Table of Figures v

Table of Tables vii

Abstract viii

Authorship x

Glossary xi

I. Introduction 1

II. Literature Review 2

2.1.1 Genetics 2

2.1.2 Patient Characteristics 3

2.1.3 Treatment Methods 3

2.2 Drug delivery 5

2.2.1 Routes of Administration 5

2.2.2 Localized Drug release 6

2.3 Hydrogel systems 8

2.3.1 Hydrogels 8

2.3.2 Bioconjugation 12

2.3.2.1 Physical crosslinking 12

2.3.2.2 Covalent crosslinking 13

2.3.3 PEG 14

2.3.3.1 PEG Based Hydrogels 15

2.3.3.2 Effectiveness in DDS 16

2.4 Injectability 16

2.4.1 Injection force 16

2.4.2 Viscosity 17

2.5 Chondroitin Sulfate 18

2.5.1 Properties of Chondroitin Sulfate 18

2.5.2 Chondroitin Sulfate Uses 22

2.6 Chemotherapeutic agent: Anthracyclines 23

2.7 Chemistry 24

2.7.1 Click Chemistry 24

2.7.1.1 Diels-Alder Reaction 25
2.7.1.2 1,3 - Dipolar cycloadditions and hetero - Aiels – Alder cycloaddition 25
2.8 Activating agents 27
2.8.1 Carbodiimide 27
2.8.2 N- Hydroxysuccinimide 28
2.8.3 Tetrazine 29
2.8.4 (4-(4,6-dimethoxy-1,3,5-triazin-2-yl)-4-methyl-morpholinium chloride) (DMTMM) 30
2.8.5 Furfurylamine 31
III. Project Strategy 33
3.1 Initial Client Statement 33
3.2 Design Requirements 33
3.2.1 Design Objectives 33
3.2.2 Design Constraints 35
3.3 Design Specifications 38
3.3.1 Specification 1: Reproducibility 39
3.3.2 Specification 2: Injectability 40
3.3.3 Specification 3: Sustained Release 40
3.3.4 Specification 4: Content Uniformity 40
3.3.5 Specification 5: Water-Insoluble 40
3.4 Design Standard Requirements 41
3.5 Revised Client Statement 42
3.6 Project Approach 43
3.6.1 Project Work Completed in A-term (Aug-Oct 2022) 43
3.6.2 Project Work to be Completed in B-term (Oct-Dec 2022) 43
3.6.3 Project Work to be Completed in C-term (Jan-Mar 2022) 43
3.6.4 Project Work to be Completed in D-term 43
IV. Design Process 44
4.1 Needs Analysis 44
4.2 Concept Map 45
4.3 Alternative Design Approaches 46
4.3.1 PEG-MI/ CS-F Hydrogel 46
4.3.2 PEG-NB/ CS-T Hydrogel 46
4.3.3 PEG−(NH2)6/ CS-NHS Hydrogel 47

4.4 Design Approach Selection 47
V. Design Verification 50
5.1 Experimentation Summary 50
5.1.1 PEG-MI/CS-F Hydrogel Fabrication 51
5.1.2 Injection Force Testing 54
5.1.3 Swelling Assay 54
5.1.3.1 Hydrogel Visual Analysis 55
5.1.4 Drug Loading Assay 55
5.1.5 Drug Release Assay 57
5.2 Design Results 58
5.2.1 Formulation Ratios 58
5.2.2 NMR Spectra Analysis 60
5.2.3 Injection Force Testing 65
5.2.4 Swelling Assay 69
5.2.5 Drug Loading Assay 70
5.2.6 Drug Release Assay 73
VI. Final Design and Validation 75
6.1 Overview of the Final Design 75
6.2 Final Design Impact 77
6.2.1 Economic Viability 77
6.2.3 Societal Implications 77
6.2.4 Environmental Impact 78
6.2.5 Issues with Health and Safety 78
6.2.6. Ethics 78
VII. Discussion 80
7.1 CS-F Hydrogels 80
7.1.1 Injection Force Testing 80
7.1.2 Swelling Study 81
7.1.3 Drug Loading Assay 81
7.1.4 Drug Release Assay 82
VIII. Conclusions and Recommendations 83
8.1 Conclusion 83
8.2 Future Studies 83

8.2.1 DMMB Assay 83
8.2.2 Degradation Assay 84
8.2.3 Hyaluronidase 85
8.2.4 Biocompatibility Assay 85
8.2.5 Drug Activity Assay 85
8.2.6 Alternative PEGs 85
8.2.7 PEG:CS Ratio 86
8.2.8 Chemotherapeutic Agents 86
VI. References 87
VII. Appendix 96
Appendix A: Gannt Charts A – D term 96
Appendix B: Protocol for PEG-MI/ CS-F Synthesis 97
Appendix C: Protocol for PEG-MI/ CS-F Hydrogels 99
Appendix D: Protocol for Instron Testing 101
Appendix E: Protocol for DNR Loading and Release Studies 104

Table of Figures

Figure 1: Hydrogel Characteristics. 10
Figure 2: Basic visual of various polymer morphology structures. 11
Figure 3: Crosslinking mechanism of action for different bond patterns. 12
Figure 4: Chemical structure of poly(ethylene glycol). 14
Figure 5: Chemical structure of CS. 19
Figure 6: Photo-cross linkable methacrylated CS synthesis. 21
Figure 7: Chemical structure of DOX (left) and DNR (right). 24
Figure 8: Diels Alder mechanism. 25
Figure 9: 1,3 - dipolar cycloadditions and hetero-Diels-Alder cycloaddition. 25
Figure 10: This is the proposed HDAC mechanism. Ligands are labeled with an R3. These can be many compounds but may vary due to the catalyst being used. 26
Figure 11: Chemical structure of carbodiimide. 27
Figure 12: Resonance structures (triple bond on left and triple bond on the right). 27
Figure 13: Chemical structure of EDC. 28
Figure 14: Mechanism of EDC and Carboxylic acid and amine to create an amide bond. 28
Figure 15: Chemical structure of NHS. 29
Figure 16: Carboxylic acid reaction with NHS to create active intermediate. 29
Figure 17: Chemical structure of Tetrazine. 29
Figure 18: Reaction and final structure of CS and tetrazine. 30
Figure 19: Chemical Structure of DMTMM. 30
Figure 20: Reaction between DMTMM and carboxylic acid. 31
Figure 21: Chemical structure of Furan. 31
Figure 22: Resonance structure of Furan. 31
Figure 23: Furan reaction with Maleimide. 32
Figure 24: Conceptual map for the injectable CS-based hydrogel DDS. 46
Figure 25: Process of hydrogel fabrication from start to finish. 52
Figure 26: Modifications made to hydrogel gelation technique showing (A) gelation in a 1.5 mL centrifuge tube, (B) gelation in a 2 mL centrifuge tube, and (C) gelation in a modified humidification chamber designed by the team. 53
Figure 27: Apparatus of the injection force testing of the tetra PEG hydrogel loaded with DNR being pushed out of the syringe onto a Petri dish. 54
Figure 28: 20 µL hydrogels loaded with DNR in PBS at different stages of visual analysis with (A) being a 1 on the scale, (B) being a 2 on the scale, (C) being a 3 on the scale, and (D) being a 4 on the scale. 55
Figure 29: Schematic of pre-loading gels. 56
Figure 30: Schematic of post-loading hydrogels. 56
Figure 31: DNR concentration standard curve. 57
Figure 32: DNR drug loading of 20 µL hydrogels without PBS on day 8 for (A) tetra PEG-MI/CS-F and (B) linear PEG-MI/CS-F. 58
Figure 33: Chemical formulation process from chondroitin sulfate modification through PEG-MI/CS-F polymer network. 59

Figure 34: NMR spectra for unmodified CS. 61
Figure 35: NMR spectra for CS-F (1:2:4 molar ratio). 61
Figure 36: NMR spectra for CS-F (1:0.5:4 molar ratio). 62
Figure 37: NMR spectra for CS-F (1:0.5:2 molar ratio). 62
Figure 38: NMR spectra for CS-F (1:1:1 molar ratio). 63
Figure 39: NMR spectra for CS-F (1:0.5:4 molar ratio) run 2. 63
Figure 40: NMR spectra for CS-F (1:2:4 molar ratio) run 2. 64
Figure 41: (A) Injection force testing data of 50 µL linear and tetra PEG-MI/CS-F hydrogels (n=3) . (B) Injection force testing data 50 µL linear and tetra PEG-MI/CS-F hydrogels post-loaded with daunorubicin (n=3). 65
Figure 42: (A) Injection force testing data of 50 µL linear and tetra PEG-MI/CS-F hydrogels post-loaded with daunorubicin injected onto Petri dish (n=3). (B) Injection force testing data 50 µL linear and tetra PEG-MI/CS-F hydrogels post-loaded with daunorubicin. 67
Figure 43: Swelling study of 20 µL linear and tetra PEG-MI/CS-F hydrogels in PBS (n=6). 69
Figure 44: Swelling study of 100 µL linear and tetra PEG-MI/CS-F hydrogels in PBS (n=6). 70
Figure 45: Mass of DNR loaded depending on PEG- Study 1. Data is presented as mean ± standard deviation of 9 independent samples. 71
Figure 46: Percent of loaded depending on PEG- Study 1. Data is presented as mean ± standard deviation of 9 independent samples. 71
Figure 47: Mass of DNR loaded depending on PEG- Study 2. Data is presented as mean ± standard deviation of 4 independent samples. 72
Figure 48: Percent of DNR loaded depending on PEG- Study 2. Data is presented as mean ± standard deviation of 4 independent samples. 72
Figure 49: DNR release profile for 20 µL hydrogels fabricated from linear PEG-MI/CS-F and tetra PEG-MI/CS-F, labeled as trial 1. Cumulative mass release in µg from the hydrogels over a period of 23 days, or until the hydrogel fully release the loaded drug. Data is presented as mean ± standard deviation of 3 independent experiments. 73
Figure 50: DNR release profile for 50 µL hydrogels fabricated from linear PEG-MI/CS-F and tetra PEG-MI/CS-F, labeled as trial 2. Cumulative mass release in µg from the hydrogels over a period of 23 days, or until the hydrogel fully released the loaded drug. Data is presented as mean ± standard deviation of 3 independent experiments. 74

Table of Tables

Table 1: Design Objectives and Definitions 33
Table 2: Pairwise comparisons chart for Design Objectives 35
Table 3: Definitions of design constraints 36
Table 4: Design Constraint weights 37
Table 5: Design Attribute/Function and Associated Specifications 38
Table 6: Design Specifications Weights. 39
Table 7: Standards for design requirements 41
Table 8: Objectives and sub-objectives ranked 44
Table 9: Design selection matrix for the design sub-objectives 48
Table 10: Design selection matrix for the design constraints 49
Table 11: Total Score of design approaches 49
Table 12: Summarized formulation ratios with corresponding weight measurements per reagent. 59
Table 13: Summary of formulation ratios with corresponding % modification of furan to CS 64
Table 14: Average injection force data calculated from linear region between 5-7 mm for three 50 µL linear and tetra PEG-MI/CS-F hydrogels with and without daunorubicin 67
Table 15: Average injection force data calculated from linear region between 3-4 mm for 50 µL linear and tetra PEG-MI/CS-F hydrogels with daunorubicin injected onto a Petri dish and raw chicken breast. 68

Abstract

Neuroblastoma is an embryonic cancer derived from the sympathetic nervous system that typically targets children under the age of 5, it is the most common and deadly solid tumor in children. High dose chemotherapy is the primary treatment for neuroblastoma patients; however, it is administered systemically and kills off-target cells, leading to a multitude of undesirable effects. In comparison to chemotherapy, intra-tumoral drug administration is a more suitable option to deliver therapeutics since it can be administered at high concentrations locally, while limiting off-target cytotoxicity. Hydrogel-based drug delivery systems are expected to be an efficient model to produce a locally administered controlled drug release system with a sustained release. The goal of this project is to identify, design, fabricate, and validate a chondroitin sulfate-based hydrogel drug delivery system with an acceptable injection force and drug release profile for localized intra-tumoral delivery of chemotherapeutic agents. Three design approaches were taken into consideration before the final hydrogel formulation was chosen based on the various design constraints determined during the initial stages of this project. Efficacy of the final hydrogel formulation was then evaluated via swelling, degradation, drug loading, drug release, injection force, and dimethyl-methylene blue assays. It was concluded that CS – Linear PEG-MI and CS – Tetra PEG-MI hydrogels were able to produce a hydrogel drug delivery system that not only showed compatibility with daunorubicin loading but also maintained a low injection force and insolubility throughout. In addition, both CS – Linear PEG-MI and CS – Tetra PEG-MI hydrogels showed reproducible drug loading and drug release profiles over a 28-day timeline, respectively. Injection force testing using a 2 kN Instron showed that CS – Linear PEG-MI produced softer gels with an injection force of 7.95 ± 1.67N, in comparison to the CS – Tetra PEG-MI hydrogels which were more rigid and produced an injection force of 18.63 ± 3.88 N. Upon further testing, it was determined that loading the hydrogels with daunorubicin, CS – Tetra PEG-MI experienced greater loading, on average, compared to CS – Linear PEG-MI. Variability in drug release readings for both samples created a challenge when comparing the drug release profiles, although further analysis is needed, CS – Linear PEG-MI hydrogels produced a quicker rate of release during the early timepoints. Despite meeting objectives, further conclusions and recommendations were made to help establish what can be done to improve and optimize the drug delivery system design.

Acknowledgements

The team would like to thank the entirety of Coburn Lab at the Gateway Biomedical Engineering Department of Worcester Polytechnic Institute (WPI) for supervision during lab experiments. We would also like to thank our advisor Dr. Jeannine M. Coburn for her guidance, support, and thorough feedback on all aspects of the project. Without her this project would not have been possible. Additionally, the team would like to thank Melissa Wojnowski for her guidance and her expertise in the relevant materials and testing procedures. Lastly, the team would like to thank Lisa wall for her help to order and gather any additional project materials we needed.

Authorship

All team members contributed equally to this project.

Glossary

A

Ad-HA

Adamantane-modified Hyaluronic Acid

ALK

Anaplastic Lymphoma Kinase

ALT

Alternating Lengthening of Telomeres

ASCT

Autologous Stem Cell Transplant

ASTM

Amerizan Society for Testing and Materials

ATRA

All-trans Retinoic Acid

C

CD-HA

Cyclodextrin-modified Hyaluronic Acid

CS

Chondroitin Sulfate

CS-A

Condroitin-4-sulfate

CS-B

Chondroitin-6-sulfate

CS-F

Chondroitin Sulfate-Furan

CS-MA

Methacrylated Chondroitin Sulfate

CS-NHS

Chondrotin Sulfate Succinimidyl Succinate

CS-T

Chondroitin Sulfate-Tetrazine

D

DDS

Drug Delivery System(s)

DHBC

Double Hydrophilic Block Copolymers

DMMB

Dimethylmethylene Blue

DMTMM

(4-(4,6-dimethoxy-1,3,5-triazin-2-yl)-4-methyl-morpholinium chloride)

DNA

Deoxyribonucleic Acid

DNR

Daunorubicin

DOX

Doxorubicin

E

ECM

Extra Cellular Matrix

EDC

1-ethyl-3-(3-dimethylaminopropyl) carbodiimide hydrochloride

F

FDA

Food and Drug Administration

FRP

Free-radical Polymerization

G

GAGs

Glycosaminoglycans

GalNAc

N-acetyl-galactosamine

GlcA

D-glucuronic Acid

GI

Gastrointestinal

GMA

Glycidyl Methacrylate

H

HA

Hyaluronic Acid

HDAC

Hetero-Diels-Alder Cycloaddition

HDC

High-dose Chemotherapy

HPNs

Hybrid Polymer Networks

I

IDR

Idarubicin

INRG

International Neuroblastoma Risk Group

IPNs

Interpenetrating Networks

ISO

International Organization for Standardization

M

MES

2-Morpholinoethanesulfonic Acid Monohydrate

MTX

Methotrexate

N

NB

Neuroblastoma

NHS

N- Hydroxysuccinimide

NMR

Nuclear Magnetic Resonance Spectroscopy

O

OA

Osteoarthritis

P

PEI-PLA

Polyethyleneimine-block-polylactic acid

PBS

Phosphate Buffer Solution

PEG

Poly (ethylene glycol)

PEG-PAsp

poly(ethylene glycol)-block-poly(l-aspartic acid sodium salt)

PEG-GAG

Poly (ethylene glycol)-Glycosaminoglycan

PEG-NB

Poly (ethylene glycol)-Norbornene

PEG-MI

Poly (ethylene glycol)-Maleimide

PEG-PAsp

Poly(ethylene glycol)-Block-Poly(L-aspartic acid sodium salt)

PEG-PNIPAM

Poly(ethylene glycol)-poly(N-isopropylacrylamide)

PEI

Polyethyleneimine

PEO

Polyethylene Oxide

PLA

Polylactic Acid

PWC

Pairwise Comparison Chart

R

RNA

Ribonucleic Acid

S

SNS

Sympathetic Nervous System

SOPs

Standard Operating Procedures

T

TMM

Telomere-maintenance Mechanisms

U

UV

Ultraviolet

V

VLR

Valrubicin

W

WPI

Worcester Polytechnic Institute

I. Introduction

Neuroblastoma (NB) is a type of embryonic cancer that is derived from neural crest cells within the sympathetic nervous system (SNS), most commonly in and around the adrenal gland (Brodeur, 2003). Tumors typically grow in places along the SNS due to the neural crest cells relocating there during their development (Heck et al., 2009). NB is the most common and deadly solid extracranial tumor in children; patients less than 18 months are deemed low-risk and can experience spontaneous tumor regression, whereas those above that age are deemed high-risk (Newman et al., 2019). High-dose chemotherapy (HDC), followed by an autologous stem cell transplant (ASCT), is the primary treatment for high-risk NB patients (Smith et al., 2018). Chemotherapy is administered systemically and although it is effective in killing cancer cells, the treatment may also kill off healthy cells in the process, leading to a multitude of undesirable side effects. To reduce systemic exposure, and thus reduce the negative effects, an intratumoral drug delivery system (DDS) can be used to deliver therapeutics locally.

Hydrogels are a three-dimensional, water-insoluble, crosslinked polymer network that is typically hydrophilic, amorphous, and biocompatible (E. Ahmed, 2015; Chauhan et al., 2022). Click chemistry is a commonly used method for crosslinking polymer chains to attain high yield products; the click bonds are not reversible by water and oxygen as the covalent bonds are not susceptible to hydrolysis and oxidation. This chemistry aids in the synthesis of hydrogels, making hydrogels an efficient model for DDS due to their ability to elicit a controlled drug release, encapsulate drugs within their network, and protecting the potency. For cancer treatment, these devices may pose a very effective means of producing a locally administered controlled drug release while limiting off target cytotoxicity. Hydrogels also can be injected by needle, which would allow the delivery to be intratumoral, eliciting a localized drug administration. The controlled drug release is dependent on the density of the crosslinking within the hydrogel, allowing it to be manipulated depending on the need. Since it is being injected intratumorally rather than the conventional systemic delivery, the drug load can be higher while remaining safe.

The project goal is to design an injectable chondroitin sulfate (CS) based hydrogel network loaded with daunorubicin (DNR) to treat NB that has a sustained release profile of 21-28 days and an injection force that can be used in clinical applications. The maximum injection force is 38 N through a 28-gauge needle with a needle length of 0.5 in.

II. Literature Review

2.1 Neuroblastoma

2.1.1 Genetics

NB is an embryonic cancer stemming from primitive cells within the SNS and is the most common and deadly extracranial solid tumor in children. NB is derived from neural crest cells; these cells develop during the third to fourth week of embryonic development, a time in which some of the cells relocate to create the SNS (Heck et al., 2009). NB tumors most commonly arise in the adrenal medulla but can also arise in a paraspinal location such as the neck, chest, pelvis, or abdomen (Brodeur, 2003; Newman et al., 2019).

NB is a heterogenous disease that typically follows an autosomal-dominant inheritance pattern, where up to 22% of tumors may be due to germinal mutation (Brodeur, 2003). These tumors have various immune evasion strategies, such as molecular expression at immune checkpoints, immunoregulatory mediator emissions, and immunosuppressive stromal and myeloid cell initiation (Wienke et al., 2021).

NB survival rate is highly dependent on patient age and the biological characteristic of the tumor (Heck et al., 2009). Clinical phenotypes of NB are induced by MYCN amplification, molecular alterations that affect telomere maintenance, and mutation of anaplastic lymphoma kinase (ALK) (Ackermann et al., 2018). Amplification of the MYCN oncogene is associated with a poor outcome for patients and is seen in 5-10% of infants younger than 1 year old, and 20-30% in children (Heck et al., 2009). MYCN amplification is a genetic aberration, causing uncontrolled cell growth and proliferation, which could be why it is associated with more aggressive tumor progression and poor outcomes (Brodeur, 2003). Amplification of MYCN can lead to promotion of telomere-maintenance mechanisms (TMM) (Akter et al., 2021). Telomere maintenance affects both cell proliferation and genomic stability and is crucial for cancer cells to attain everlasting proliferation capacity; patients that harbor TMM typically are at a higher risk (Ackermann et al., 2018). Alternating lengthening of telomeres (ALT) can lead to NB prognosis, where the longer the length of the telomere, the worse the outcome (Akter et al., 2021). Patients with TMM and a mutation in the RAS and/or p53 pathway are expected to have a poor prognosis due to an increase in tumor aggression, and these mutations are detected in relapsed NB

(Ackermann et al., 2018). Amplification of the ALK oncogene is also associated with MYCN amplification, and is a common somatic mutation, as well as the primary causes of hereditary NB (Allinson, 2022). This ALK mutation is overexpressed in NB and present in roughly 8-14% of diagnosis, and 26-43% of relapses (Allinson, 2022). It was found that somatic mutations account for > 98% of diagnoses, particularly amplification of the MYCN and ALK oncogene (Spencer et al., 2022).

2.1.2 Patient Characteristics

The age that a patient is diagnosed with NB is important in identifying the clinical course for the patient, since typically those under the age of 18 months are deemed low-risk patients, and those older than 18-months are deemed high-risk patients (Newman et al., 2019). For patients <18 months, it is common for tumors to spontaneously regress, or to regress with minimal therapy, whereas older patients with metastatic disease commonly experience relentless growth, despite undergoing intensive multimodality therapy (Brodeur, 2003). Patients that have a genetic predisposition typically have multifocal primary tumors at an early age (Brodeur, 2003). Roughly 700 children are diagnosed in the United States per year, with NB representing 8% of all pediatric cancer and roughly 15% of childhood cancer deaths (Newman et al., 2019). A mass screening between the age of 6-12 months led to an increased detection in NB, however, it did not decrease mortality (Brodeur, 2003).

2.1.3 Treatment Methods

A system of classification is used by the International Neuroblastoma Risk group (INRG) to stratify patients into pre-treatment risk stages which include stage 1 (low risk), stage 2 (intermediate risk), or stage 3 and 4 (high risk) (Smith et al., 2018). Patients with high-risk neuroblastoma are the hardest to treat since they require multi-modal therapy. Current popular treatment methods include chemotherapy, radiation therapy, immunotherapy, and aggressive surgery (Newman et al., 2019).

Treatment is divided into three different phases: induction, consolidation, and maintenance (Smith et al., 2018).

During the induction phase, patients typically receive between 5-8 cycles of intensive chemotherapy which can include topoisomerase agents, platinum containing agents, or alkylating agents (Smith et al., 2018). In North America, vincristine, cyclophosphamide, cisplatin,

etoposide, and doxorubicin (DOX) regiments are also commonly used. These cycles are typically followed by stem cell collection, commonly harvested from bone marrow, in preparation for an ASCT. Towards the end of induction chemotherapy, after the tumor has shrunk, the patient will undergo surgery to remove more of the tumor.

After the induction phase, the consolidation phase begins. The consolidation phase aims to eliminate any remaining disease; this typically includes HDC and ASCT, or radiation therapy (Smith et al., 2018). Intensive multimodal treatment is necessary to increase high-risk NB patients' chance of survival. An aggressive treatment involving HDC is needed for patients with high-risk NB, and patient prognosis continues to improve if this HDC is followed by ASCT (Haghiri et al., 2021). These treatments allow for dose escalation since HDC utilizes a combination of high-dose drugs (i.e., etoposide, carboplatin, busulfan, melphalan, etc.) to kill cancer cells (Smith et al., 2018). When paired with ASCT, stem cells that may have been killed in the process of HDC can be recovered so that the body is still able to produce new cells. Radiation therapy can occur after the ASCT for a higher rate of local control and is usually administered to the main tumor bed. The last phase of treatment is maintenance, where any residual disease is treated, typically with immunotherapy, to combat relapse and increase survival (Smith et al., 2018).

Chemotherapy is the standard treatment for NB, as well as for all cancer types. Although this is the standard treatment, the systemic administration of chemotherapy targets cells within the whole body rather than a localized area, which often kills healthy dividing cells, such as bone marrow stem cells. Since HDC results in undesirable toxicity towards regular proliferating cells, it is not a sustainable treatment method (Schirrmacher, 2019). There are a multitude of toxic effects that include immediate signs of toxicity, along with late signs of chronic toxicity, ranging from mild to life threatening. All organs, including essential organs, can be affected by HDC. More severe side-effects include paralysis, spasms, drug resistance, carcinogenicity, infertility, and relapse. In comparison to chemotherapy, intratumoral drug administration is a more attractive option since it can be administered at high concentrations locally, while limiting off-target cytotoxicity.

2.2 Drug delivery

2.2.1 Routes of Administration

The most common drug delivery method is orally administered drugs, this is because they are easily administered and non-invasive (Homayun et al., 2019). The route of the drug when administered orally follows the digestive tract and is ultimately released in the lumen of the gastrointestinal (GI) tract, where it is absorbed through the gut wall and enters the bloodstream. The variability for oral drug administration is due to the administration route, as well as the need to be metabolized by the gut prior to being exposed to the bloodstream. Metabolism can be highly affected by a myriad of factors. This variability from patient to patient regarding the absorption and metabolism of drug rates is the main concern for oral administration of chemotherapy drugs. These drawbacks can result in dosing that is too low or too high.

Chemotherapeutic drugs are primarily administered intravenously. This route allows the drug to be administered directly into the bloodstream. This skips the first pass metabolism and therefore the variability of the rate of metabolism of the drug. Other common types of drug administration include transdermal delivery, which is delivered through the skin. The skin is another barrier that is difficult to permeate and can alter how the drug is absorbed, though this method is convenient and self-administrable (Verma et al., 2010). Intravenous is immediately administered into the bloodstream, but for strong drugs, this route can produce harmful effects. This is a convectional route for chemotherapeutic drugs, although systemic toxicity can arise from the direct route to the vein, thus requiring the dose to be limited to ensure the safety of other organs. This causes the drug concentration to not be at its strongest, leading to it not be as effective while still having high off target toxicity (Coburn et al., 2017). The route of administration is dependent on the need and the target. For health disparities that are not systemic, or stem from a specific location, it is more efficient to create a targeted approach.

Cancer treatment benefits from localized drug delivery because highly tumor cell-concentrated areas can be targeted with high concentrations of drug. By targeting those areas, other surrounding tissue remains viable. This introduces a different type of administration called intratumoral, where the drug is injected directly into the tumor. Intratumoral deliveries are more accurate and make certain that the drug is sent to the tumor site, whereas with systemic delivery that is not certain. Due to anticancer drugs being extremely toxic, when enduring systemic

administration, the dosing must be lowered due to its ability to affect other parts of the body. With intratumoral delivery, dosing can be at a higher concentration since it is being delivered straight to the affected area with less off target toxicity (De Lombaerde et al., 2021). There is a lot of work being done on different ways to create localized drug release options due to its promising effectiveness, which will be discussed in the following section.

2.2.2 Localized Drug release

There are a multitude of ways to achieve a localized approach for drug delivery. For certain maladies, this type of therapy is necessary. In the case of tumors, the only area that needs the drug is the tumor site. In addition, the harmful side effects of anticancer drugs can be extreme, such as myelosuppression, kidney malfunction, hearing malfunction, heart malfunction, nerve damage, etc. (Chatterjee et al., 2010). For a more localized drug delivery, there are intratumoral methods, as well as other methods where an encapsulated drug complex will be delivered intravenously, and then released locally through chemical modifications and/or triggering stimuli.

Nano vehicles are a new type of technology that can deliver multiple chemotherapy drugs through the help of nanotechnology. Through this method, the drug system can be injected intratumorally, or through a different route, and will be modified so that the drug is released only at the desired site. Nano vehicles include micelles, inorganic nanoparticles, polymeric nanoparticles, dendrimers, and lipid-based nanoparticles.

Micelles are block copolymers with a hydrophobic center and hydrophilic exterior. This allows the center to easily absorb hydrophobic molecules, which includes many therapeutic drugs, while the outside allows for easy travel through the body and stability. In one study, a pH responsive hybrid micelle was created out of polyethyleneimine (PEI) and polylactic acid (PLA) for delivery of paclitaxel and siRNA (Jin et al., 2018). The PEI-PLA copolymer created a pH response dependent drug release, so that when the micelle reached the tumor site and experienced the change in pH (to about 5-6 pH), the poly(ethylene glycol)-block-poly(L-aspartic acid sodium salt) (PEG-PAsp) coating would detach and promote the PEI and siRNA to leave the endosomal area. Since the pH environment in a tumor site is more acidic than that of a regular cellular environment, the dependent pH external factor allows the delivery to be more specific.

Inorganic nanoparticles are another type of nano vehicle that are receiving attention due to their ability to be activated through magnetism or lasers as stimuli. Inorganic nanoparticles can include metallic materials such as iron oxide, gold, and silver, but also nonmetallic materials such as oleic acid and Pluronic's (Zeinali et al., 2020). In one study, an oleic acid and Pluronic coated iron oxide nanoparticle complex was created for delivery of DOX and paclitaxel for a more targeted delivery (Jain et al., 2005). Due to the iron oxide nanoparticle addition, when magnetic resonance imaging was applied to the tumor site, initiation of the delivery of the cancer drugs occurred. The complex showed a sustained release profile as well as high margins (74-95%) for encapsulation of the cancer drugs.

Polymeric nanoparticles are usually chemically modified on the surface with ligands in conjunction with overexpressed ligand binding sites on cancer cells (Zeinali et al., 2020). The polymeric materials used are normally hydrophilic in order to better protect the drugs at the core, such as polyvinyl alcohol, polyethylene glycol, and monomethoxy polyethylene glycol. Nanoparticles made of PEGylated gelatin were created in one study for the delivery of DOX and betanin (Amjadi et al., 2019). Betanin was used in efforts to reduce toxicity effects of the DOX on healthy cells. The PEGylated gelatin nanoparticles allowed for a pH responsive system illustrating controlled release of the drug. The complex showed results of both decreasing overall breast cancer cell count while showing a safe and controlled drug release.

Dendrimers are highly branched macromolecules synthesized by materials such as peptides, poly(L-lysine), Poly amidoamine, and other dendritic polymers (Tekade et al., 2009). Dendrimers normally have issues being able to hold drug for controlled releases, so one conventional method to combat this is to synthesize them to be externally triggered. An example of this is a pH responsive PAMAM dendrimer complex encapsulating methotrexate (MTX) and all-trans retinoic acid (ATRA) for ovarian cancer. Through a cytotoxicity study, the dendrimer drug matrix release profile was found to be more controlled and efficient than just the drug itself.

Lipid based nanoparticles can also group together with liposomes, which are used in many drug delivery mechanisms since they are easy to prepare and do not require organic solvent as other nanoparticles do (Zeinali et al., 2020). They have phospholipid bilayer membranes which allows them to ease through the body while protecting the drug within. These

subgroups within nano vehicles are consistently being worked on, as well as combined, for new hybrid drug delivery systems that have the potential to be triggered by external factors.

Another drug delivery method that is well studied and has been clinically approved for targeted therapies is the Gliadel Wafer (Westphal et al., 2006). The Gliadel wafer is a dime shaped wafer made up of polyanhydride entrapping carmustine (chemotherapy drug) to combat brain cancer. When using the treatment, a maximum of eight wafers can be placed after surgical excision of the tumor. The wafers degrade in two steps; first hydrolysis wears down the anhydride bonds, corroding the polymers that make up the external area, followed by the release of the drug over a ~5-day period. The wafers finally degrade after about 6-8 weeks. The wafers are a good use of drug delivery mechanisms, but since they are an additive to excision surgery, they are not cheap, safe, or easily administered. There are many other clinically approved drug delivery systems, the first of many liposomes encapsulated drugs being Doxil in 1995 (Kraft et al., 2014). This is through an intravenous route, but there is no external trigger and so the drug can start to release even if not at the tumor site, thereby creating adverse toxicity effects (Bochot et al., 2012).

Hydrogels provide an alternative route for drug delivery where their favorable hydrophilic properties and ability to uphold localized and sustained drug release have made them subject to gaining the attention of multiple research centers. To cover the benefits and efficacy of hydrogels in drug delivery, a more in-depth analysis will follow in the succeeding section.

2.3 Hydrogel systems

2.3.1 Hydrogels

Hydrogels possess a great opportunity in DDS as they are capable of encapsulation and controlled localized delivery of molecules (Larraneta et al., 2018). The inherent hydrophilic nature of hydrogels allows for integration of differently charged and/or soluble molecules for targeted drug delivery. This may prove to be especially useful in cancer therapies where many of these drugs rely on the hydrophilic/ hydrophobic interactions within the body for the drug to release. With drug therapeutics it is also important to consider the cytotoxicity that they carry, so in order to control the molecular release kinetics, gel permeability is adjusted by tuning the density of the crosslinks as well the molecular weights of the crosslinks (Lin et al., 2010). By adjusting the size of the crosslinks one can manipulate the amount of drug release over time

because the drug will release slower over time if the crosslink molecular weights are smaller and will release faster through the hydrogel network if the molecular weights between the crosslinks are large. In just the past decade researchers have begun using PEG to modify anti-cancer drugs in order to improve potency and reduce cytotoxicity (Li et al., 2013). PEGylation is a form of chemical surface medication often used to improve permeability via covalently bonding PEG polymers to therapeutic molecules. Primary advantages of using PEG as a molecular modifier is that it attributes to prolonged drug releases locally and decreased biodegradation creating a predictable and controlled release profile, as well as reducing the immunogenic response in the body. Products such as Oncaspar, Mircera, and Somavert are some of the top FDA-approved PEGylated drugs released out on the market for tumor and/or cancer therapies. DOX, a common anticancer drug, was conjugated with PEG molecules to study the potency and toxicity upon release *in vivo* that showed 10 times less cytotoxicity than just DOX on its own (Li et al., 2013). The tumor targeting response and plasma residence time was also an improvement on just DOX alone, signaling PEG as a potential vehicle in DDS. A novel hydrogel platform consisting of a PLGA-PEG-PLGA triblock copolymer network encapsulating the active pharmaceutical ingredient, Docetaxel, is a thermo-responsive hydrogel that has been identified as a subcutaneous route of administration for lung cancer (Larraneta et al., 2018). It is water soluble and free flowing at low temperatures such as 2-15 °C but once administered and exposed to body temperature (~37 °C), it will transition into a gel, allowing for a steady release of drug over time. The immense opportunities PEG provides in DDS lends itself to why it has several proven results already and why researchers are still finding fresh and innovative ways to use the material in therapeutics.

The use of 3D polymeric models in material science and engineering applications has become a popular course of action for researchers over the past decade, for the purpose of this project, the team will be looking at hydrogels (Chauhan et al., 2022). Hydrogels are three-dimensional polymer networks that consist of crosslinked hydrophilic polymer chains that are swollen with water (E. Ahmed, 2015; Chauhan et al., 2022). These polymer chains can be naturally and synthetically derived, or a combination of both, which gives them the capability to be modified based on the desired application. (E. Ahmed, 2015). These polymer chains can be interwoven to create a mesh network that swells upon contact with fluid.

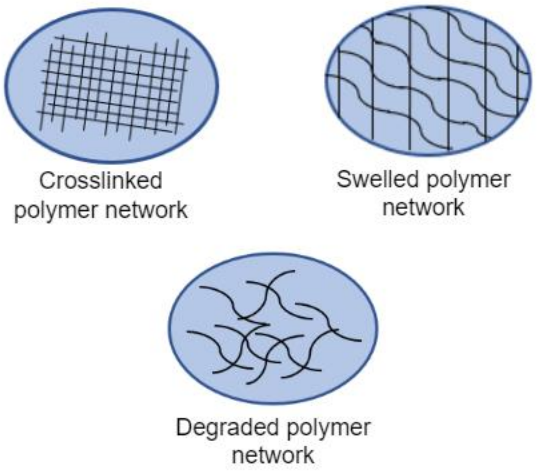

Figure 1: Hydrogel Characteristics.

The water solubility component of hydrogels arises from their hydrophilic polymer backbone. They contain polar functional groups such as hydroxyl, carboxyl, and amino groups that make them soluble and swellable by water (Yang et al., 2022). Figure 1 shows some important hydrogel characteristics to consider when it comes to formulation and fabrication. The mesh size refers to the size of the links between each molecule in the polymer network and the swelling refers to the intake of water into that polymer network. The degradation and mechanical properties of the hydrogel come because of the polymer network that is synthesized and thus will depend highly on the type of polymers used, as well as their specific properties (Bustamante-Torres et al., 2021).

The hydrophilicity of hydrogels allows for them to swell, as water enters the crosslinked polymer mesh network, the water molecules become absorbed into the polymer network, as depicted in Figure 1 (Ahmed, 2015). Depending on the properties of the polymers being used under equilibrium, or without the presence of any stimuli such as the molecular weight and density of the crosslinks, they can maintain varying volumes of water inside during its swollen state. When the hydrogel becomes exposed to water like this, the ratio of water inside the hydrogel is typically higher than the ratio of the polymer inside. This water retention capability makes hydrogels optimal in not only material science research, but also in the clinical setting as well.

To have an effective hydrogel, the inherent mechanical properties are important to consider. Polymer morphology can be classified into three groups: amorphous, crystalline, and semicrystalline, each having their own advantages and disadvantages; it should be made clear what the differences are (Aswathy et al., 2020).

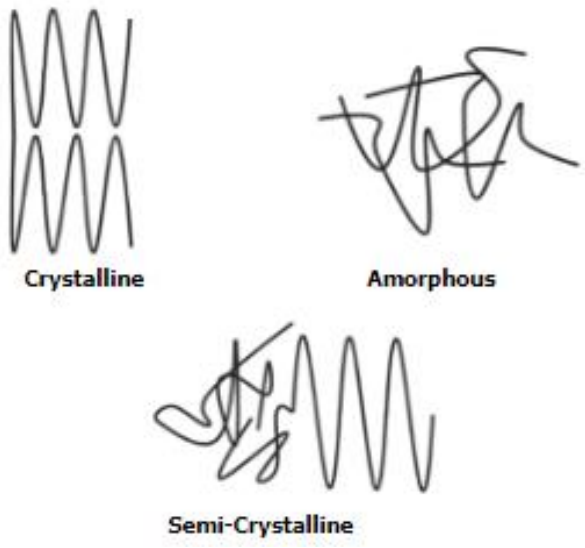

Figure 2: Basic visual of various polymer morphology structures.

As depicted in Figure 2, an amorphous polymer structure has no defined structure to it, so generally water-swollen hydrogels do not have any ordered structure to them at the molecular level (Miyazaki et al., 2001). Although this may increase the permeability of the material, it may also come at a loss for mechanical properties such as strength, stiffness, and toughness (Beckett et al., 2020). There is then the crystalline morphology, which is highly ordered with molecules densely packed together. This type of morphology typically results in a stiffer and less ductile material with smaller open regions between molecules, causing the permeability to decrease. Depending on the desired application, it may be beneficial to have a mixture of both as depicted in the bottom of Figure 2. A semi-crystalline structure is a hybrid of amorphous and crystalline morphology. Semi-crystallinity gives the benefits of both morphologies, allowing for fine-tuning of the molecular composition and crosslinks of materials.

With a brief overview of the novel hydrogel platform in place, the following section will go into finer detail as to how these hydrogel networks may be synthesized for clinical application to achieve optimal patient treatments.

2.3.2 Bioconjugation

In recent years, the use of biomaterials in medical application has increased rapidly and shown great results in tissue engineering and regenerative medicine (Wang et al., 2022). Their innate biocompatibility and water retention properties make them an attractive option in biomedicine due to the similar water content of molecules in the human body. Despite their positive capabilities, their effectiveness can be reliant on the type of crosslinks that are formed between the molecules: physical and covalent.

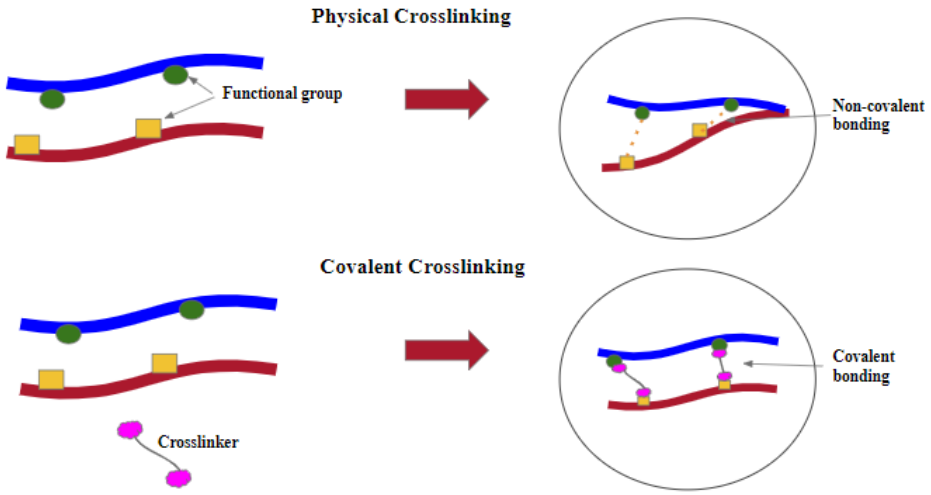

Figure 3: Crosslinking mechanism of action for different bond patterns.

2.3.2.1 Physical crosslinking

Physical crosslinking commonly refers to a self-assembled reversible linkage of molecules based on weak interactions such as ionic bonds (Chauhan et al., 2022). This type of crosslinking is the most prevalent since it does not require a crosslinking agent to initiate bonding between molecules. Crosslinking is dependent on the physical interactions occurring between the distinct polymer chains. The ionic charges of the molecules often determine the bonding patterns that will occur. Weak chemical bonding patterns such as Van der Waals and hydrogen bonding, are commonly seen in physically crosslinked hydrogel networks. Aside from the bonding patterns, mechanisms such as hydrophobic surface interactions between the

molecules and the synergistic interactions between small molecules, or polymer chains, that have the same chemical composition but different stereochemistry, also go into the physical crosslinking process (Parhi, 2017). Due to the lack of crosslinkers, or chemical modification, physical crosslinked hydrogels have an inflexible gelation time, gel pore size, chemical functionalization, and degradation profile, leading to them not being the go-to mechanism for hydrogel formation for *in-vivo* applications.

2.3.2.2 Covalent crosslinking

Covalent crosslinking, also known as chemical crosslinking, on the other hand utilizes covalent bonding to link adjacent molecules. As depicted in Figure 3, a crosslinker is used to covalently bond the functional group from one polymer to a functional group on another polymer. Covalent crosslinking typically yields hydrogels with stronger mechanical integrity due to the covalent bonds between molecules (Chauhan et al., 2022). Since these covalent linkages are largely non-reversible, the stability and the end-product are permanent. In contrast to physical crosslinked hydrogels, chemical crosslinked networks allow for the absorption of water and other bioactive agents without dissolution, as well as drug release via diffusion, which is vital in many drug delivery systems (Parhi, 2017). Various methods of inducing chemical crosslinked hydrogel networks include hybrid polymer networks (HPNs), photo crosslinking, enzymatic crosslinking, as well as interpenetrating networks (IPNs).

In HPNs, crosslinking occurs between a structural unit from one polymer chain and a structural unit from another polymer chain, resulting in a network with a composition of two different polymer chains covalently bonded together (Parhi, 2017). For this method, the polymers need to be pre-functionalized with reactive end groups that will allow for crosslinking to occur when the covalent bond is made. The biggest advantage with this approach is that there is no need for crosslinker molecules and in-situ formation of covalent bonds. Although beneficial to negate the crosslinker, this method also requires significant polymeric modification to attach functional groups to the polymer chain. This pre-functionalization may sometimes elevate the cytotoxicity which in turn affects the overall biocompatibility of the application.

Photo crosslinking considers the photo sensitivity of the functional groups, so by linking a photo sensitive functional group to the polymer chain, it enables the polymer to form crosslinks under light induced stimuli such as ultraviolet (UV) light (Parhi, 2017). An example of a photo

crosslinked hydrogel may come in the form of a chitosan based polymeric backbone chain incorporated with azide functional groups. The azide groups get converted into a nitrene group after exposure to UV light, thus allowing it to bind to the free amino acid groups of chitosan, inducing an in-situ hydrogel formation within a minute. This type of approach is more straight forward to facilitate but its downside is the lengthy exposure to irradiation which could result in a rise in internal temperature, potentially damaging surrounding cells and tissues.

Enzymatic crosslinking is a newer approach that uses enzymes as a catalyst to promote crosslinking of adjacent molecules (Parhi, 2017). The biggest advantage when using enzymes is that it speeds up the formation and crosslinking, usually resulting in a faster gelation time, but this comes at the cost of variability and inconsistency. It is hard to fine tune and control since once the catalyst has been added there is no reversable process or step-back that can be taken (Perin et al., 2022).

IPNs are hydrogel networks that consist of three or more polymers in which one polymer is crosslinked in the presence of the other (Parhi, 2017). They are like alloys of crosslinked polymers, formed without any covalent bonds, meaning that the networks cannot be separated unless the chemical bonds between the molecules are broken. Polymers used in IPNs need to have similar kinetics to the polymer that it is crosslinked in the presence of, and there should not be a significant phase separation between the two molecules. IPNs are unique in the fact that they do not have any viscoelastic properties, they can swell within solution, but they will not dissolve. Multicomponent IPNs offer the best route due to their increased mechanical strength and swelling response.

2.3.3 PEG

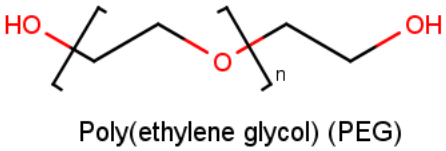

Poly(ethylene glycol) (PEG)

Figure 4: Chemical structure of poly(ethylene glycol).

Poly (ethylene glycol) (PEG) is a synthetic polymer comprised of repeating units of ethylene glycol (HO-CH_2-CH_2-OH), yielding a chemical structure that its commonly expressed

as H-(O- CH_2-CH_2)n-OH (Peng et al., 2020). This structure yields a nontoxic, and non-immunogenic polymer that exhibits excellent hydrophilic properties as well (Li et al., 2013). It is hydrolytically nondegradable and has good water solubility (Tessmar et al., 2007). In addition, PEG is uncharged, allowing it to form highly hydrated coils on biomaterial surfaces that can repel proteins. This shielding effect can also be used to create modified surfaces that respond to some molecular cue. As a result of its superior properties such as nontoxicity, non-immunogenicity, good water solubility, and biocompatibility, the Food and Drug Administration (FDA) has approved PEG in the biomedical space (Peng et al., 2020). The customizability and additive properties that PEG may give when incorporated into a polymer network make this molecule an option to strongly consider when looking into biocompatible hydrogels.

2.3.3.1 PEG Based Hydrogels

PEG is a common polymer used in hydrogel platforms over the last couple of decades due to its advantageous properties both *in vitro* and *in vivo* (Aswathy et al., 2020). Researchers recently developed a protein-peptide based hydrogel for spinal cord injury repair where multi arm poly(ethylene glycol)-poly(N-isopropylacrylamide) (PEG-PNIPAM) copolymer was used to conjugate protein rich peptides to create a hydrogel network capable of encapsulating Schwann cells (Wang et al., 2022). Upon *in vivo* delivery, the self-healing properties of the copolymer yielded greater cell adhesion and transplantation efficiency at the site leading to an overall successful spinal cord injury treatment plan. Hydrogels may also be conducive in treatments where properties will need a form of external stimuli to achieve molecular release or gelation. For this reason, stimuli responsive material may prove to be a route of interest for some. For example, photo-responsive or light responsive material can be considered for their steady degradation profiles (Yang et al., 2022). An *in vitro* experiment was performed where modified 4-arm PEG was copolymerized with photo-sensitive molecule 2-nitrobenzyl, and phenol forming a crosslinked hydrogel network with horseradish peroxidase and hydrogen peroxide where once exposed to UV light, the hydrogel had begun to degrade. This type of approach may be considered for both longer- and short-term hydrogel degradation profiles, depending on the copolymer network used. Due to the harmful radiation that chemotherapy may induce on the body during treatment, having the ability to control cell fate is something that has piqued the interest of researchers recently. Novel hydrogels utilizing polysaccharide glycosaminoglycans (GAGs) have shown that that this may be possible now (Chauhan et al., 2022). A star shaped

PEG-GAG hydrogel was fabricated via in-situ bio-orthogonal crosslinking that showed hydrogel structure could effectively control cell morphogenesis as well as the survival rate of embedded mesenchymal stem cells. During the in-situ synthesis process the researchers were able to adjust the charge on GAG which then allows for regulating the biomolecular signals that are responsible for determining cell fate. For *in-vivo* hydrogel applications it is important to consider the internal pH of the site to ensure biosafety and biocompatible delivery. For this reason, researchers fabricated pH- responsive Ag+ nanoparticles loaded into a PEG-methacrylic acid copolymer hydrogel which opened the door for applications such as biosensing, nanomedicine, and drug delivery as well (Thoniyot et al., 2015).

2.3.3.2 Effectiveness in DDS

To understand the capabilities of PEG, it is important to note the breakdown process of its subunits. Due to their inability to hydrolyze in the body, PEG molecules undergo limited metabolism before they release their polymer blocks, which is either through the kidneys if the molecular weight of the polymer chains are less than 30 kDa, or through the liver if its more than 30 kDa. PEGs can have a molecular weight up to 100 kDa depending on the number of repeating subunits of ethylene glycol there are (Peng et al., 2020). To ensure safety of patients and efficacy, molecular weights of less than 50 kDa are considered for tissue engineering and drug delivery applications (Tessmar et al., 2007).

2.4 Injectability

2.4.1 Injection force

Hydrogels pose as an effective DDS due to their ability to be administered via syringe. They can be fabricated with many different polymers and polymer weight content affecting the composition of the polymer network and its inherent viscosity (Alonso et al., 2021). This is important because the viscosity affects the syringeability and injectability of the hydrogel since it needs to get pushed through a needle to be injected. Syringeability is the ability of the hydrogel to be released through a needle point. Injectability is the evaluated force value needed to administer the substance through a syringe and is also dependent on needle gauge, needle length, and flow rate (Alonso et al., 2021). Mechanical testing for the injection force can be done using a mechanical testing machine with a force sensor and loading a syringe with the hydrogel. By putting the machine on tensile extension mode, it is able to have a set linear rate as desired, and

then the displacement can begin to be applied (Chen at al,. 2017). A more viscous hydrogel will result in a higher injection force. A smaller needle diameter and shorter needle length will result in a lower injection force.

$$F = F_{friction} + \frac{8\,Ql\,R^2}{r^4}\eta$$

Equation 1: Hagen-Poiseuille's adapted equation (Krayukhina et al., 2020).

The above equation is an adapted version of Hagen-Poiseuille's equation specifically for the motion of fluid through a needle (Krayukhina et al., 2020). Hagen-Poiseuille's equation normally is used to analyze the connection between pressure and flow rate in a pipe but can be adapted so that a needle acts as a pipe. The equation is solving for F which will act as injection force in units of Newtons (N). R is the inner radius of the syringe (m), r is the inner radius of the needle (m), l is the length of the needle (m), Q is the volumetric flow rate (m^3/s), and n is the dynamic viscosity (Pa * s).

In one study, adamantane-modified hyaluronic acid (Ad-HA) and cyclodextrin-modified hyaluronic acid (CD-HA) hydrogels were fabricated and compared through mechanical testing. Different total polymer content ranging in 5-7.5 wt. % in the hydrogels were compared while keeping the flow rate and needle parameters constant (Chen at al., 2017). The 5 wt. % hydrogel had an injection force of about 5 N, while the 7.5 wt. % hydrogel showed a 15 N injection force. These results show that a smaller increase for the polymer component in a hydrogel can significantly increase the injection force through increasing viscosity of the complex.

2.4.2 Viscosity

For injectable hydrogels, viscosity is an important parameter that is in relation to the injection force needed as well as the chemical and physical properties of the hydrogel. The Coburn Lab did a study using photocrosslinkable methacryloyl groups (MA) to covalently modify CS, methacrylated CS (CS-MA) injectable hydrogels were fabricated (Ornell et al., 2019). To test the hydrogel's ability to be injected, Coburn executed an injection force test on different hydrogels. These hydrogels varied in reaction times from 2 hours (h) to 24 h, as well as

CS-MA concentration range, comparing 10% and 20%. Injection force testing was performed on the following hydrogels: 2 h 20% CS-MA showing an average of 17.6 N injection force, 24 h 10% CS-MA showing 38.6 N, and 24 h 20% CS-MA with 94.3 N. Hydrogels that were methacrylated for longer showed a higher injection force, this could be due to the higher amount of crosslinking. In addition to this finding, the results showed that the higher the polymer concentration of the hydrogel, the higher the viscosity. Photo crosslinking forms the crosslinks the create the CS-MA hydrogel, which plays a large role in determining the viscosity of the gel. This determination is based on the density of crosslinking. There are other ways to crosslink hydrogels; physical crosslinking, chemical crosslinking, enzyme initiated crosslinking, and ionic crosslinking (Overstreet et al., 2012). Different crosslinking can result in different hydrogel properties. Chemical crosslinking can increase elastic properties within the hydrogel. Enzyme-initiated crosslinking can decrease the gelation time making it a rapid reaction as well as a highly specific reaction during formation. Physical crosslinking can increase the hydrogel's mechanical properties; these factors are dependent on the requirements for the hydrogel.

2.5 Chondroitin Sulfate

2.5.1 Properties of Chondroitin Sulfate

CS is a polymer that is widely used in biomedical applications due to its composition and functionalities, which will be explained in greater detail throughout this section. CS is a sulfated GAG that is naturally occurring and consists of repeating disaccharide units of D-glucuronic acid (GlcA) and *N*-acetyl-galactosamine (GalNAc) linked by β-(1,3) glycosidic bonds (Pat et al., 2019; Shi et al., 2014). CS is sulfated in different carbon positions and is typically modified by OH groups being replaced by sulfate groups on C-2 and C-3 of GlcA, and C-4 and C-6 of GalNAc; these sulfate group placings, along with composition and concentration, determine the type and classification of CS (Shi et al., 2014). The chemical structure can be seen in Figure 5. There are two main structural categories, condroitin-4-sulfate (CS-A) and chondroitin-6-sulfate (CS-B), where there is a sulfate group on position 4 and 6 of GalNAc on the disaccharide units (Di Muzio et al., 2022). These modifications can generate a wide variety of forms, each with different applications. The bioactivity of CS is directly related to the structure, so it is important to note the structure of the CS being used in each application so the relationship between the structure and function can be understood (Lauder, R.M., 2009).

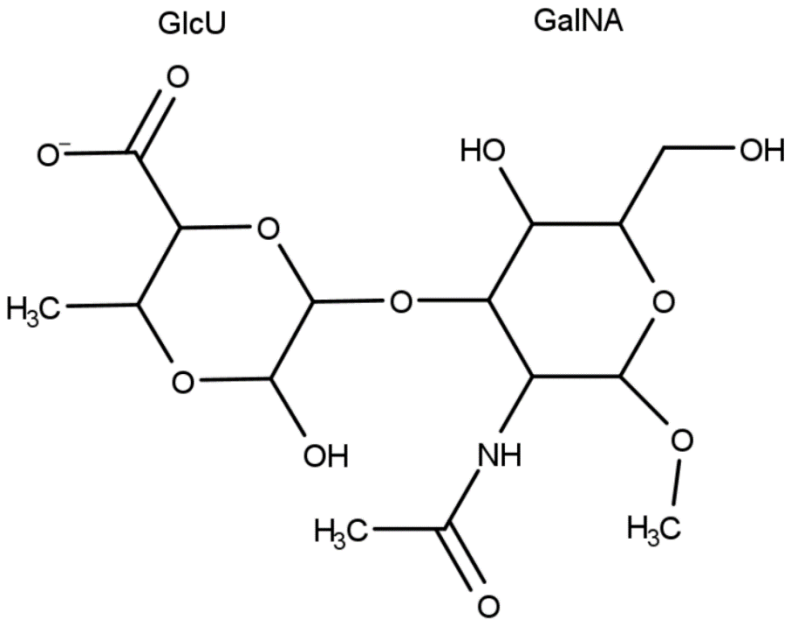

Figure 5: Chemical structure of CS.

CS is typically extracted from the cartilage of porcine, bovine, chicken, or shark, and the average molecular weight is $1 - 4\,x\,10^4$ Da, depending on the origin; CS chain size varies based on where they come from, but they are always heterogenous with respect to their size (Yang et al., 2020; Shi et al., 2014). CS chain structure is not random, allowing for it to impact different biological processes, and can take on a diverse range of structures based on the sulfate group (Lauder, 2009; Shi et al., 2014). The structure of CS impacts the function and the bioactivity properties for that molecular type, which can have different therapeutic impacts (Shi et al., 2014). These interactions may stem from certain saccharide domains that are within the CS chain, allowing for it to interact with a wide variety of molecules (Asimakopoulou et al., 2008).

CS is non-toxic, biocompatible, and is typically ingested by humans, or non-humans, orally, as a food/drink additive, topically, or in medical applications (Lauder, 2009). CS is an important component of cartilage that can work to promote regeneration of tissues and is naturally found in the extra cellular matrix (ECM), particularly in connective tissues and the brain, and has a high affinity towards growth factors by electrostatic interaction (Li et al., 2018; Tang et al., 2019). CS can form a network with collagen in connective tissues that allows for macromolecule transport, such as globular proteins (Wang, 2003). Collagen is one of the main proteins in connective tissues, and works to provide strength, structure, and support. CS shows

many properties including anti-inflammatory, antioxidant, antithrombic, anticoagulation, stem cell niche creation, immunomodulatory, cell recognition, enzymatic activity, and apoptosis, along with other types of bioactivities (Shi et al., 2014; Strehin et al., 2010).

One of the main ways that CS can be modified is through chemical crosslinking, which allows for hydrogels to be formed since the water solubility is reduced (Sintov et al., 1995). In the Sintov study, products with a reduced water solubility were created by crosslinking CS with 1,12-diaminododecane, this product was later mixed with indomethacin to create tablets. This study found that the higher the crosslinking, the slower the drug is released into the system. It is recommended that the amount of crosslinking be manipulated based on the desired drug release profile. Enzyme penetration is important since it degrades the hydrogel, thus impacting the degradation profile (Meyer et al., 2022). Since swelling is a key factor in enzyme penetration into a polymer, it is important to determine the effect that the degree of crosslinking has on swelling properties (Sintov et al., 1995). This also influences the drug release profile by impacting the diffusion rates of both the drug into the hydrogel and the hydrogel into the body. The modification of this crosslinked CS allows for it to be used for other biomedical purposes, such as hydrogels.

To form a hydrogel, CS must be functionalized so that it can photo-crosslinked (Chen et al., 2018). There is a wide variety of chemical options that can be used to modify a polymer so that it can be crosslinked. As seen in Coburns lab, methacrylate can be used as a functionalization group for the development of photo-crosslinked, injectable CS hydrogels (Ornell et al., 2019). The Coburn Lab used glycidyl methacrylate (GMA) as a means of adding methacrylate groups to CS due to its reaction efficiency and lower production of cytotoxic byproducts (Li et al., 2004). CS-MA macromers are created when the hydroxyl side groups in CS react with GMA (Chen et al., 2018). The percentage of methacrylate groups on CS impacts the water absorption capability of the hydrogel, since it is connected to crosslinking density and pore size (Li et al., 2004). The reaction between CS and GMA can be accomplished through epoxide ring-opening or transesterification (Li et al., 2003). When under heterogenous-phase conditions, the reaction occurs via both mechanisms and results in the outcome being influenced by the medium's pH value (Di Muzio et al., 2022). The reaction occurs through epoxide ring-opening

when GMA reacts with carboxyl and hydroxyl, the two functional groups in CS, allowing for methacrylate insertion. This synthesis can be seen in Figure 6.

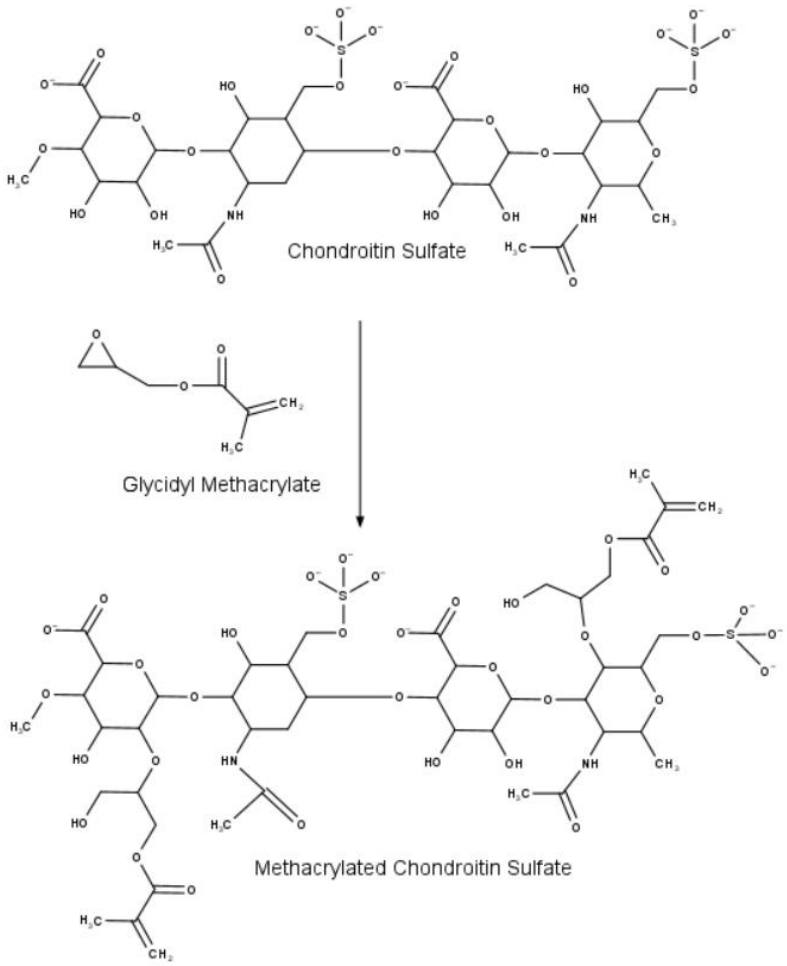

Figure 6: Photo-cross linkable methacrylated CS synthesis.

The CS-MA can be formed into a hydrogel through free-radical polymerization (FRP). Typically, an added chain-transfer agent will use a chain-transfer reaction to terminate the propagating chain (Gao, 2020). This works to avoid macro gelation since the primary chain length is short and each primary chain has an average number of crosslinks that is greater than 1. FRP forms a polymer change using free-radical groups that are generated from a reaction, while crosslinking of the acrylate group will form a hydrogel network (Matyjaszewski, 2002). When CS-MA reacts with a double bonded carbon in the methacrylate group, the radicals transfer to a carbon in the acrylate group forming a bond (Carvalho, 2022). A crosslink is formed when the radical containing group reacts with a different polymer chain. These radical groups can be

formed on CS-MA through external stimuli. Irgacure®2959 is used as an initiator, it is exposed to UV light resulting in photolysis of Irgacure®2959, which forms free radicals. These free radicals are transferred to the methacrylate group in the CS-MA chains. The two radicals on the CS-MA chains react with other methacrylate groups, thus forming a crosslinked network, or a hydrogel.

2.5.2 Chondroitin Sulfate Uses

CS has many properties, as stated above, that can aid in a multitude of biomedical applications. One of the main uses of CS is in combination with glucosamine, where it is used as an anti-inflammatory drug for osteoarthritis (OA) to reduce pain (Jin et al., 2020). OA is musculoskeletal condition that is the most common cause of joint pain, arthritis or disability in elderly patients; there are no drugs to prevent or slow OA progression, and the current therapies are often ineffective (Simental-Mendia et al., 2018). The impact of CS on OA has been explored due to its ability to positively impact joint health and aid in treatment, and more recently has been looked at to prevent OA (Lauder, 2009). Studies have shown that when CS is used as a supplement in animal's diets, articular cartilage degradation was prevented (Simental-Mendia et al., 2018). CS can stimulate hyaluronic acid (HA) and proteoglycan synthesis, as well as inhibiting nitric oxide and proteolytic enzyme synthesis, which works to have an anti-inflammatory and immunomodulating effect. As stated before, CS is typically used in combination with glucosamine to treat OA due to their joint ability to suppress cytokines that can affect cartilage catabolism, as well as producing a symbiotic effect that works to moderate articular cartilages matrix metabolism.

CS is a biomaterial with a wide range of pharmacological applications, whether it be in a DDS or in the tissue engineering field; it is a multifunctional signal molecule and regulator with a series of bioactivities (Yang et al., 2020). CS can be used to create scaffolds for bone tissue engineering through mechanisms such as 3D bioprinting, covalent crosslinking, electrostatic interactions, etc. Researchers have begun to identify the role of CS in hydrogel networks as a form of drug delivery since it is biocompatible, biodegradable, non-toxic, has good anionic properties, and has no side effects. The system can be created using physical crosslinking and chemical reactions and is a promising biomaterial for DDS.

2.6 Chemotherapeutic agent: Anthracyclines

One of the most common antitumoral agents that researchers investigate when developing anticancer therapeutics is anthracyclines, which are derived from gram positive Streptomyces spp. Bacteria. Some of the most common types of anthracyclines available for treatment are agents such as DOX, DNR, idarubicin (IDR), and valrubicin (VLR) (Vankatesh et al., 2022). The biggest difference between anthracycline derivatives is the substitution patterns on the anthraquinone or the carbohydrate unit, this in turn can translate to varying levels of targeted antitumor activity and cytotoxicity.

The biggest driver in the usage of anthracyclines for anticancer therapies is their efficacy in preventing cancer cells from reproducing (Shandilya et al., 2020). Aside from this, they are capable of dose limiting cytotoxicity and possess evolved drug resistance properties as well (Shaul et al., 2013). DOX has been widely used in chemotherapy treatments for various metastatic cancers such as breast, lung, and NB, whereas DNR is more commonly used as a chemotherapeutic agent in acute lymphocytic and myelogenous leukemias (Venkatesh et al., 2022). Research performed in the Coburn Lab yielded results showing that DNR can be a viable option for an injectable hydrogel that delivers anticancer therapeutic agents intratumorally (Carvalho, 2022).

The general structure of anthracyclines includes a tetracyclic aglycone structure containing a chain of 4 cyclohexane rings with a daunosamine sugar moiety at carbon C7 on the primary ring, with adjacent quinone-hydroquinone groups in the secondary and tertiary rings, a methoxy substituent carbon C4 in the quaternary ring, a carbonyl group carbon C13, as well as a short side chain in carbon C9 (Shaul et al., 2013). As shown in Figure 7, the only chemical structural difference between DOX and DNR is their short side chains, DOX has a primary alcohol side chain whereas DNR has a methyl group said chain.

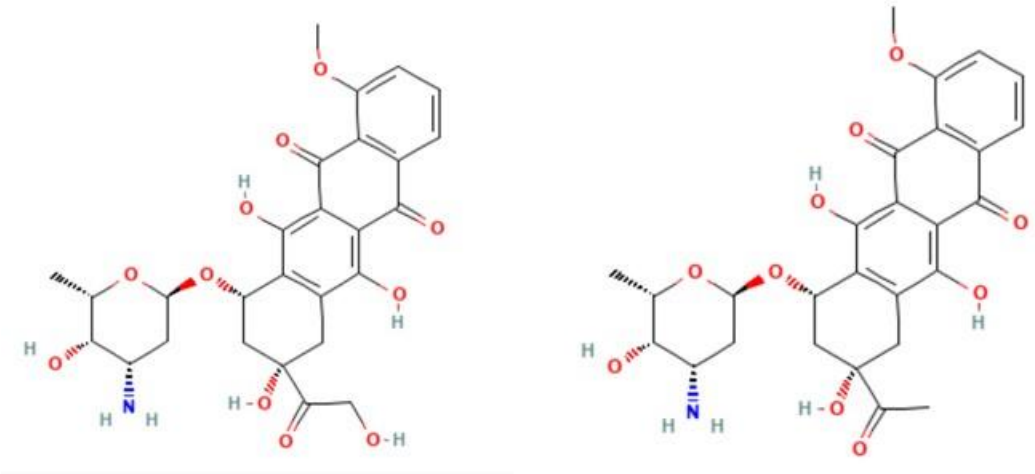

Figure 7: Chemical structure of DOX (left) and DNR (right).

The primary mechanism of action for anthracyclines is via topoisomerase-II interactions (Venkatesh et al., 2022). Topoisomerase-II induces double strand deoxyribonucleic acid (DNA) breaks for the purpose of counteracting DNA entanglement and coiling, providing new strand replication. Anthracyclines have a chromophore moiety that allows for cellular conformational changes to occur. This intercalating function allows the drug to insert itself between adjacent DNA base pairs when localized to the cell nucleus, in turn inhibiting DNA and ribonucleic acid (RNA) synthesis, thus leaving broken strands of DNA and inducing cell apoptosis in highly replicating cells. Their ability to efficiently induce apoptosis can be advantageous when creating localized drug delivery methods.

2.7 Chemistry

2.7.1 Click Chemistry

Click chemistry is a class of chemical reactions commonly used for bioconjugation, defined as the process of combining two molecules, with at least one being a biomolecule (Hein et al., 2008). At its essence, click chemistry utilizes the natural interactions between two smaller biomolecules to combine them into one. These reactions tend to be simple reactions that are not affected by the presence of oxygen or water; therefore, the products are compatible in physiological conditions. Click reactions are thermodynamically driven, have high yields, and lead to only one product. There are four groups of Click reactions: cycloadditions, nucleophilic ring- openings, carbonyl chemistry of the non-aldol type, and additions to carbon-carbon multiple bonds.

2.7.1.1 Diels-Alder Reaction

Diels-Alder reactions are a subsection of cycloadditions. These reactions are specifically between a diene and a dienophile to create a cyclohexene (Domingo et al., 2009). The reaction is shown in Figure 8.

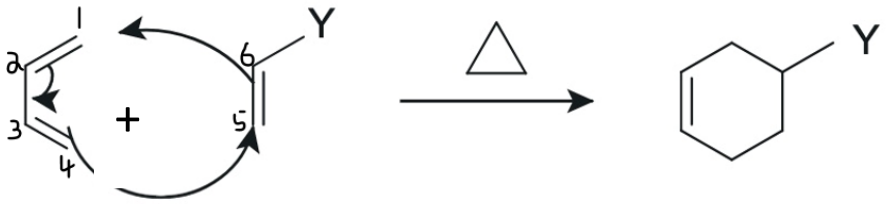

Figure 8: Diels Alder mechanism.

Diels-Alder reactions are exothermic, releasing 40 kcal/mol with an activation barrier of 27.5 kcal/mol (Domingo et al., 2009). The driving force behind this reaction is the creation of sigma bonds that tend to be much stabler than the pi bonds that currently exist (Berski et al., 2003). The double bond between carbons 1 and 2 moves down as a double bond forms between carbons 2 and 3. This causes the electrons to be pushed from carbon 3 and 4 to create a sigma bond between carbons 4 and 5. Similarly, this pushes the double bond between carbons 5 and 6 to create a sigma bond between carbons 6 and 1, resulting in the creation of the cyclohexane. This mechanism scheme can be translated into a more complex reaction like the 1,3 - dipolar cycloadditions and hetero-Diels-Alder cycloaddition, as seen in Figure 9 (Hein et al., 2008).

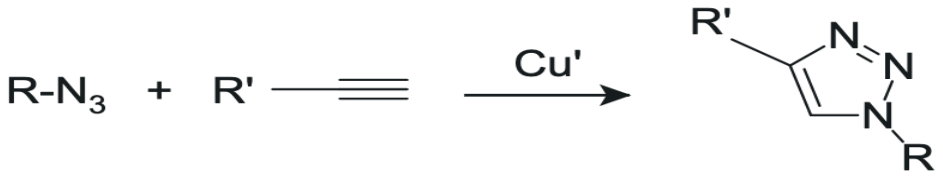

Figure 9: 1,3 - dipolar cycloadditions and hetero-Diels-Alder cycloaddition.

2.7.1.2 1,3 - Dipolar cycloadditions and hetero - Aiels – Alder cycloaddition

Most cycloadditions that fall under click chemistry are 1,3 - dipolar cycloadditions and hetero-Diels-Alder cycloaddition (HDAC) (Hein et al., 2008). A prime example of click chemistry is the Cu^{I}-catalyzed Huisgen 1,3-dipolar cycloaddition of azides and terminal alkynes

to form 1,2,3-triazoles (Sarpong et al., 2022). This reaction follows all of click chemistries criteria. It creates only 1,4 – substituted products, has no solvent preference, is unaffected by oxygen and water, stereospecific, and can be done over a large pH range (5-12) (Hein et al., 2008). These reactions are special in their ability to create cyclic products, leading to them being named cycloadditions (Hein et al., 2008). The HDAC reactions favor a stepwise catalyzed reaction with an activation barrier of 16.8 KJ/mol. The starting components are the alkyne and the Cu^{I} dimer. It is theorized that a pi bond exists at this junction (1), as seen in Figure 10 below.

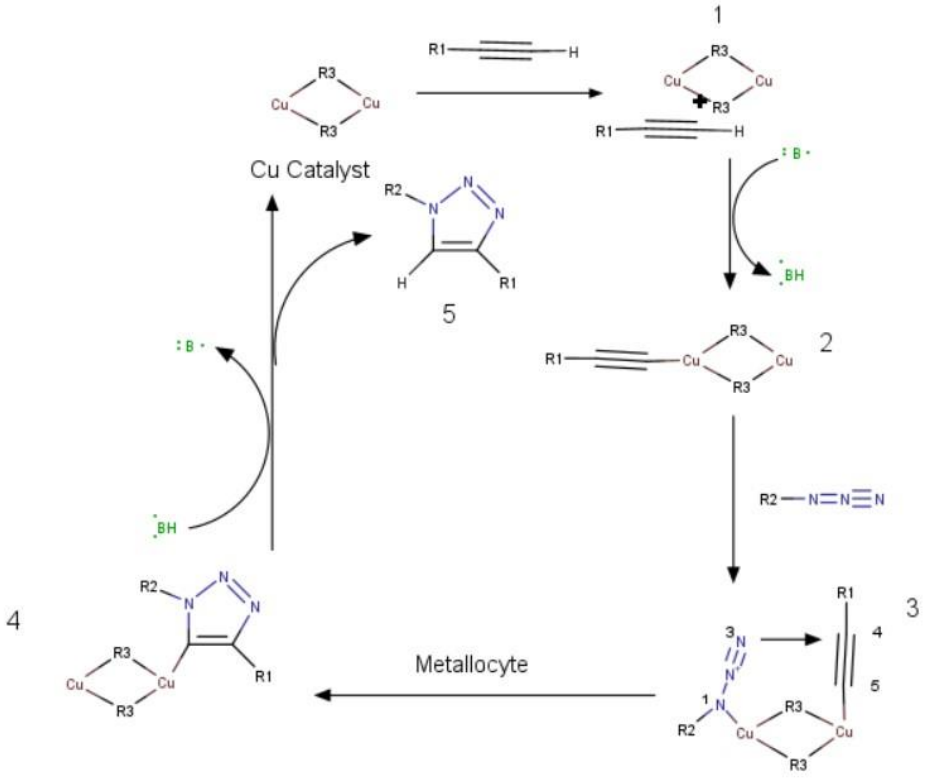

Figure 10: This is the proposed HDAC mechanism. Ligands are labeled with an R3. These can be many compounds but may vary due to the catalyst being used.

Because of the pi bond, hydrogen is deprotonated to form a Cu-acetylide. In step 3, N^{1} creates a slight bond with the Cu^{I} giving the azide the potential required for nucleophilic attack. N^{3} attacks C^{4} on the alkyne, leading to the formation of a metallocycle. The triazole in step 4 is created with the lone pair on the metallocycle when the lone pair on N^{1} attacks C^{5}. Finally, a step of protonation occurs to allow the Cu^{I} dimer to bring a Cu catalyst, thus allowing for the product

1,2,3 triazole to form. This reaction is a good example of a general click chemistry cycloaddition, however, this specific reaction uses a Cu catalyst which has been shown to produce toxicity in vivo, making it unsuitable to be injected into the body (Kim & Koo, 2019).

2.8 Activating agents

Double hydrophilic block copolymers (DHBC) have received ongoing attention and research for controlled drug delivery systems. In DHBC's one block is usually PEG or polyethylene oxide (PEO). The main purpose of this component is for solubilization in water, whereas the other block's purpose is to interact with the external environment. To combine CS with PEG, the CS first must be activated. The process of functionalizing grants CS the ability to make the bonds necessary for bioconjugation.

2.8.1 Carbodiimide

Carbodiimide is a functional group with a chemical composition shown in Figure 11, although this is not its only structure (Williams et al., 1981).

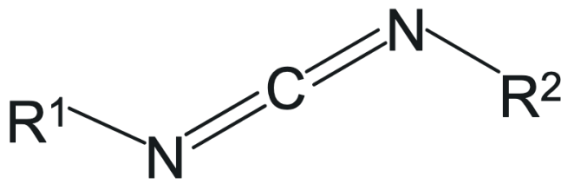

Figure 11: Chemical structure of carbodiimide.

It has two resonance structures, one being a triple bond on the left of the alpha carbon and one with the triple bond on the right, shown in Figure 12.

Figure 12: Resonance structures (triple bond on left and triple bond on the right).

Carbodiimides are another way to create amide bonds (Hermanson, 2013). An example of carbodiimides is 1-ethyl-3-(3-dimethylaminopropyl) carbodiimide hydrochloride (EDC) is shown in Figure 13.

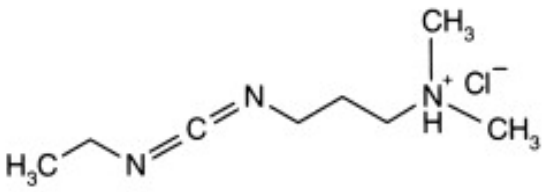

Figure 13: Chemical structure of EDC.

EDC is the most used carbodiimide in the bioconjugation of two groups that contain carboxylate and primary amines. It is often used together with N- Hydroxysuccinimide (NHS) to create efficient bonding with the amines. As seen in Figure 14, carboxylic acid must again be forced into its carboxylate state, where it then reacts with the alpha carbon in the carbodiimide to create an anhydride *O*-acylisourea as an intermediate while waiting for amine nucleophilic attack (Williams et al., 1981). The primary amine reacts to the carboxylate in a similar way to the NHS functionalized carboxylate, but the byproduct is now Isourea, which is a form of urea, instead of NHS leaving group.

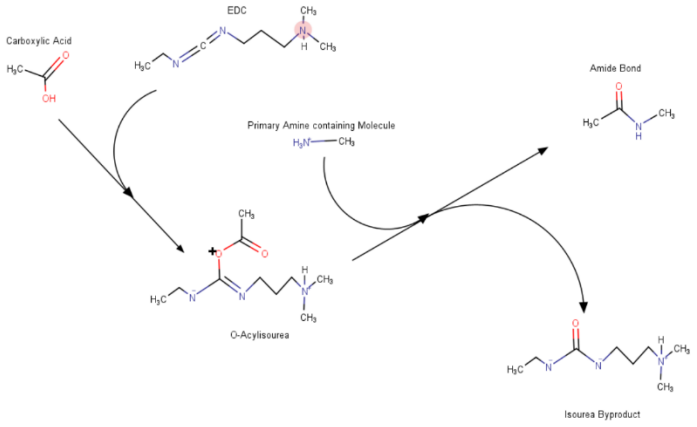

Figure 14: Mechanism of EDC and Carboxylic acid and amine to create an amide bond.

2.8.2 N- Hydroxysuccinimide

NHS is an organic ester that is commonly used for activating chemical compounds (Hermanson, 2013). This reagent has a composition of $(CH_2CO)_2NOH$, as shown in Figure 15.

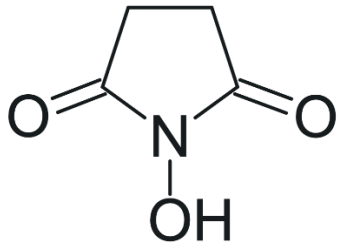

Figure 15: Chemical structure of NHS.

NHS specifically targets carboxylic Acid. While trying to react with carboxylic acid, it creates a covalent bond, thus creating an active intermediate, as shown in Figure 16. This results in a desirable leaving group for nucleophilic attack by a primary amine.

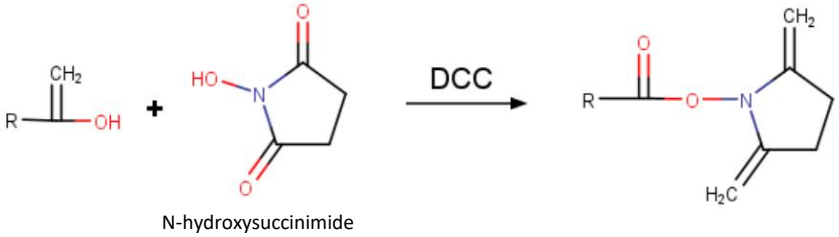

Figure 16: Carboxylic acid reaction with NHS to create active intermediate.

When NHS bonds to carboxylic acid on the CS it creates chondroitin sulfate succinimidyl succinate (CS-NHS) (Strehin et al., 2010). This new group allows binding with amines to create amide bonds. The PEG amine nucleophile attacks the electron deficient carbonyl group making the NHS group leave (Hermanson, 2013). This action causes the creation of stable amide bonds. This is the mechanism NHS modified CS bonds to PEG (Strehin et al., 2010).

2.8.3 Tetrazine

Tetrazine is another organic group that can functionalize CS to bond to PEG, it has a composition shown in Figure 17 (Sousa et al., 2022).

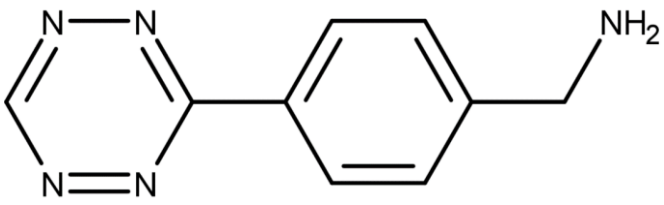

Figure 17: Chemical structure of Tetrazine.

However, using tetrazine means a different formation of bonds (Sousa et al., 2022). Tetrazine also targets the carboxylic acid on CS, but tetrazine functionalized groups bond to the unbonded norbornene groups on the PEG amine instead of the amine groups.

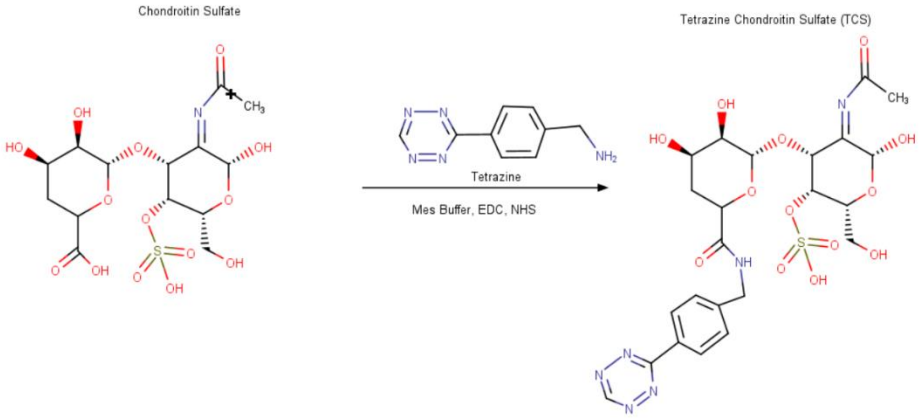

Figure 18: Reaction and final structure of CS and tetrazine.

2.8.4 (4-(4,6-dimethoxy-1,3,5-triazin-2-yl)-4-methyl-morpholinium chloride) (DMTMM)

DMTMM is the activating agent, like EDC, and is used for the activation of Carboxylic acids on the Chondroitin Sulfate. Its structure is shown in Figure 19.

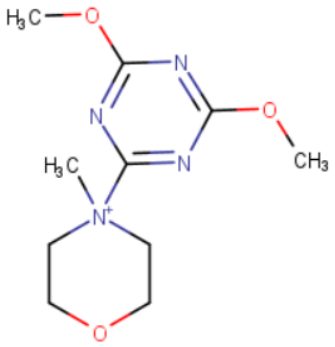

Figure 19: Chemical Structure of DMTMM.

The DMTMM reacts with the carboxylic acid to create an active ester, this releases *N*-methyl morpholinium. This active ester is highly reactive and can undergo nucleophilic attack easily, this reaction is shown in Figure 20 (D'Este et al., 2014).

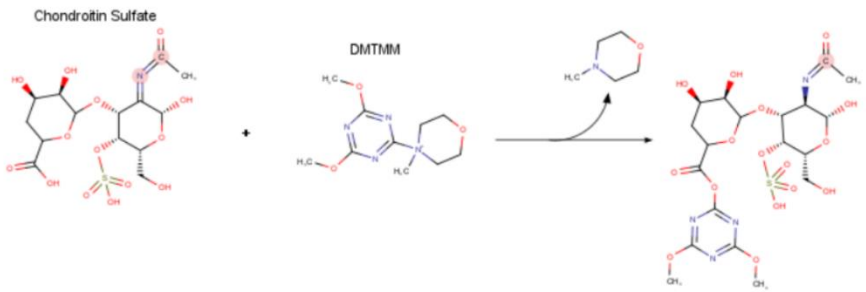

Figure 20: Reaction between DMTMM and carboxylic acid.

2.8.5 Furfurylamine

Furfurylamine (referred to as furan from here on out) is an aromatic compound. Furan is a heterocyclic organic compound that consists of four carbons with one oxygen. Its composition can be seen in Figure 21. Additionally, it has a lone pair on the oxygen allowing it to have a resonance structure, which can be seen in Figure 22.

Figure 21: Chemical structure of Furan.

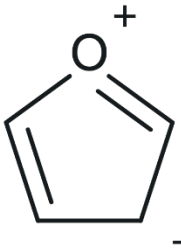

Figure 22: Resonance structure of Furan.

Similar to NHS, Furan also modifies the active intermediate created by DMTMM. It attaches to the end of the carboxylic acid; this modification allows the CS-Furan (CS-F) to covalently bond with Maleimide modified PEG. This reaction can be seen in Figure 23.

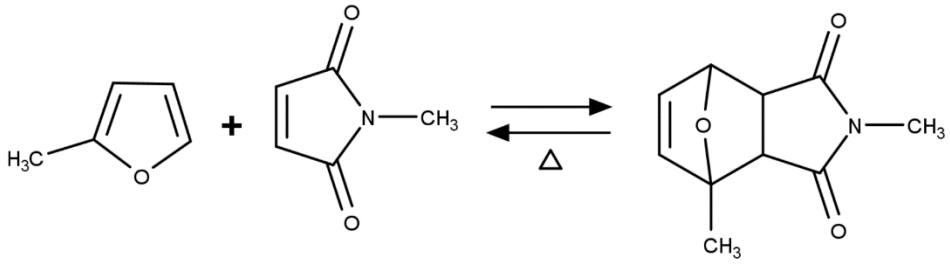

Figure 23: Furan reaction with Maleimide.

This reaction shows that furan is the diene and maleimide is the dienophile. Due to Furan's properties, it allows the CS PEG crosslinking to be devoid of side reactions, very selective, thermodynamically controlled, and have reversibility of cross linking (Gandini, 2013).

III. Project Strategy

3.1 Initial Client Statement

The initial client statement, provided by Professor Jeannine M. Coburn, PhD is:

"Develop a fabrication technique to obtain water-insoluble, injectable chondroitin sulfate drug delivery vehicles and characterize the resulting chondroitin sulfate material."

As our project progressed and we were able to gain more in-depth knowledge on the topic, as well as feedback from the advisor, the client statement was revised and is presented in Section 3.5.

3.2 Design Requirements

3.2.1 Design Objectives

The design objectives for this project revolve around creating a CS-based DDS that is water insoluble and within the optimal range for injection force and drug release. Additionally, more objectives were identified in terms of reproducibility, functionality, ease of use and more. These objectives were developed through the initial client statement and modified based on the advisor and project team's discussion. These categories and objectives are highlighted in Table 1 below.

Table 1: Design Objectives and Definitions.

Main Objective	Sub- Objective	Definitions
Injectable Hydrogel	Low Injection Force	The injection force must be 38 N through a 28- gauge needle with a needle length of 0.5 in.
	Reproducible Injectability	The injectability process must be repeatable and predictable.
	Reproducible Gelation Time and Process	The gelation time and process must be repeatable and predictable.

	Maintains Content Uniformity through Injection	The hydrogel must maintain structural integrity, stability, consistency pre- and post-injection.
Drug Delivery System Properties	Sustained Drug Release Profile	Target drug release profile is between 21- 28 days.
	Water Insoluble	The chondroitin sulfate-based hydrogel must stay water insoluble.
Market Scalability	Safe to Handle	The hydrogel must not expose the handler to danger or risk, thus making it safe to manipulate and create.
	Sterilization	Hydrogel must be created in a sterile environment to produce a sterile product or be able to be sterilized after creation.
	Effective Procedure	The procedure must be repeatable, efficient, and successful in the creation of a hydrogel that contains the desired properties.

To understand the difference in importance between design objectives, a Pairwise Comparison Chart (PWC) was created, as seen in Table 2 below. This chart was utilized to filter out what objectives are necessary. When an objective was deemed more important, it was given a value of 1, when it was deemed of equal importance, it was given a 0.5, and when it was deemed of lesser importance, it was given a 0. The total weights of each specification were added for a better understanding of where priorities would be along the project planning and execution process. This standard is used for the rest of the paper.

Table 2: Pairwise comparisons chart for Design Objectives.

Sub-objective	Low Injection Force	Reproducible Injectability	Reproducible Gelation Time & Process	Maintain Content Uniformity through Injection	Sustained Drug Release Profile	Water Insoluble	Safe to Handle	Sterilization	Effective Procedure	Total
Low Injection Force		½	1	1	1	0	1	1	½	6
Reproducible Injectability	½		1	½	½	0	1	1	½	5
Reproducible Gelation Time & Process	0	0		½	0	0	1	1	0	2.5
Maintain Content Uniformity through Injection	0	½	½		½	0	1	1	0	3.5
Sustained Drug Release Profile	0	½	1	½		0	1	1	0	4
Water Insoluble	1	1	1	1	1		1	1	1	8
Safe to Handle	0	0	0	0	0	0		½	0	0.5
Sterilization	0	0	0	0	0	0	½		0	0.5
Effective Procedure	½	½	1	1	1	0	1	1		6

Through this PWC, we found water insolubility to be the most important design objective with a weight of 8. Injection force and effective procedure were found to be the second most important objectives, with a weight of 6. Reproducible injectability was the next most important objective with a weight of 5. A sustained drug release profile was found to be the next most important objective, with a weight of 4. Maintaining content uniformity through injection was ranked next with a weight of 3.5, followed by reproducible gelation time and process with a weight of 2.5. Sterilization and safety to handle were ranked last with a weight of 0.5.

3.2.2 Design Constraints

Constraints are one of the key considerations to the design process, since if they are not met, then the project cannot be completed. The team was able to identify 7 major design constraints, which are described in Table 3 below.

Table 3: Definitions of design constraints.

Constraints	Description
Money	The team has a total budget of $1000, with $250 granted per member.
Time	The project work must be completed by April 21, 2023, thus giving the team ~8-month to complete all the project work.
CS Chemical Compatibility	CS must be able to covalently bond to adjacent molecules for crosslinking formation of the hydrogel network.
CS Biocompatibility	CS must be able to be compatible for in-body use.
Material Availability	All materials necessary for the project must be available in the given lab space or be purchased in a cost-efficient manner.
Equipment Availability	All equipment necessary for the project must already exist and be readily available through WPI laboratory spaces.
Intellectual Resource Availability	All project requirements must be supported through past knowledge, research, and lab equipment availability.

A PWC was constructed to rank the design constraints according to their importance. The design constraints identified include money, time, CS chemical compatibility, CS biocompatibility, material availability, equipment availability, and intellectual resource availability. All the design constraints described throughout this section were deemed important, regardless of some being weighed higher than others. The PWC shown in Table 4 below is used to summarize all the design constraints for this project, along with their weights.

Table 4: Design Constraint weights.

Goals	Money	Time	CS Chemical Compatibility	CS Biocompatibility	Material Availability	Equipment Availability	Intellectual Resource Availability	Total
Money		1	1	1	1	1	1	**6**
Time	0		1	1	1	1	1	**5**
CS Chemical Compatibility	0	0		½	0	½	0	**1**
CS Biocompatibility	0	0	½		0	½	0	**1**
Material Availability	0	0	1	1		1	0	**3**
Equipment Availability	0	0	½	½	0		0	**1**
Intellectual Resource Availability	0	0	1	1	1	1		**4**

Through this PWC, we found money to be the most important design constraint, with a weight of 6. Time was found to be the second most important constraint with a weight of 5. The third ranked design constraint was intellectual resource availability with a weight of 4, the fourth being material availability with a weight of 3. Lastly, CS chemical compatibility, CS biocompatibility, and equipment availability were found to be of equal importance, each having a weight of 1.

As seen in the PWC above, money is one of the largest constraints for the project since the WPI Biomedical Engineering Department grants each team member $250 per MQP project, which allows for a total budget of $1000. This influences experimentation since outside sources, such as materials (i.e., PEG), must be purchased, causing each purchase made to be well thought out and deemed necessary. The next important design constraint is time since all the project deliverables must be completed by the required deadline of April 21, 2023, which is Project Presentation Day. The WPI school year spans from the end of August to the beginning of May, which gives the team eight months to complete all the required deliverables. The next design constraint is intellectual resource availability. The project team must be able to intellectually research, support, and complete the design process given the equipment and material constraints stated before. The next design constraint is material availability; materials that are necessary for

the project must be bought at a reasonable cost, within the budget, and in a timely fashion. The materials must be purchased, shipped, and received in a manner that allows for the project team to utilize it when needed. The next design constraint is CS chemical compatibility. CS must be able to covalently bond to adjacent molecules in the project design to achieve a copolymer network and this network is what will be used to create the hydrogel. The next design constraint is CS biocompatibility. CS must be biocompatible in the body and not elicit an autoimmune response within the project design to meet the goals stated in our client statement. The final design constraint is equipment availability. The team can only perform experiments that are possible to complete with lab equipment that is available for use at sanctioned WPI laboratory spaces.

3.3 Design Specifications

To meet the specified objectives and constraints in the previous section, the team had identified a list of six design specifications that will be considered during the various stages of this project. These specifications can be seen in Table 5 below.

Table 5: Design Attribute/Function and Associated Specifications.

Attribute/Function	Specification
Reproducibility	Hydrogel injection must produce a consistent product through each batch. The drug binding and drug loading must be quantifiable and repeatable within 5% variability between batches.
Injectability	Extrusion of the hydrogen through a 28-gauge needle must not go above a maximum force of 38 N.
Sustained Release	Must allow for daunorubicin release for at least 21 days.
Content Uniformity	The drug loading must be persistent throughout the entire hydrogel network.
Water-insoluble	Hydrogel network must maintain insolubility for a minimum of 21 days to allow for the sustained release of the drug.

Using these design specifications, the team developed a PWC to weigh out the significance of each design which would further determine our timeline and plan for the project.

All design specifications shall be met, regardless of their weight. Table 6 outlines the design specifications with their weights and was created to assist in the project planning process.

Table 6: Design Specifications Weights.

Specification	Reproducibility	Injectability	Sustained Release	Content Uniformity	Water-insoluble	**Total**
Reproducibility		1	1	1	1	**4**
Injectability	0		1	1	0	**2**
Sustained Release	0	0		½	0	**0.5**
Content Uniformity	0	0	½		0	**0.5**
Water-insoluble	0	1	1	1		**3**

Based on Table 6, reproducibility had the highest weight of 4. The second largest weighted specification was water-insolubility at 3. Next was injectability with a weight of 2. The content uniformity obtained a weight of 0.5, along with content uniformity that obtained a weight of 0.5. Just to reiterate, all design specifications are important and will be addressed in the completion of this project.

3.3.1 Specification 1: Reproducibility

The first design specification is reproducibility which entails being able to reproduce formulations, fabrications, testing, and results with minimal to no error. To address this specification, the team will create Standard Operating Procedures (SOPs). These SOPs will contain the necessary information needed for anyone to reproduce the work for any potential future applications.

3.3.2 Specification 2: Injectability

The second design specification the team will investigate is obtaining a max injection force of 38 N through a 28-gauge needle with a volume of 0.5 mL and needle length of 0.5 in. To verify this, the team will perform Instron mechanical testing where a force will be applied to a syringe connected to a needle with these desired specifications, and the force it took for the hydrogel to be pushed through the needle will be observed.

3.3.3 Specification 3: Sustained Release

The third design specification is obtaining a sustained drug release profile of about 21-28 days. This is important to achieve because chemotherapeutic agents are inherently cytotoxic, so allowing the drug in the site for an extended period may cause damage to the surrounding cells/tissues, and if the drug elutes too fast then this can also cause damage. As mentioned in the previous chapter, most chemotherapeutic drugs are on a 21-28 to day cycle. For this reason, the team will perform a drug release study to determine how much drug is eluting from the hydrogel over time.

3.3.4 Specification 4: Content Uniformity

The fourth design specification is maintaining content uniformity throughout the hydrogel. This is essential in maintaining a consistent drug to polymer ratio throughout the hydrogel network. If DNR is not uniformly distributed throughout the hydrogel, then the cytotoxicity of the drug upon release from the network may be at higher levels, thus causing damage to the surrounding cells/tissues. For this reason, the team will perform a drug loading study to ensure the ratio of drug to polymer in each formulation is the same.

3.3.5 Specification 5: Water-Insoluble

The fifth design specification the team will consider is water insolubility. Hydrogels need to be water-insoluble to carry a drug load to a site without dissolution and disintegration. For this reason, the team will formulate an insoluble copolymerized PEG-CS hydrogel that will not dissolve upon contact with water. To test the solubility properties of the hydrogel, it will be suspended in buffer and analyzed over time to determine if the hydrogel structure is still present or dissolved.

3.4 Design Standard Requirements

Throughout this section, relevant standards and regulations that will be used for project planning and the final design process are outlined. The categories for these standards include material characteristics, mechanical testing, cytotoxicity testing, and sterility testing. These standards are outlined in Table 7 below.

Table 7: Standards for design requirements.

Category	Standard	Title	Purpose
Material Characteristics	ASTM D445-21	Standard Test Method for Kinematic Viscosity of Transparent and Opaque Liquids	This test method specifies the necessary procedures and calculations for determining material viscosity of transparent liquids
Mechanical Testing	ISO 11608-6:2022(en)	Needle-Based Injection Systems for Medical Use	This testing method will validate the process of the intratumoral needle-based drug delivery system.
	ISO 11040-8	Syringe Testing on Prefilled Syringes	Prefilled syringes are to be met with the following required safety, functionality, and quality standards.
Cytotoxicity Testing	ISO 10993-11	Biological Evaluation of Medical Devices: Testing for Systemic Toxicity	This standard test quantifies the potential systemic toxicity from the medical device.

	ISO 10993-17	Biological Evaluation of Medical Devices: Establishment of Allowable Limits for Leachable Substances	This standard will be used to quantify the leaching ability of substances being used within the drug delivery system and ensuring that it is below the standard.
	ISO 10993-20	Biological Evaluation of Medical Devices: Principles and Methods for Immunotoxicology	This standard is used to ensure that biomedical devices will have a non-immunogenic response on the body.
Sterility Testing	ISO 11737-2	Sterilization of Health Care Products: Microbiology Methods	For microbiology methods, this standard test is performed to validate sterility of the medical device.

3.5 Revised Client Statement

After taking into consideration these design constraints and specifications, we were able to develop a revised and more in-depth client statement:

"To develop a fabrication technique to obtain a water-insoluble, injectable chondroitin sulfate – polyethylene glycol copolymerized hydrogel network loaded with daunorubicin to achieve a 21-28 day sustained release profile"

3.6 Project Approach

3.6.1 Project Work Completed in A-term (Aug-Oct 2022)

From September to October 2022, the team began the project by delving into research for the design as well as creating goals and requirements. The research is illustrated in the form of a literature review, where the problem is assessed, following the current state of treatment, and the state-of-the-art technology in the field. The purpose of the literature review is to be able to understand the significance of the project as well as contextualize the technology that will be used. Further, the team completed creating a client statement that can summarize the goal. This is supported by defined design requirements, constraints, and overall approach on a term basis. This project approach will also be supported by a timeline of the goals in form of a Gannt Chart, keeping the team on track (Appendix A).

3.6.2 Project Work to be Completed in B-term (Oct-Dec 2022)

In B-term, the team will fabricate different proposed models of hydrogels. These models will have different concentrations as well as different functionalization methods in efforts to propose the best possible design for the requirements developed. These models will also be subjected to injection force testing and gelation procedures to help propose the most sensible design.

3.6.3 Project Work to be Completed in C-term (Jan-Mar 2022)

During C-term, the team will carry out a 30-day drug loading and release study due to the 21–28-day drug release profile. The hydrogels being tested will be the best fitting models based on results in B term. Following this, injection force testing will be done on the unloaded hydrogels, and then the drug loaded hydrogels. The swelling assay will also be applied on the chosen hydrogel models.

3.6.4 Project Work to be Completed in D-term

In D-term, the team will keep moving forward with testing and refining the synthesis of the drug delivery system to be as close to the created design requirements as possible. This will also include refining and finalizing the final report and final presentation towards the end of the term.

IV. Design Process

4.1 Needs Analysis

For this project, the main needs for the design are to create an injectable hydrogel with drug delivery system properties and market scalability. For the needs identified, they will be met through qualitative and quantitative testing of the prototypes created to ensure that the drug delivery system is adequate. The needs are described in Table 8 as main objectives, further defined through multiple sub objectives. Refer to Table 2 for a pairwise comparison chart comparing these design needs and their weights. The team took the top six weighted sub objectives and decided that the other four were wants instead of needs. This means that although it is a goal for the project, the needs are more important as they define the projects' success. In addition, these decided needs were then weighted by adding up the score of the chosen needs from the pairwise comparison chart, and then dividing the individual scores by the sum, giving us percentages. These sub objectives will act as checkpoints for each of the objectives, ensuring that the product will return successful. Injectable hydrogel includes the need to have a low injection force, and reproducible injectability. Drug delivery system properties require the system to have a sustained drug release profile and water insolubility. Market scalability includes having an effective procedure. Each of these sub-objectives will ensure that the needs for the product have been fulfilled.

Table 8: Objectives and sub-objectives ranked.

Main Objective	Sub- Objective	Percentage
Injectable Hydrogel	Low Injection Force	16%
	Reproducible Injectability	13%
	Reproducible Gelation Time and Process	[redacted]
	Maintains Content Uniformity through Injection	
Drug Delivery System Properties	Sustained Drug Release Profile	10%
	Water Insoluble	24%

Market Scalability	Safe to Handle	[redacted]
	Effective Procedure	16%
	Sterilization	[redacted]

4.2 Concept Map

When considering the use of hydrogels for a DDS, it is important to consider a multitude of factors to create an effective hydrogel that achieves both the desired injection force and drug release profile for treatment of NB. For the application of this project, these factors have been outlined in Figure 24. Although the following concept map was aligned with the goals of our project design, the factors can be considered and applied to other injectable hydrogel-based DDS. With the initial client statement specifying the need to use hydrogels as the vehicle to deliver the therapeutic agent, the team had to first consider how to fabricate the polymer network. Since the crosslinks formed between molecules in the hydrogel network are dependent on the molecular chemistry of the polymers involved, the team had to consider what materials would be needed to obtain the final hydrogel design. The team knew that CS had to be a component of the hydrogel design, but the team decided to investigate other polymers to see whether it be advantageous to have a multi-component polymer network that could create a more desirable release profile when loaded with DNR. After deciding on what materials would be used, it was vital to determine how these materials would react with each other to form the hydrogel. The team would need to consider both the ratios of the reagents used in the reaction, as well as how these ratios would affect the overall profile of the gel, since different polymer chemistries can affect the mechanical and chemical integrity of hydrogels. These two sub-factors would in turn help establish a reproducible gelation procedure that could be used for the future. Once a gelation procedure for the desired formulations had been established, the team could then proceed with fabrication and perform the reaction. Following the conclusion of the reaction and formation of the hydrogels, the gelation properties would be analyzed to ensure that crosslinking occurred and that the polymer chemistries were compatible in creating a gel. Injection force testing would be performed using an Instron machine to collect quantitative data for analysis. Once the team verified that the gel upholds the structural integrity needed for injection, the hydrogel would be loaded with DNR, and the release profile of drug *in vitro* would be analyzed.

This is to ensure that the desired hydrogel meets the target release profile as stated in the client statement. With these factors in place, an injectable CS-based hydrogel loaded with chemotherapeutic agent, DNR, can be fabricated for drug delivery applications.

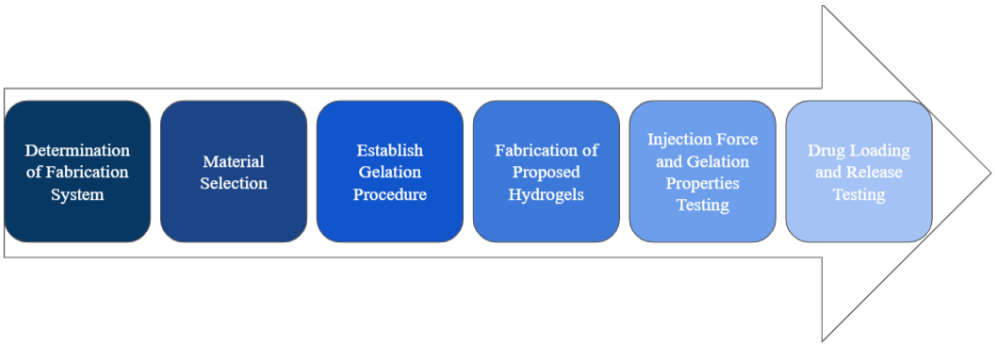

Figure 24: Conceptual map for the injectable CS-based hydrogel DDS.

4.3 Alternative Design Approaches

Below are the three designs considered to make an injectable CS based hydrogel. The three designs that were considered were PEG-MI/CS-F, PEG-NB/CS-T, and PEG–$(NH_2)_6$/CS-NHS.

4.3.1 PEG-MI/ CS-F Hydrogel

CS-F with PEG Maleimide (PEG-MI) creates a cross linked hydrogel. To create this hydrogel, CS would have to be functionalized by furan and react with the PEG-MI through click chemistry. Since click chemistry is being utilized, this reaction will have a high yield, high specificity, and not a lot of side products, making it simple to handle and replicate. Additionally, Furan functionalization can take place quickly and in temperatures ranging from 35 °C to 80 °C making it very versatile and easy to use (Gevrek & Sanyal, 2021). **There is not much prior research on CS-F formulated hydrogels, for drug delivery.** Furan and its corresponding PEG-MI are both cheap and easy to secure (Furan: $35 for 5 g PEG-MI).

4.3.2 PEG-NB/ CS-T Hydrogel

CS-Tetrazine (CS-T) with PEG-Norbornene (PEG-NB) is another option for a click chemistry-based hydrogel. Tetrazine is an alternative functional group, with PEG – Norbornene being its corresponding group. Tetrazine is a biocompatible functionalizer that has high stability in wet conditions and was found to be nontoxic to cells. This formulation has a very low gelation time (within minutes). Like the Furan functionalized hydrogel, the reaction is also highly

specific, high yields and not much by product. These gels are also extremely modifiable through changes in arms of peg, molecular weight, and size of polymer (Sousa et al., 2022). However, this formulation is unfeasible due to PEG-NB being expensive ($267 for 1 g).

4.3.3 PEG−(NH2)6/ CS-NHS Hydrogel

The third formulation that was researched was CS-NHS hydrogel. Unlike the other two formulations this formulation uses carbodiimide chemistry instead of click chemistry. Like the click chemistry reactions, CS is functionalized by NHS in order to create carboxylates to bond with peg. Research has shown that carbodiimide chemistry is less efficient in creating cross links when compared to click chemistry. Additionally, this reaction consistently creates an isourea byproduct. Though materials are available and low cost ($50 for 25 g of NHS); however, the materials and reaction are much harder to handle since EDC and NHS are very moisture sensitive and need to be kept completely dry (Thorek et al., 2009).

4.4 Design Approach Selection

The design approaches stated in section 4.3 were compared using a design selection matrix that uses the design criteria that was stated and weighed in section 4.1. The design approach was assigned a value of 1 if the project team believed it could meet the engineering criteria, a value of 0.5 if the project team was unsure, or a value of 0 if the criteria could not be met. The values assigned for each design criteria were totaled and then multiplied by the weight for the sub-objective that was assigned in section 4.1. The total score for each design was out of 51 points. The design selection matrix for the sub objectives can be found in Table 9, whereas the matrix for the design constraints can be found in Table 10. The total score of the design approaches is represented in Table 11.

Table 9: Design selection matrix for the design sub-objectives.

Sub Objective		PEG-MI/CS-F Hydrogel	PEG-NB/CS-T Hydrogel	PEG-(NH2)6/*CS-NHS* Hydrogel
Injectable Hydrogel	**Low Injection Force**	1	½	½
	Reproducible Injectability	1	½	½
	Reproducible Gelation Time & Process	½	1	½
	Maintain Content Uniformity through Injection	1	1	½
DDS Properties	**Sustained Drug Release Profile**	1	1	1
	Water Insolubility	1	1	1
	Degradation Time Profile	1	½	0
Market Scalability	**Safe to Handle**	1	1	0
	Effective Procedure	1	1	½
Total Score		8.5	7.5	4.5

Table 10: Design selection matrix for the design constraints.

Design Constraint	PEG-MI/CS-F Hydrogel	PEG-NB/CS-T Hydrogel	PEG-(NH2)6/*CS-NHS* Hydrogel
Cost	1	0	1
Time	1	1	1
CS Chemical Compatibility	1	1	1
CS Biocompatibility	1	1	1
Material Availability	1	0	0
Reagent Availability	1	0	1
Intellectual Resource Availability	1	1	1/2
Total Score	7	4	5.5

Table 11: Total Score of design approaches.

Design Approaches	Total Score
PEG-MI/CS-F Hydrogel	46.5
PEG-NB/CS-T Hydrogel	34.5
PEG-$(NH_2)_6$*NH26*/CS-NHS Hydrogel	30.0

The team chose to pursue design verification on the design approach with the greatest score, which was a PEG-MI/CS-F hydrogel. Creating a PEG-NB/CS-T hydrogel was also considered, however, due to the high cost and long shipping time, it was deemed unfeasible. The experimentation that the PEG-MI/CS-F hydrogel endured is outlined in Chapter 5.

V. Design Verification

5.1 Experimentation Summary

The final design formulation that the team proceeded with was the PEG-MI/CS-F formulation, as stated above. This formulation's materials adhered to the price constraints, ease of handling, and aligned with the needs of the project. The fabrication procedure was adapted from a procedure previously used to create hyaluronic acid (HA) hydrogels. The weights and disaccharide units were converted to make up for the difference between molecular weight of HA and CS. Once the proposed hydrogel fabrication procedure could be executed, the team could then proceed with testing.

The first objective was to figure out the reaction scheme. Variables like CS, DMTMM, and furan concentration can be adjusted to create CS-F with differing furan content, which would ultimately result in hydrogels with different properties. Ideally, the functionalization of CS with furan should be 100% as this would allow for more site for crosslinks to form when reacted with the PEG-MI during the gelation process; therefore, the team considered a variety of reaction schemes to determine which provided the greatest amount of functionalization. The functionalization was then verified using Proton Nuclear Magnetic Resonance (NMR) Spectroscopy.

After deciding on which reaction scheme to proceed with, the PEG-MI/CS-F hydrogel characteristics were studied. This was done through swelling assays and degradation assays. For the swelling assay, the hydrogels were submerged in phosphate buffer solution (PBS) and wet weight gel measurements were studied over a period of 28 days. For degradation, hydrogels were submerged in PBS then washed with MilliQ water and lyophilized to obtain the dry weight gel measurements.

The drug release profiles were quantified using UV-Vis spectrophotometry. Several serial dilutions with DNR and standard curves were made to relate absorbance to concentration of drug in PBS. The drug release study was also run for 28 days to understand how the gel released drug.

Injection force testing was done to ensure that the maximum of 38N was not exceeded. Hydrogels that were both loaded and not loaded with drug were transferred into Insulin syringes

with a 28-gauge, 0.5 mL volume capacity, and 0.5 in needle size. These syringes were then placed into the Instron to measure the amount of force required to push the gel out of the syringe.

5.1.1 PEG-MI/CS-F Hydrogel Fabrication

Figure 25 shows the process in which the team used to create the PEG-MI/CS-F hydrogels for the various tests that will be described throughout this section. To start, the team diluted the available MES buffer solution, down from 500 mM to an 83.33 mM concentration, which would be used as the solvent in the subsequent steps. Next, 0.485 g of CS was added 40 mL of MES buffer in a round bottom flask with constant stirring on a magnetic stir plate until fully dissolved. Once CS had been dissolved, 1.1214 g of DMTMM was added. After 10 minutes of mixing, 188.8 µL of furan was added dropwise. The flask was then capped with a rubber stopper and the solution was set to react for 24 h to allow for the attachment of furan to CS. This step is known as the chemical modification step, which creates the furan modified CS component of the hydrogel, which will be referred to as CS-F. After 24 h, the solution was then transferred into dialysis tubing and purified for 72 h. Water baths changes were done at 1, 3 and 5 h post-start of dialysis on day 1. For days 2 and 3, water bath changes were done in the morning, afternoon, and evening. At the end of the 72 h, the solution was taken out of the tubing and transferred into centrifuge tubes with no more than 30 mL of solution per tube. These tubes were then frozen before being lyophilized for 72 h. The lyophilized CS-F and PEG-MI were dissolved in MES buffer separately and then combined and vortexed until mixed thoroughly. The mixed solution is then pipetted onto a glass slide lined with parafilm for easier handling after gelling. The PEG-MI/CS-F solution was then allowed to gel over 24 h and checked with a pipette tip to check whether the solution was still in a liquid state. Formed gels were then used for tests such as swelling, degradation, drug loading and release, as well as injection force.

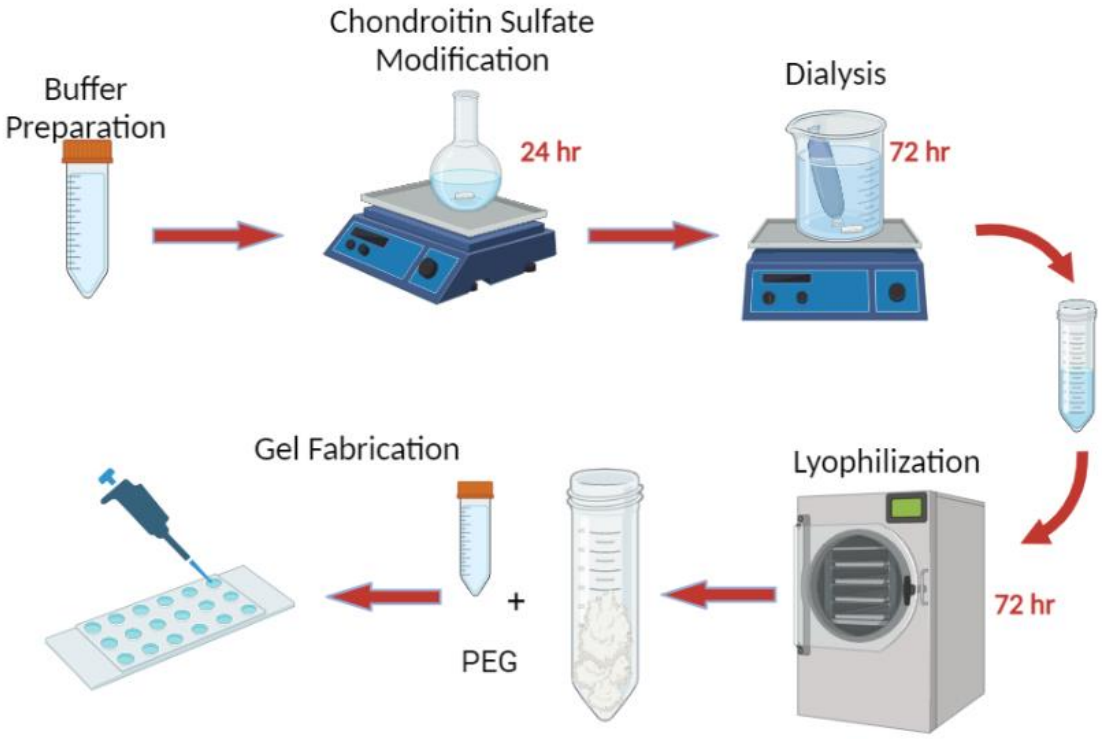

Figure 25: Process of hydrogel fabrication from start to finish.

5.1.1.1 NMR Sample Preparation

As mentioned previously, NMR was chosen to assess the CS-F functionalization and to do this, 60 µg of lyophilized CS-F was dissolved in 600 µL of D2O in a 2 mL centrifuge tube and then vortexed until the solution was homogenous. Once the solution had been mixed thoroughly with no clumps of CS-F suspended, the solution was transferred into NMR tubes and a peak analysis was done via Proton NMR Spectroscopy to identify the rate of modification. A bench line of at least 85% modification was deemed desirable by the team as this would show sufficient attachment of the furan to the CS end group.

5.1.1.2 Fabrication Method Modifications

Before getting to the final fabrication method for the PEG-MI/CS-F hydrogels, the team went through 3 iterations of gelation techniques which can be seen in Figure 26 below.

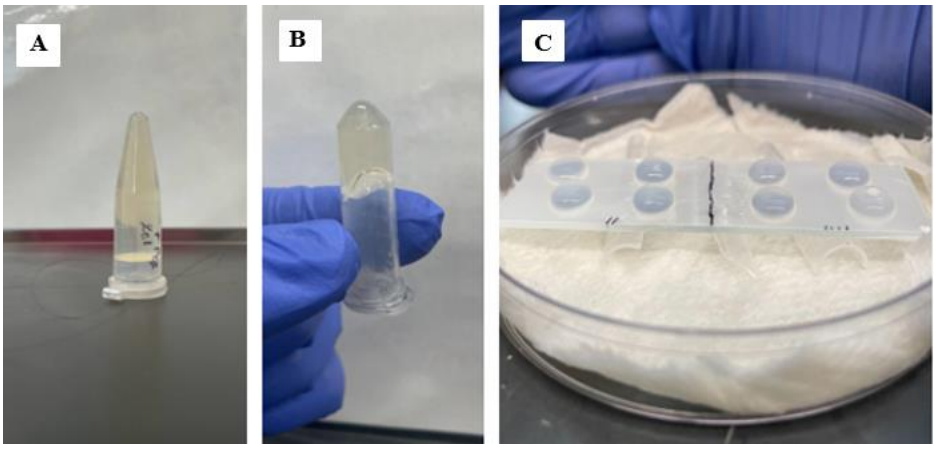

Figure 26: Modifications made to hydrogel gelation technique showing (A) gelation in a 1.5 mL centrifuge tube, (B) gelation in a 2 mL centrifuge tube, and (C) gelation in a modified humidification chamber designed by the team.

In the initial gelation process, as shown in Figure 26A, PEG-MI/CS-F solution was transferred into 1.5 mL centrifuge tubes and allowed to gel over 24 h at room temperature (68-72 °F). The tube was then inverted to see if a gel had formed. If the tube had been inverted and no solution was seen to run down the inside walls, then solution was said to be gelled. If there was solution that still moved when the tube was inverted, then the solution was allowed to sit at room temperature until gelled. Difficulties with material transfer after gelation led the team to alter the gelation technique as seen in Figure 26B, where the PEG-MI/CS-F solution was transferred into a 2 mL centrifuge tube and allowed to gel. Similar to the initial process, the gelation was checked by tube inversion and visually analyzing whether a gel had formed at the bottom of the centrifuge tube. Although this technique was an improvement on the initial iteration, a similar challenge in material transfer after gelation was seen. For this reason, the team developed a modified humidification chamber as seen in Figure 26C. In this gelation technique, the bottom of a petri dish would be lined with damp paper towels and then two micropipette tips would be laid down over the paper towels. A glass slide would then be carefully wrapped in parafilm and placed onto the micropipette tips so that it is slightly elevated. The PEG-MI/CS-F solution would then be pipetted onto the glass slide, at the desired volume per gel, with adequate space between gels. The petri dish cover was then placed back on, and the pipetted volumes would be allowed to gel at room temperature for 24 h. The gels would then be checked by removing the cover of the petri dish and gently tapping them with a pipette tip to see whether there is any residual

solution stuck to the pipette tip. If nothing sticks to the pipette tip, then the solution had gelled. If there was any solution on the pipette tip then it would be allowed to sit until fully gelled.

5.1.2 Injection Force Testing

For injection force testing, 50 µL hydrogels were pushed into a 0.5 mL volume and 0.5 in needle size insulin syringe with a 28-gauge needle. The team tested linear homo-bifunctional PEG and tetra homofunctional PEG with and without drug. 3 gels were tested for each individual parameter, the results were then averaged and graphed. The injection force required to extrude water from the syringe was used as a control. Overall, the injection forces of the hydrogels are very low, making them easily injectable. In Figure 27 below, the apparatus created within the Instron machine for injection force testing is shown.

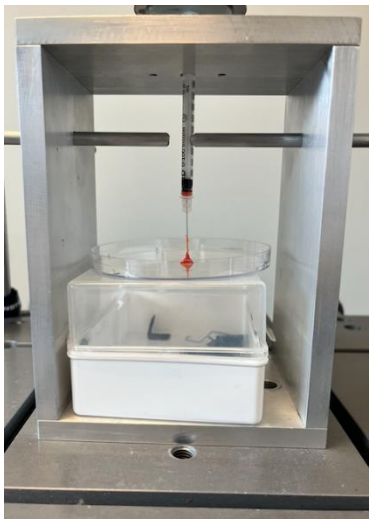

Figure 27: Apparatus of the injection force testing of the tetra PEG hydrogel loaded with DNR being pushed out of the syringe onto a Petri dish.

5.1.3 Swelling Assay

To test swelling, 20 µL hydrogels were weighed and placed in 1 mL of PBS (pH 7.4). The weight of the hydrogel was calculated using Equation 1. Before the weight of the hydrogel was measured, the entire volume of PBS solution was removed; 1 mL of fresh PBS was added after the weighing process was over. The amount of swell was evaluated at regular intervals.

[weight of hydrogel in microcentrifuge tube (g) - weight of empty microcentrifuge tube (g)] = weight of hydrogel (g) **(Equation 1)**

5.1.3.1 Hydrogel Visual Analysis

The hydrogels were characterized on a scale of 1 to 4, with 1 being an exploded gel that could barely be visually spotted when moving around the solution, and 4 being a fully uniform hydrogel. The uniformity of the gel was evaluated at regular intervals. Throughout this study, the hydrogel remained consistent and there did not appear to be any significant swelling. Most, if not all, of the hydrogels stayed as a 4 throughout this study. Figure 28 shows an example of how each scale would look visually; however, the pictures were taken using drug loaded samples so that the hydrogel could be seen since the swelling samples were without drug and translucent.

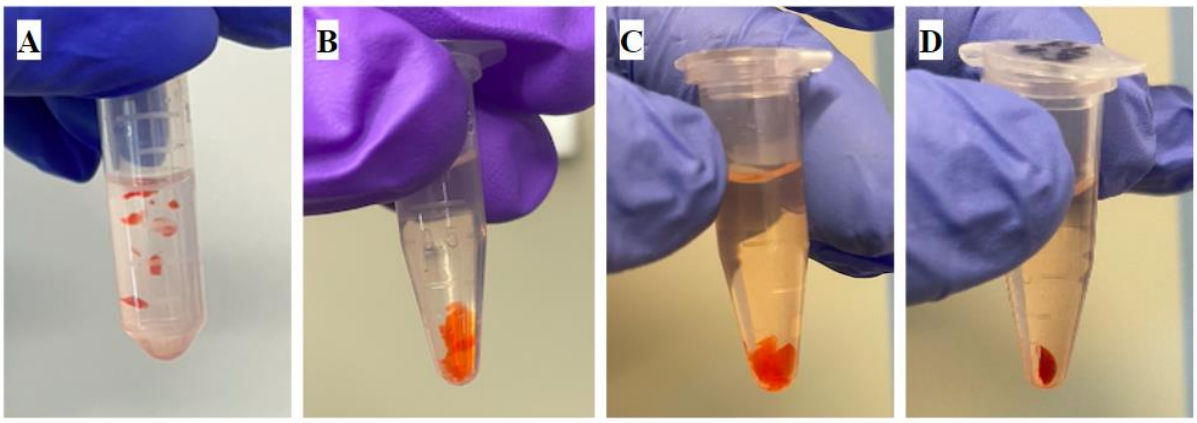

Figure 28: 20 µL hydrogels loaded with DNR in PBS at different stages of visual analysis with (A) being a 1 on the scale, (B) being a 2 on the scale, (C) being a 3 on the scale, and (D) being a 4 on the scale.

As stated before, Figure 28 was used as a scale to measure all the swelled hydrogels against, as a way of visual analysis. Since all the hydrogels remained at a 4, it was concluded that the hydrogels remained uniform throughout the study, were water insoluble, and were able to maintain structural integrity over time in an aqueous environment.

5.1.4 Drug Loading Assay

Drug loading was done using two methods, pre-loading and post-loading. The pre-loading method attempted to have the hydrogel form a gel around the drug. To do this, the 2-MES buffer was switched out for water, which eliminates potential side reactions from the drug. This method of post loading is outlined in Figure 29; however, it was not used again since when this was attempted, the preloaded sample solution did not gel.

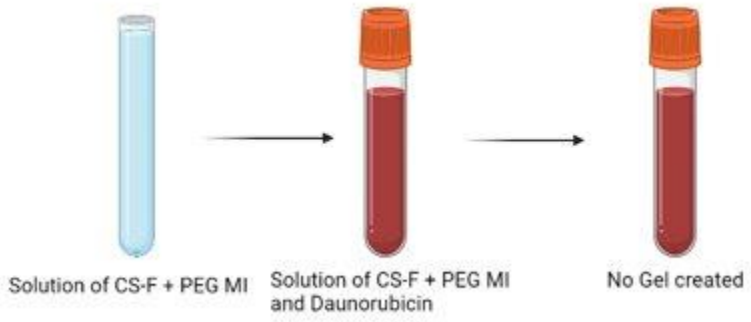

Figure 29: Schematic of pre-loading gels.

For post-loading, 50 µL gels were put into 2 mL centrifuge tubes with 1 mL of 200 µg/mL of drug solution. These gels were loaded with drug for 48 h and could be seen when the gel turned orange/red. This method is outlined in Figure 30, as seen below.

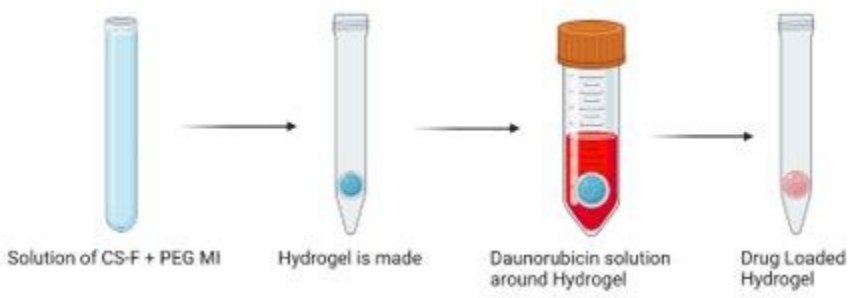

Figure 30: Schematic of post-loading hydrogels.

After each gel was loaded with drug, the supernatant was taken out and ran through the UV/Vis spectrophotometer to determine the concentration of drug in the gel. The drug concentration was determined using a standard curve of DNR as shown in Figure 31.

The standard curve was created by doing serial dilutions. 7, 2 mL centrifuge tubes were set up with 500 µL of water. 1 centrifuge tube had 1 mL of 200 µg/mL DNR solution. A serial dilution was then done starting with this concentration. 500 µL of the 200 µg/mL was taken and put into a tube of 500 µL of water. Then 500 mL of the new solution was taken and put into the next 500 µL of water. The absorbances of each sample were taken through the UV/Vis Spectrophotometer.

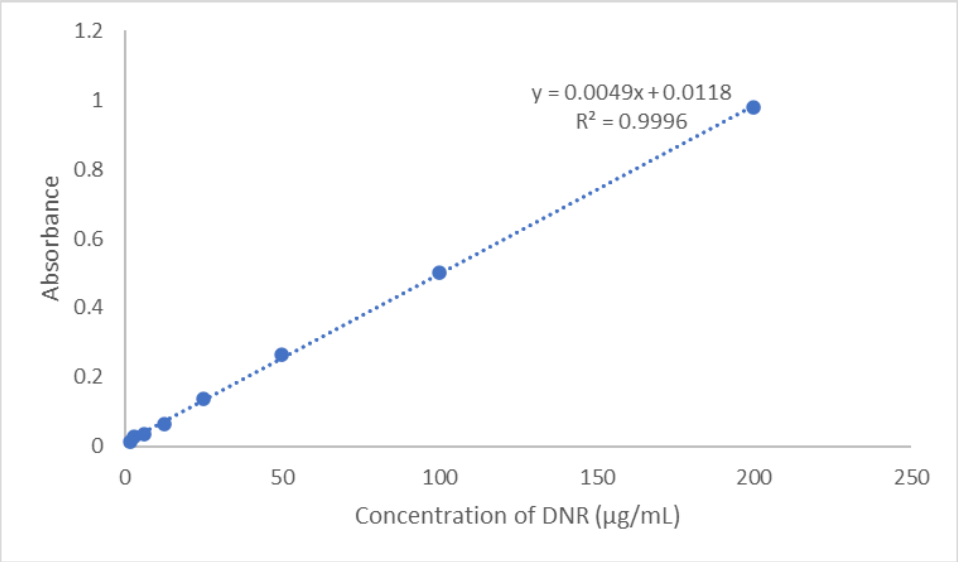

Figure 31: DNR concentration standard curve.

5.1.5 Drug Release Assay

The hydrogels were placed in 1 mL of PBS (pH 7.4) for the drug release study and stored at 37 °C in a humid environment to mimic the human body. 200 µL of supernatant was collected to be ran through the UV/Vis spectrophotometry, which was used to evaluate the drug concentration. Data points were taken on day 0, day 1, day 2, and then every other day for two weeks, or until the drug was fully released. After 200 µL of supernatant was collected, the rest of the PBS solution was removed and replaced with fresh PBS.

To determine how the difference of PEG used in the fabrication of the hydrogel would affect drug loading, samples were made with both linear PEG and tetra PEG. The methodology for drug release studies was followed for both 20 µL linear PEG and tetra PEG hydrogels. The difference was visually confirmed due to the shape and uniformity of the hydrogel; the gel made from tetra PEG remained completely uniform and appeared as a darker orange, whereas the gel made from linear PEG appeared more spread out with a duller, more translucent orange, as shown in Figure 32.

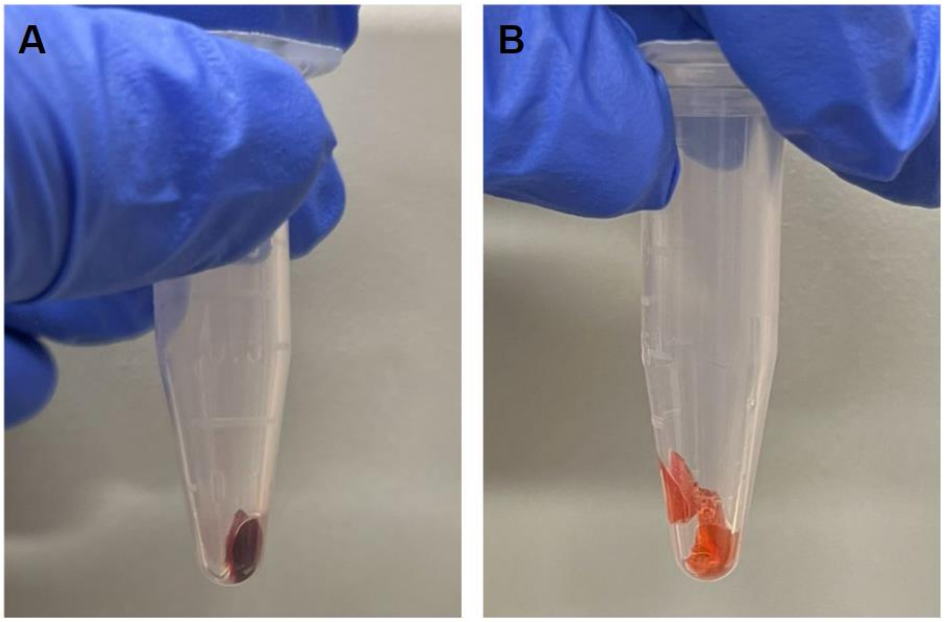

Figure 32: DNR drug loading of 20 µL hydrogels without PBS on day 8 for (A) tetra PEG-MI/CS-F and (B) linear PEG-MI/CS-F.

5.2 Design Results

5.2.1 Formulation Ratios

Through the team's design process, a variety of hydrogel formulations were developed and studied to determine which would meet the specifications and objectives as best as possible. Figure 33 displays the chemical formulation process taking part in the addition of the reagents in the steps of the process. To start, DMTMM reacts with CS to create reactive end groups to which furan can attach to when added. This in turn makes the CS a functionalized molecule that, once introduced to PEG-MI in an aqueous environment, forms crosslinks between modified PEG-MI ends groups and the now modified CS-F end groups. This reaction creates the hydrogel network, shown in Figure 33, that will be tested and analyzed further with various experiments that will be covered later.

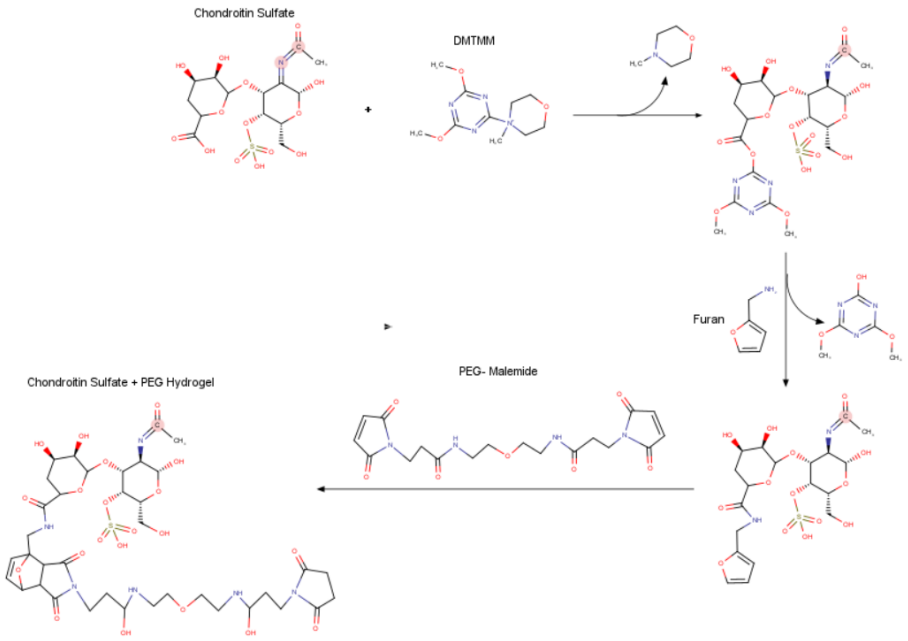

Figure 33: Chemical formulation process from chondroitin sulfate modification through PEG-MI/CS-F polymer network.

In Table 12 below, the molar ratios used in each formulation can be seen as well as the corresponding masses per reagent used.

Table 12: Summarized formulation ratios with corresponding weight measurements per reagent.

Formulation #	CS (g)	Furan (µL)	DMTMM (g)	Molar Ratio
1	0.4860	188.8	1.1315	1:2:4
2	0.4850	47.2	1.1214	1:0.5:4
3	0.4855	47.2	0.5590	1:0.5:2

4	0.4841	94.4	0.2842	1:1:1
5	0.4860	47.2	1.1300	1:0.5:4
6	0.4850	188.8	1.1337	1:2:4

Formulation 1 and 2 were repeated, as shown in the molar ratios for 5 and 6, respectively. All hydrogel formulation variations were done to determine whether a gelling reaction would occur upon contact with MES and PEG-MI. Formulation ratios in which no gelling reaction was observed were ruled out for the final testing. Molar ratios 1:2:4 as well as 1:0.5:2 created firm gels that were easy to handle whereas molar ratios 1:0.5:4 and 1:1:1 created soft gels that were delicate.

5.2.2 NMR Spectra Analysis

As mentioned in Chapter 3, one of the team's objectives was to make a hydrogel formulation that could be reproduced. This is why it was important for the team to duplicate one of the formulations and see if the NMR spectra for the corresponding formulation show a high rate of CS to furan modification. The higher the rate of modification, the greater the degree of crosslinking there will be in the hydrogel. With more crosslinks present in the polymer network, the gel is more likely to be stable and easier to handle. Figure 34 below shows the NMR spectra for an unmodified CS sample which will be used as a control (modification rate 0%).

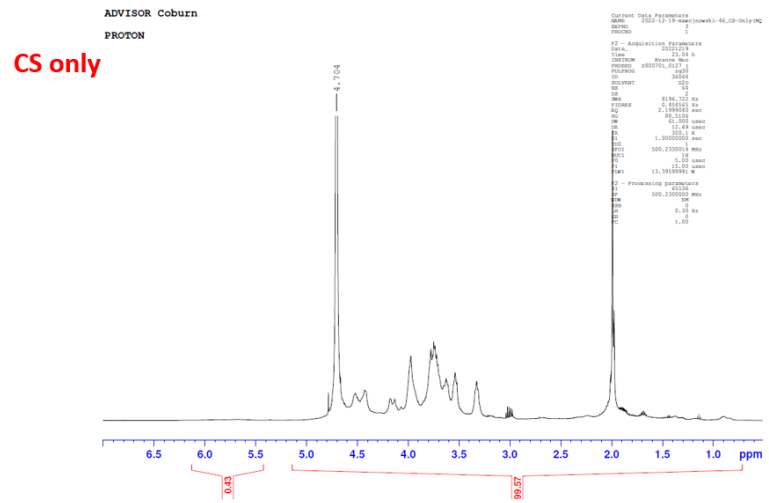

Figure 34: NMR spectra for unmodified CS.

The NMR spectra for formulation 1 was then analyzed, the modification rate based on the area under the curve was found to be 86%. The NMR spectra for formulation 1 can be seen below in Figure 35.

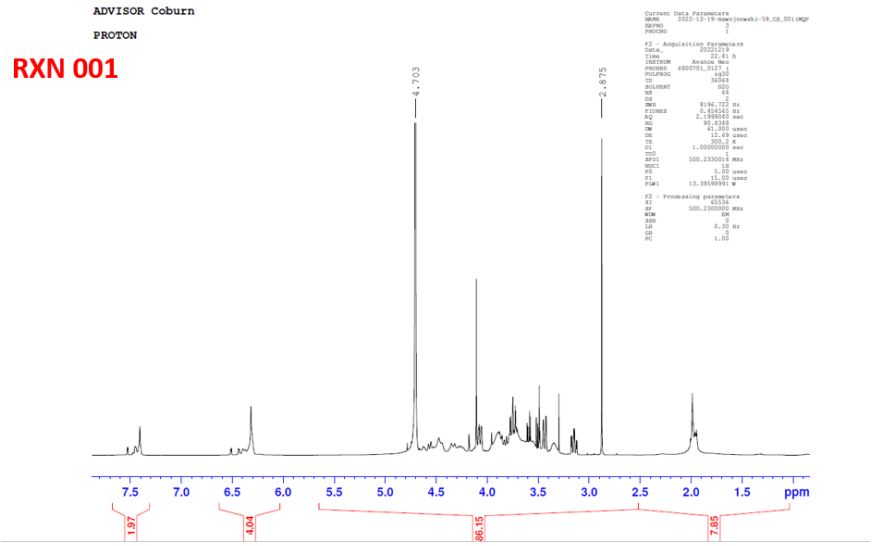

Figure 35: NMR spectra for CS-F (1:2:4 molar ratio).

The NMR spectra for formulation 2 was then analyzed and the modification rate based on the area under the curve was found to be 65%. The NMR spectra for formulation 2 can be seen below in Figure 36.

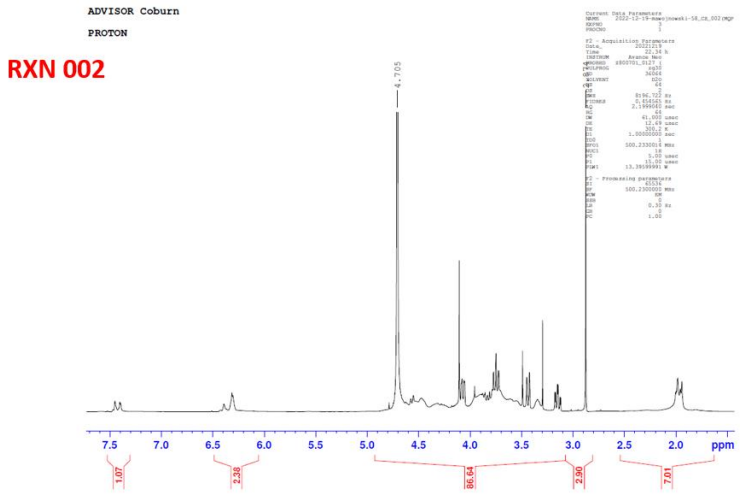

Figure 36: NMR spectra for CS-F (1:0.5:4 molar ratio).

The NMR spectra for formulation 3 was then analyzed, the modification rate based on the area under the curve was found to be 65%. The NMR spectra for formulation 3 can be seen below in Figure 37.

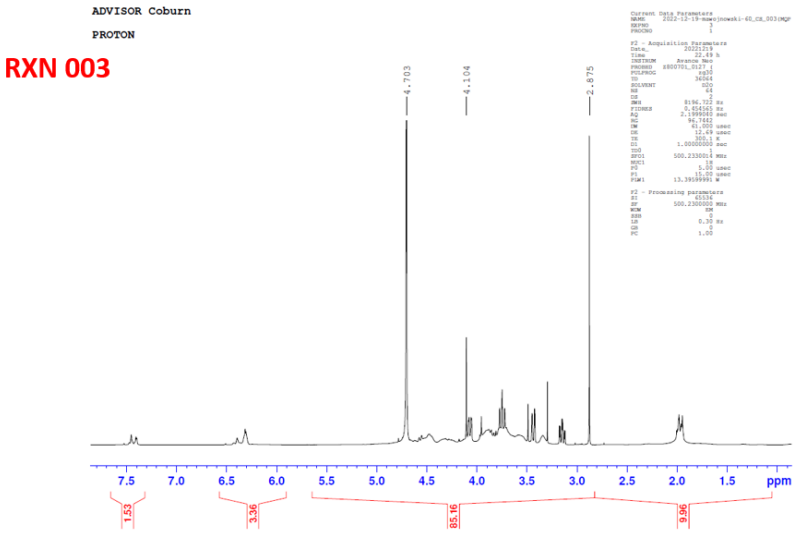

Figure 37: NMR spectra for CS-F (1:0.5:2 molar ratio).

The NMR spectra for formulation 4 was then analyzed, the modification rate based on the area under the curve was found to be 58%. The NMR spectra for formulation 4 can be seen below in Figure 38.

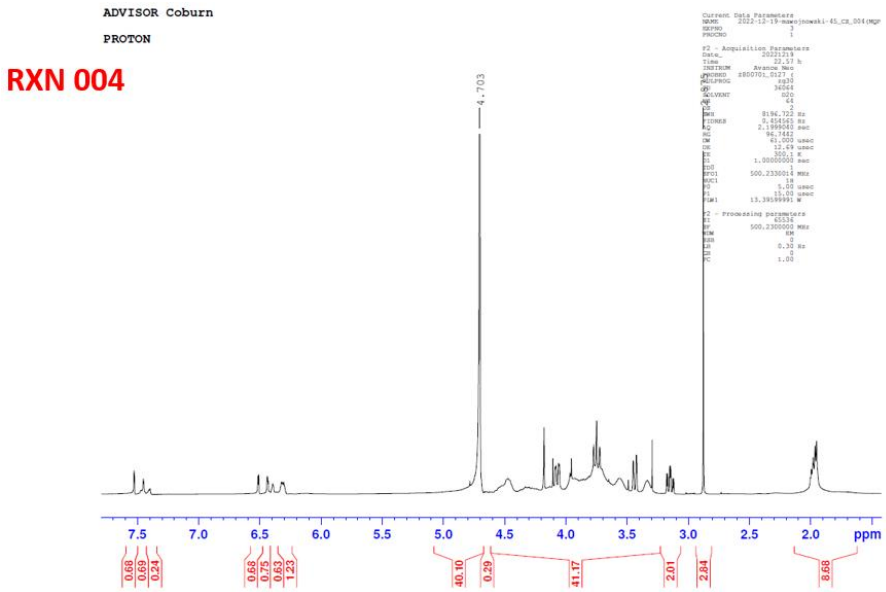

Figure 38: NMR spectra for CS-F (1:1:1 molar ratio).

The NMR spectra for formulation 5 was then analyzed, the modification rate based on the area under the curve was found to be 54%. The NMR spectra for formulation 5 can be seen below in Figure 39.

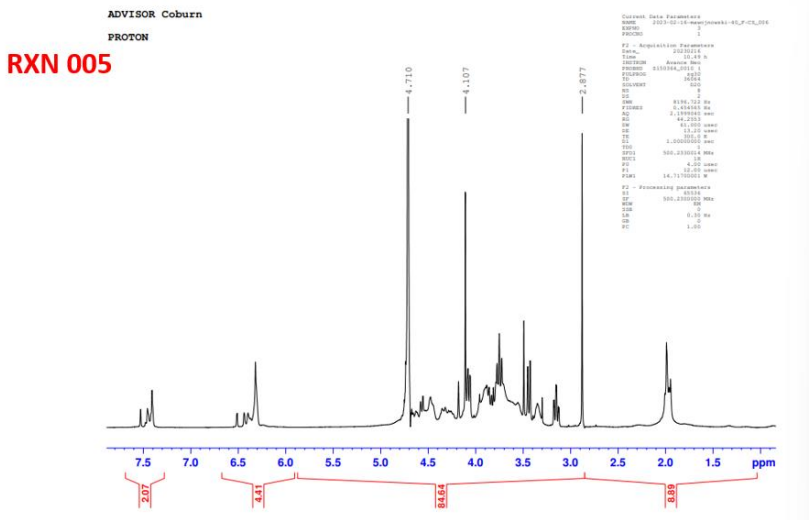

Figure 39: NMR spectra for CS-F (1:0.5:4 molar ratio) run 2.

The NMR spectra for formulation 6 was then analyzed, the modification rate based on the area under the curve was found to be 68%. The NMR spectra for formulation 6 can be seen below in Figure 40.

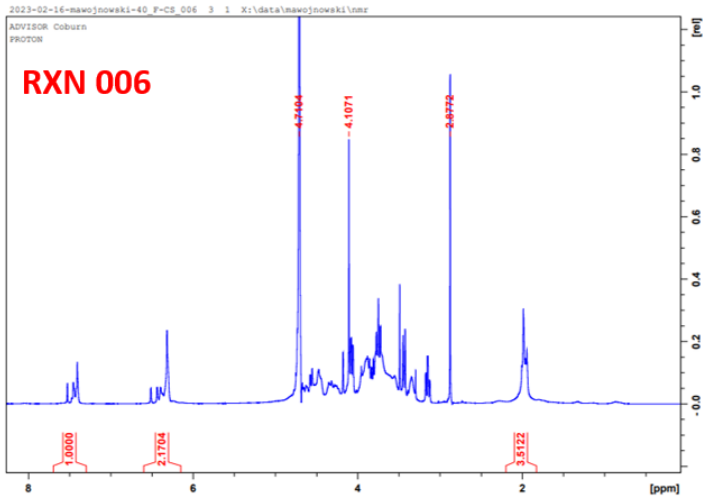

Figure 40: NMR spectra for CS-F (1:2:4 molar ratio) run 2.

Once all NMR spectra results were collected a table was created to display the corresponding formulation with the molar ratio used and the rate of modification. This data can be seen in Table 13 below.

Table 13: Summary of formulation ratios with corresponding % modification of furan to CS.

Formulation #	Molar Ratio	% Modification
1	1:2:4	86
2	1:0.5:4	65
3	1:0.5:2	58
4	1:1:1	54
5	1:0.5:4	68

6	**1:2:4**	**93**

5.2.3 Injection Force Testing

The team aimed for the injection force to be below 38 N, which was achieved throughout these tests. One challenge the team faced was the amount of air bubbles in the syringe during the testing. This caused the force readings to quickly go up and down in a drastic manner, thus leading the data to be clouded with extraneous data. Figure 41A depicts the injection force results for the non-drug loaded hydrogels, whereas Figure 41B depicts the data on the hydrogels loaded with daunorubicin.

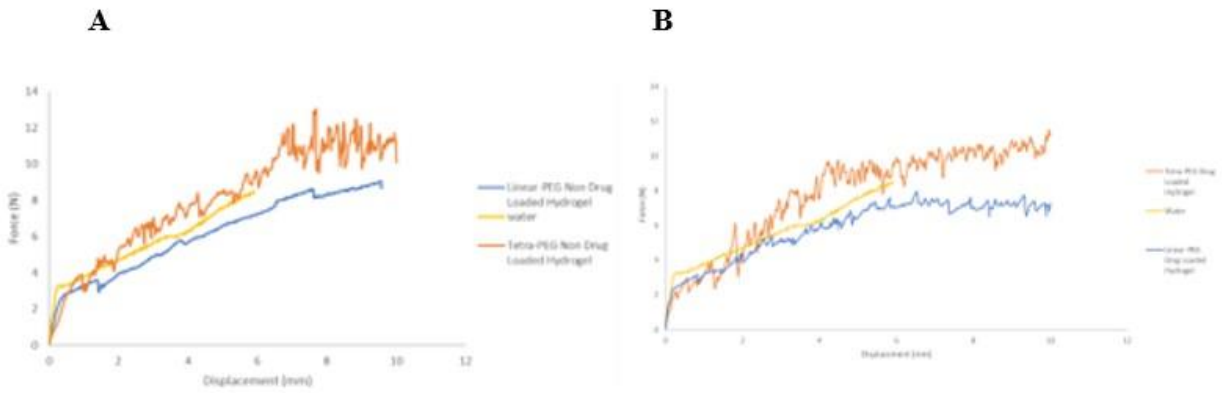

Figure 41: (A) Injection force testing data of 50 µL linear and tetra PEG-MI/CS-F hydrogels (n=3) . (B) Injection force testing data 50 µL linear and tetra PEG-MI/CS-F hydrogels post-loaded with daunorubicin (n=3).

In Table 14, the maximum injection force and average injection force were calculated using the injection force data from the different gel subjects. The average injection force was calculated from the most linear region between all the graphs, being between 5-7 mm of displacement. The tetra PEG hydrogels overall had a higher injection force than linear PEG. The team hypothesized this through visual analysis of the gels since they seemed to have a better structural integrity and were not as soft as the linear PEG hydrogels. A two-way ANOVA test was performed on the average injection forces of both PEG samples, within the linear region, for both drug-loaded and non-drug loaded samples. The results show that drug-loading does not

significantly affect the injection force. Although the different PEGs used during hydrogel fabrication did show a significant change in the injection force, with a *p-value* of 0.002. These results show that the drug did not have a significant effect on the structure of the gels, but the different PEGs did.

Table 14: Average injection force data calculated from linear region between 5-7 mm for three 50 µL linear and tetra PEG-MI/CS-F hydrogels with and without daunorubicin.

	Linear PEG w/ Drug	Tetra PEG w/ Drug	Linear PEG w/o Drug	Tetra PEG w/o Drug
Max Injection Force (N)	8 +/- 2	19 +/- 4	10 +/- 2	13 +/- 3
Average Injection Force (N)	7 +/- 0	9 +/- 1	7 +/- 0	9 +/- 1

The team executed a second study for injection force testing on drug-loaded hydrogels formulated differently with linear and tetra PEG. This round of testing used the Instron to push the gel onto a Petri dish. Following this study, the team pierced a raw chicken breast with the needle and then performed injection testing. This was done to mimic tissue to simulate the hydrogel being injected into human skin, as that is its original design. This test provided data on how the injection force would be affected from being pushed into 'phantom tissue'. Figure 42 below shows the results obtained from this test.

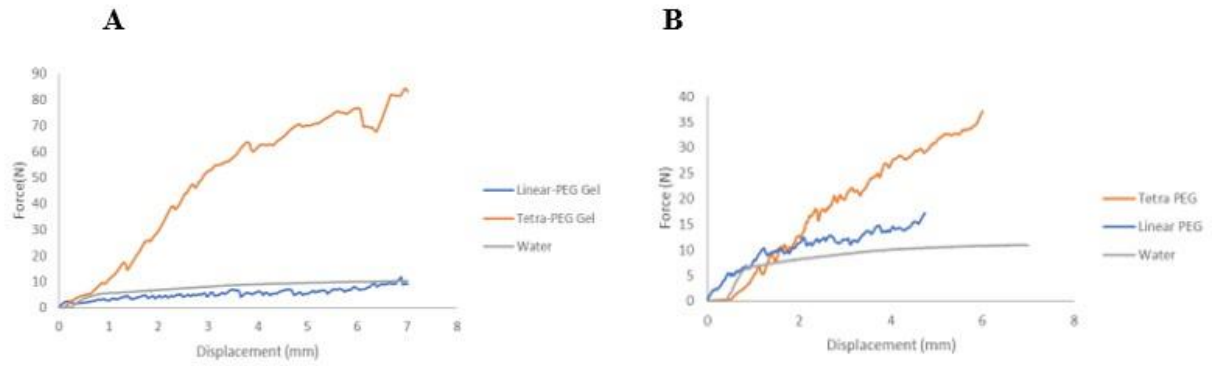

Figure 42: (A) Injection force testing data of 50 µL linear and tetra PEG-MI/CS-F hydrogels post-loaded with daunorubicin injected onto Petri dish (n=3). (B) Injection force testing data 50 µL linear and tetra PEG-MI/CS-F hydrogels post-loaded with daunorubicin.

During this second study, the team decided to prime the syringes, preemptively pushing out all extra air in the syringes prior to testing. This was done so that the air bubbles wouldn't affect the force calculated by the Instron for analysis.

Table 15 below summarizes the quantitative analysis results of the second injection force study. For this study, the most linear region in the graphs were found to be between 3-4 mm of displacement. From these areas, the average force was calculated and compared. The difference in linear region based off displacement can be accounted for by the fact that the syringes pushed down prior to testing in efforts to prime them and offset air bubbles in the results. To determine if the raw chicken breast and different PEGs used during this study showed significant changes in the injection force, a two-way ANOVA was performed. The results of the ANOVA showed that the different PEGs used during fabrication showed a significant change in force, consistent with the results of the first study. Being injected into raw chicken breast, or 'phantom tissue', did not have a significant effect on the injection force.

Table 15: Average injection force data calculated from linear region between 3-4 mm for 50 µL linear and tetra PEG-MI/CS-F hydrogels with daunorubicin injected onto a Petri dish and raw chicken breast.

	Linear PEG w/ Drug in Chicken	**Tetra PEG w/ Drug in Chicken**	**Linear PEG w/ Drug in Air**	**Tetra PEG w/ Drug in Air**
Max Injection Force (N)	17 +/- 47	47 +/- 12	12 +/- 2	84 +/- 25
Average Injection Force (N)	13 +/- 4	23 +/- 2	6 +/- 1	58 +/- 3

5.2.4 Swelling Assay

The weights of the centrifuge tubes for the respective gels were weighed prior to the gels being placed in them. The weights of only the gels were then able to be determined and were graphed against the respective time intervals. The first study below used 20 µL linear and tetra PEG hydrogels. The data was found to be inconclusive due to the high standard deviations in Figure 43 below. With the gels being extremely small, the changes in weight were too insignificant for the scale to register and there was greater chance of human error.

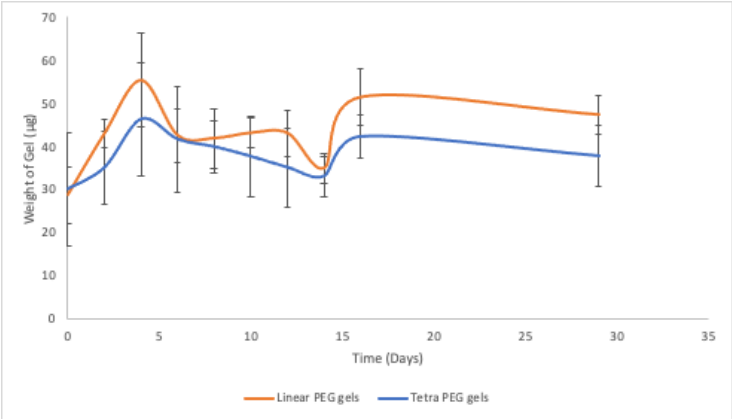

Figure 43: Swelling study of 20 µL linear and tetra PEG-MI/CS-F hydrogels in PBS (n=6).

The team decided to run another swelling study using 100 µL gels to account for the small gels in the prior study. This study was graphed in Figure 44 below. As depicted, the standard deviations were much lower, and conclusions can be made from the data. The tetra PEG gels swelled about 1.5 times their original size within the first two days, and then their liquid uptake plateaued. The linear PEG gels swelled about 2 times their original size within the first two days, then followed a similar pattern of plateau. The linear PEG gel had a higher liquid uptake than the tetra PEG gel. A one-way ANOVA test was performed on this data and showed that there was a significant difference between the swelling of the linear and tetra PEG gels.

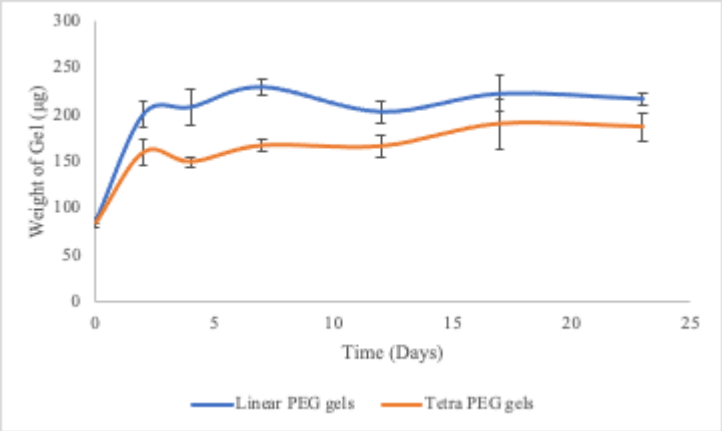

Figure 44: Swelling study of 100 µL linear and tetra PEG-MI/CS-F hydrogels in PBS (n=6).

5.2.5 Drug Loading Assay

The mass of drug loading into linear gels and tetra gels is shown in Figure 45. The figure shows that there was an average loading of 74.7 µg/mL ± 35.7µg/mL for linear PEG and that tetra PEG had an average loading of 134.5 µg/mL ± 57 µg/mL. In general tetra PEG loaded more DNR than linear. However, because the error bars were very large, accounting for almost half of the loaded drug. The t-test gave a p-value of .017. Because the p-value is less than 0.05, the test shows that the data is statistically significant of different loading profiles. Figure 46 shows a percent loading of study 1. Due to the large error in the data, a second study was done in hopes of receiving more consistent data.

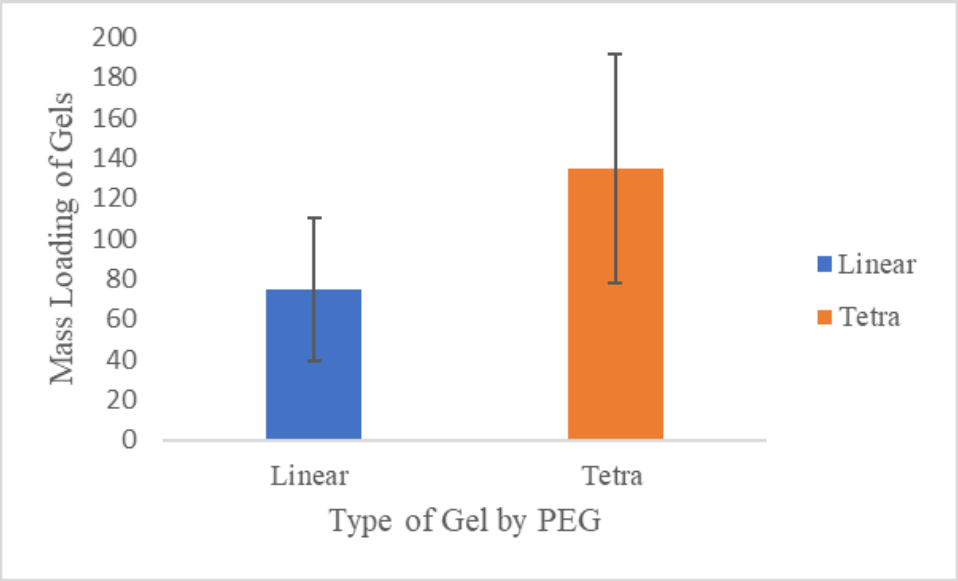

Figure 45: Mass of DNR loaded depending on PEG- Study 1. *Data is presented as mean ± standard deviation of 9 independent samples.*

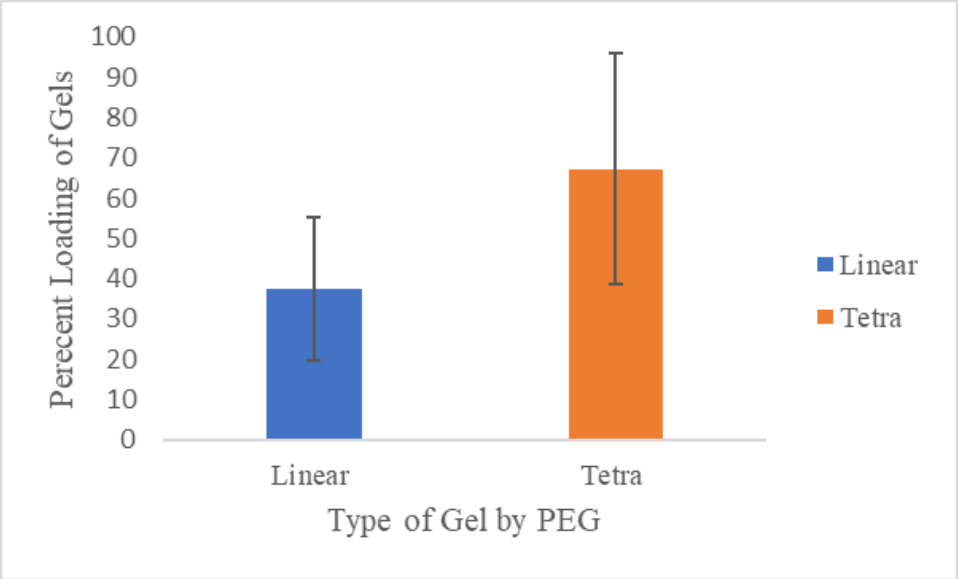

Figure 46: Percent of loaded depending on PEG- Study 1. *Data is presented as mean ± standard deviation of 9 independent samples.*

The second study to determine drug loading had much more consistent data. Error bars were much lower than the first study. The second study found that linear gels loaded an average of 77.4 µg/mL ± 2.3 µg/mL and the tetra gels loaded 172.3 µg/mL ± 20.6 µg/mL, as seen in Figure 47. The t-test gave a p value of 9.7E-05 meaning these results were statistically

significant. The tetra gels did load more than the linear gels. Percent loading graph is shown below in figure 48 for ease of analysis between both gels.

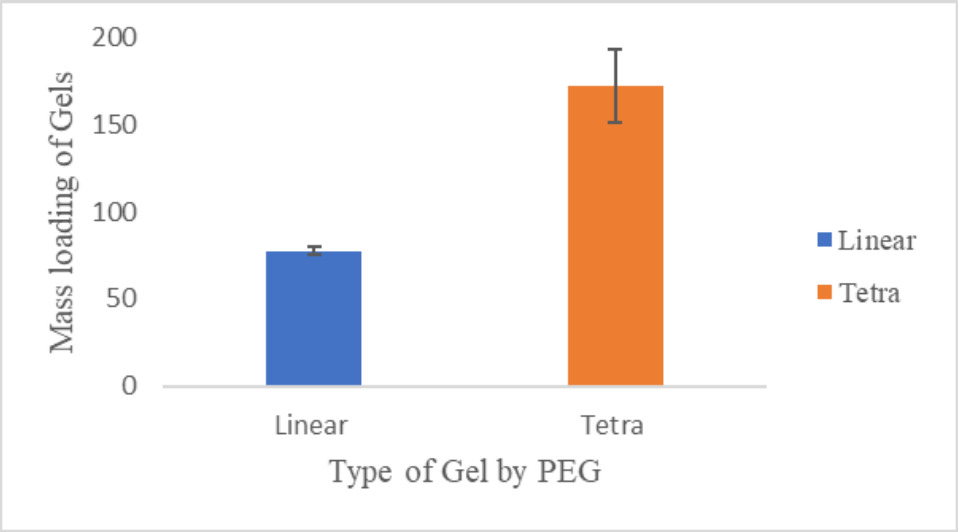

Figure 47: Mass of DNR loaded depending on PEG- Study 2. Data is presented as mean ± standard deviation of 4 independent samples.

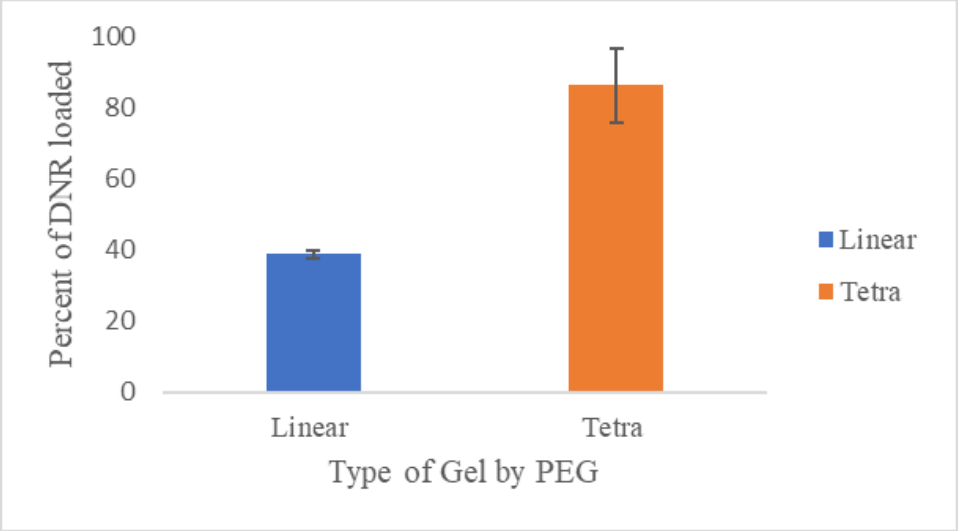

Figure 48: Percent of DNR loaded depending on PEG- Study 2. Data is presented as mean ± standard deviation of 4 independent samples.

5.2.6 Drug Release Assay

The release profile of both formulations from drug release trial 1 of the hydrogels studied is shown in Figure 49, whereas the release profile of the formulations from drug release trial 2 is shown in Figure 50. Both the 20 µL linear PEG-MI/CS-F hydrogels and tetra PEG-MI/CS-F hydrogels from trial 1, as well as the 50 µL linear PEG-MI/CS-F hydrogels and tetra PEG-MI/CS-F hydrogels from trial 2, were able to withstand the release study for 23 days without dissolving. The linear PEG hydrogels from trial 1 appeared to have a larger initial release of drug than that of the tetra PEG hydrogels, which can be seen in the first two time points in Figure 49, whereas tetra PEG appears more linear. This is due to the cumulative mass release of drug for linear PEG being greater than the cumulative mass release of tetra PEG. For trial 2, the linear PEG and tetra PEG had similar initial releases of the drug, with the cumulative mass release of tetra PEG being a bit greater than the cumulative mass release on linear PEG.

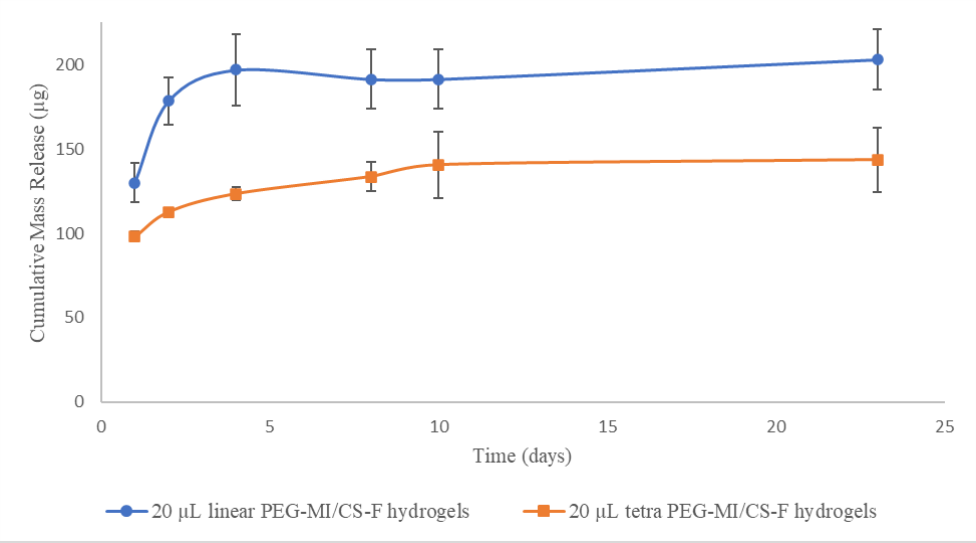

Figure 49: DNR release profile for 20 µL hydrogels fabricated from linear PEG-MI/CS-F and tetra PEG-MI/CS-F, labeled as trial 1. Cumulative mass release in µg from the hydrogels over a period of 23 days, or until the hydrogel fully release the loaded drug. Data is presented as mean ± standard deviation of 3 independent experiments.

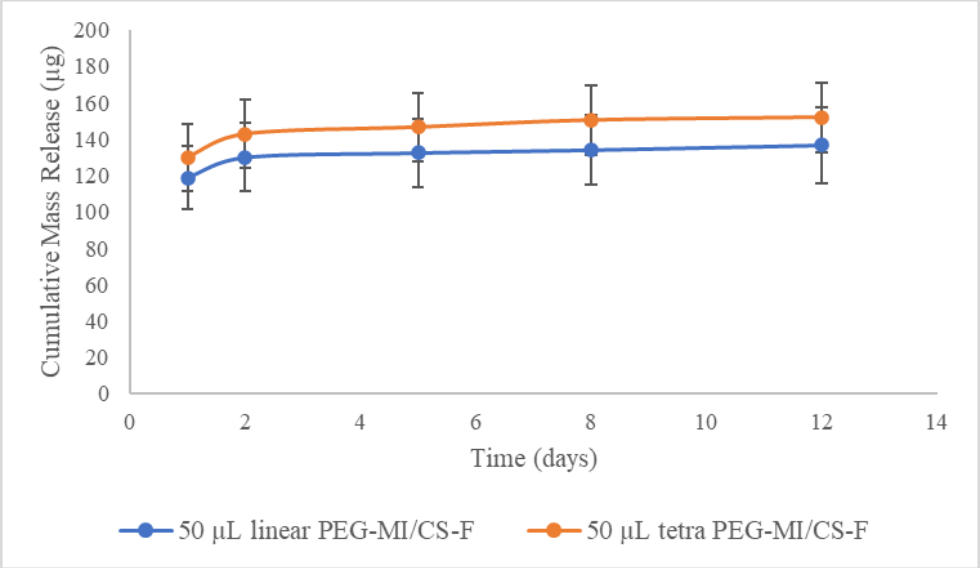

Figure 50: DNR release profile for 50 µL hydrogels fabricated from linear PEG-MI/CS-F and tetra PEG-MI/CS-F, labeled as trial 2. Cumulative mass release in µg from the hydrogels over a period of 23 days, or until the hydrogel fully released the loaded drug. Data is presented as mean ± standard deviation of 3 independent experiments.

VI. Final Design and Validation

Various tests were run on the design approaches to determine which would lead to the most successful final design. Throughout this chapter we will discuss how well the final design met the initial goals that were stated, how it was validated, and how industry standards play a role in the design process.

6.1 Overview of the Final Design

The final design for a water insoluble, injectable CS-PEG based hydrogel DDS is a furan modified chondroitin sulfate (CS-F) copolymerized with PEG-Maleimide (PEG-MI) hydrogel network loaded with DNR. To create this DDS, first the team investigated various formulation ratios to determine which would yield the highest rate of chondroitin sulfate modification via NMR analysis. The result of this process, as shown in table 12 showed that the 1:2:4 molar ratio yielded the highest rate of furan to CS modification, and therefore would be the formulation ratio for all future tests containing CS-F. The process of fabricating the hydrogels was then followed as described in chapter 5.1.1. Fabricated hydrogels were made in sizes of 20 µL, 50 µL, and 100 µL depending on the specific test that was going to be run and allowed to gel under room temperature for 24 h.

The first experiment run on the hydrogel formulation was the swelling assay as described in Chapter 5.2.4. In this experiment, initial swelling data was collected over 28 days on 20 µL hydrogels containing linear PEG-MI and CS-F as well as tetra PEG-MI and CS-F but results, as shown in Figure 44, yielded inclusive data due to large standard deviations. For this reason, the team chose to increase the gel volume and run the same assay but with 100 µL volumes instead. Results from this study, as shown in concluded that linear gels, on average, swelled 2-fold within the first two days and the tetra gels, on average, swelled 1.5-fold. The study was conducted over 23 days and yielded that linear gels have a greater swelling capacity than tetra gels in an aqueous environment.

The second experiment run was then injection force testing as outlined in appendix D, in which 50 µL linear and tetra hydrogels were extruded through 0.5 mL syringe with 0.5 in needle length and 28-gauge needle size. Testing was performed using an Instron E1000 with a 2 kN load cell (Catalog #2527-129) and custom compression fixture set up as shown in Figure 28. In

addition, a Bluehill script for compression testing was used in accordance with the Instron as outlined in Appendix D with specifications of 4 mm/min and measurements for extension and load collected every 250 ms. The experimentation done on linear and tetra drug and non-drug loaded hydrogels resulted in an injection force profile showing that drug loading hydrogels did not greatly affect the injection force profile so for the remainder of samples only drug load linear and tetra gels were compared. These gels were tested by injecting into chicken breast, to act as surrogate tissue and simulate injection into human tissue, and into air onto a petri dish following the same set up as the previous test. From this testing, linear drug loaded gels were found to be within acceptable injection force range of under 38 N for injection into chicken breast and injection into air onto the petri dish.

The third and final experiment involved performing a drug loading and release assay according to protocol outlined in Appendix E. In both experiments linear and tetra gels were loaded with a 200 µg of DNR and set aside to load for 48 h before results were compared to see which sample is more compatible with drug loading. Drug loading results yielded that tetra gels generally load a higher dose of DNR over 48 h. Specifically, tetra gels loaded 86 ± 10% of the total DNR dose whereas linear gels loaded 38 ± 1%. After drug loading was determined gels were placed into a fresh 1 mL of PBS and a drug release assay was performed as outlined in Appendix E. To obtain drug concentrations, a Molecular Devices SpectraMax M2 Multilabel Microplate Reader was used with an absorbance reading at 485 and then a standard curve containing known concentrations of DNR was used to calculate the DNR concentration of the supernatant readings. The first drug release assay was run over the course of 23 days and the mass of DNR release and the cumulative DNR mass release results can be seen in Figure 50. Linear gels were shown to release a greater amount of drug during the first couple of days in comparison to tetra gels but over time, both linear and tetra gel release profiles began to plateau as the remainder of the drug was released. In the second drug release assay as shown in Figure 50, the linear and tetra gels exhibited similar release profiles with a higher drug concentration being released in the first couple days and the remainder of DNR being released in a sustained manner over the remainder of the 17 day study.

6.2 Final Design Impact

6.2.1 Economic Viability

With the short scheme of this project, it is difficult to predict the economic viability and costs. The project cannot move forward as it might have been able to with more resources. It is expected that if it was to continue yielding positive data and keep moving forward, it would require more testing, requiring more money. The product does have the potential to be less expensive than other treatment options currently on the market due to its ability to decrease hospitalization and treatment visits, thereby lowering costs. It would also decrease the chance of side effects because it is an intratumoral delivery. Other treatment options such as intravenous delivery of cancer drugs would put the patient at risk for a long list of side effects, also placing the risk of more unpredicted costs.

6.2.2 Marketability

This project has some marketability concerns. The designed DDS requires an intensive amount of time, maintenance, and management; the fabrication of the hydrogel alone calls for around-the-clock care. This poses manufactural concerns regarding the marketability of this product, since the market typically favors efficiency and minimal human input. The materials necessary for the fabrication of the hydrogel are limited, although they are quite expensive, which can pose an issue for a future scale-up of this DDS fabrication method. As previously stated, there are minimal materials required to fabricate the hydrogel, therefore the amount of material lost is insignificant. The main material used in the fabrication process is CS; as stated in section 2.5, CS is a naturally derived substance that can also be synthetically fabricated in a lab. Therefore, the DDS has a low sustainability impact with room to improve overall sustainability.

6.2.3 Societal Implications

Due to the limitations of time and money, the societal implications of this project are minimal. Without more resources, the product will not be able enter preclinical and clinical trials, requiring more adequate resources. Should data consistently prove to be positive, this would further the product along and allow it to be a viable option for neuroblastoma patients. The future prospect of this project would implicate a larger and significant impact on society in the way that it would provide a new neuroblastoma treatment that is less invasive and requires less treatments than currently on the market.

6.2.4 Environmental Impact

The future scaled-up environmental impacts of the DDS must be considered to ensure that the system is environmentally friendly and will not lead to any adverse effects. The materials that are used in the lab are in such small quantities that there is little to no environmental concern. This can also be attributed to disposing of these materials in accordance with the lab standards, leading to minimal waste. Energy heavy processes must also be considered regarding the environmental impact of this fabrication process. Lyophilization of the CS results in excessive energy consumption which does raise environmental concerns due to negative impacts.

6.2.5 Issues with Health and Safety

The health and safety concerns of this project revolve around the Daunorubicin more than the hydrogel. The hydrogel is made up of CS, furan, and PEG MI. Both CS and PEG MI are biocompatible materials that do not pose a threat to the body. However, both the Daunorubicin and furan are dangerous when it encounters the body. Furan is commonly used to create other reagents that encounter the body, and Daunorubicin is a common hazard that is handled for cancer patient use so general safety in handling this drug would be followed.

6.2.6. Ethics

With the emerging and developing field of drug delivery, laboratories and institutions are consistently looking for ways to innovate. As a result of trying to advance science, there are ethical implications that need to be considered. The research and development process in the drug delivery industry requires clinical testing to validate the efficacy and safety of the product. In the scope of this project, all designed experiments were performed *in vitro* to help characterize the novel drug delivery system. There were no human or animal subjects involved in any of the experiments. The goal with this project was to develop a drug carrier capable of injection and providing a sustained release of drug, locally, over time. This development would provide a basis for further research down the line. Additionally, with any research it is crucial to ensure that all tests, the corresponding data, and results are handled with merit and not intentionally falsified. For this reason, experiment data and results are presented raw with any exceptions being clearly explained. In the scope of this project, any exceptions made to handling of the data were made in the form of cleanup to remove any noise from graphs/figures that was not pertaining to the

teams' drug delivery system. Lastly, the research team is one entity and has no relations to third parties that may have financial stakes skewing the results of this project.

VII. Discussion

7.1 CS-F Hydrogels

7.1.1 Injection Force Testing

Injection force testing was performed on different CS-PEG hydrogels to determine if the gels were within the acceptable force range for injection. Hydrogels were loaded into a 0.5 mL , 28-gauge, and 0.5 in needle size insulin syringes and were placed within the Instron. The Instron pushed the gels out of the syringe and relayed the measurements of the force and displacement. The first injection force testing study was done on non-drug loaded linear and tetra PEG and drug loaded linear and tetra PEG. After this, the team moved forward with performing a second injection force study. The second study compared linear and tetra PEG gels loaded with daunorubicin being pushed out of the syringe onto a Petri dish and into a raw chicken breast.

From the first study, it was found and proven through a two-way ANOVA test that the drug loading did not have a significant effect on the force it takes to push the gels out of the syringe. Both linear and tetra PEG gels also showed to be within acceptable injection force range. One problem that arose during this study was the amount of air bubbles in the syringe. This caused the force readings from the Instron to quickly jump up and down. During the second study, the syringes were pushed prior to testing in efforts to remove all possible air bubbles. This caused the overall displacement available in the syringe to be much less. For the set of gels being pushed onto a Petri dish, the linear PEG had consistent results with the first study which was proven by a t test that sh, remaining within the desired range. Validated by a two tailed t-test, the p value was greater than .005 showing that there was no significant difference between the drug loaded linear PEG gels that were pushed onto a Petri dish across both studies. The tetra PEG force results were much higher than the prior study, with there being a significant change validated through a two tailed t-test. When being pushed into raw chicken breast, the linear PEG gel force results were slightly higher than without raw chicken breast but were still within acceptable range.

From both injection studies, it can be determined that the drug loading did not have a significant effect on the injection force of the gels, thereby their structural integrity remained the same. The tetra PEG gels were acceptable in the first study but did not show consistency in the second study and had force readings too high. Thereby, they did not show reproducibility, and

more tests on the tetra PEG gels will need to be run to confidently determine if they have a low injection force and can be reproducible. The linear PEG gels showed reproducible readings with and without drug, as well as being pushed onto a Petri dish and being pushed into a raw chicken breast. These reproducible results were also low and within the acceptable range of below 38 N.

7.1.2 Swelling Study

In a tumor microenvironment, the gels will be subjected to an aqueous environment. It is essential to understand how the gels react in this type of environment. This pushed the team to perform swelling tests on the different gels and analyze their liquid uptake. The team performed two swelling tests. The first study used 20 µL linear and tetra PEG gels. Many problems arose during this study due to the small volume needing to be pipetted as well as weighed. Both gels, though especially the linear PEG due to its softer characteristics, were difficult to handle during the study, causing human error and presumably causing the high variability. Therefore, the data from the first study was found to be inconclusive. For the second swelling study, the team used 100 µL gels to avoid high human error similar to the prior study. These results proved to be much more conclusive. Both gels swelled the most within the first two days and then plateaued. A one-way ANOVA test was performed on this data, and the *p* showed to be less than 0.05, showing that the linear PEG gel swelling was significantly different from the tetra PEG gels.

It can be concluded that the linear PEG gels would uptake more liquid in an aqueous environment based off the second swelling study. This was hypothesized due to the softer and less rigid structure of the linear PEG gels observed during fabrication. The swelling was found to be within the first two days, followed by a plateau in gel weight. This is significant because the gel uptakes the liquid but can hold its shape and not degrade.

7.1.3 Drug Loading Assay

Drug loading assays were done using the post-loading method. All gels were surrounded with 1 mL of 200 µg/mL DNR. There were 200 µg of drug available for loading Two studies of drug loading were done. The first study showed very inconsistent results with the error for linear and tetra gels being 35.7 µg and 57 µg respectively. The second one was much more consistent with errors for linear and tetra being 2.3 µg and 20.6 µg respectively. Both studies showed that tetra gels loaded more drug than linear gels with a p-value of .017 for study 1 and a p-value of 9.7E-05. While the results of the second study did show to be much more consistent,

reproducibility cannot be determined until further studies are done. The linear gels in this study loaded with 74.7 µg and the tetra gels loaded 134.5 µg, while the linear gels in the second study loaded with 77.4 µg and tetra gels loaded with 172.3 µg. Prior to the studies being done the drug loading goal was to be above 85% to be acceptably loaded. The only sample that surpassed this requirement was met was the tetra gels on the second study, loading an average of 86.1%. No conclusions about the loading capabilities of the gels can be drawn from this data; however, it should be observed that all studies were done on 50 µL gels and this could have a large effect on amount of DNR loaded. Studies with larger gels and larger sample size could lead to more consistent and conclusive data.

7.1.4 Drug Release Assay

Significant conclusions were able to be drawn from the drug release of both the 20 µL and 50 µL linear PEG-MI/CS-F and tetra PEG-MI/CS-F hydrogels. For trial 1, linear PEG hydrogel released 130.05 µg of drug on the first day. The drug release demonstrated a sustained release profile with 48.51 µg being released on the second day, and 18.37 µg being released on the fourth day. The sustained release appeared to plateau after day 10, as seen in Figure 48. The tetra PEG hydrogel from trial 1 also demonstrated a sustained release that appears more linear than linear PEG. This can be seen in Figure 48, where tetra PEG released 98.07 µg of drug on the first day, 14.72 µg on the second day, and 10.76 µg. For trial 2, both the linear PEG and tetra PEG hydrogels exhibited a sustained release profile. Linear PEG released 118.82 µg of drug on the first day, 11.14 µg on the second day, and became more linear around the fifth day with a release rate of approximately 2.72 µg/day. Tetra PEG released 130.02 µg of drug on the first day and became more linear around the second day with a release rate of approximately 2.57 µg/day. Our findings confirm that both the 20 µL and 50 µL linear PEG-MI/CS-F and tetra PEG-MI/CS-F hydrogels can deliver a chemotherapeutic agent at a sustained rate over the course of time, thus meeting specification 3, which can be seen in section 3.3.3.

VIII. Conclusions and Recommendations

8.1 Conclusion

In conclusion, the group successfully created and tested a Chondroitin Sulfate based hydrogel. The formulation ratio and fabrication process the team proceeded with led to the development of a water insoluble, drug loadable, and injectable hydrogel. The process was made reproducible, and the materials used were cost efficient, easy to handle, and stored. The resulting hydrogel DDS was validated by gel characterization studies, DNR loading and release profiles, and injection force data. Taking this into account we recommend moving forward with linear PEG gels. The linear gels hit design objectives that tetra gels didn't: a low injection force and a reproducible injection force. We found that tetra gels had an injection force of over 38 N in the second study and seems to be unreproducible because of the change in injection force from study 1 to study 2 (9 N to 58 N). The linear gels were able to hit these design objectives along with the rest. Some major limitations to the final DDS included the budget as well as time constraints. The reasons for this were because specific materials were chosen to be cost effective and the tests completed were under strict limits. Future directions are mentioned below as there are many variables that are unexplored.

8.2 Future Studies

8.2.1 DMMB Assay

The team collected chondroitin sulfate supernatant samples from swelling studies to be used in a DMMB that was planned to be completed in late D-term but due to scheduling and time conflicts, the team was not able to run the DMMB assay to determine the amount of CS being leached out of the hydrogel over time. Since the team was not able to obtain DMMB assay results, we suggest running a repeat swelling study using 100 µL and then to collect the supernatant samples at each time to then run a DMMB assay to collect the CS leaching data. The expected experimental design for the DMMB assay would be as follows:

Collected supernatant samples obtained from the 100 µL hydrogel swelling study are used for this assay. To start, a standard curve of known concentrations of CS is made and will later be used to determine the GAG concentration in the supernatant. Next 20 µL of the supernatant samples is added to a 96 well plate and 200 µL of the DMMB solution is added to the wells. The well plate is then immediately placed into a UV-Vis spectrophotometer at an

absorbance reading of 525 nm and 5 second pre-shake and then the absorbances are read out using SoftMax Pro software. The resulting absorbances are then converted into GAG concentrations through the CS standard curve. This general protocol has been adapted from https://www.researchgate.net/publication/308759000_Dimethylmethylene_Blue_Assay_DMMB.

8.2.2 Degradation Assay

The team prepared 100 µL linear and tetra gels to be used in a degradation assay as described in Chapter 5.1.4. The gels were frozen and were prepared for the lyophilizer but as mentioned in the previous section, due to scheduling and time conflicts at the end of D- term the team was not able to get access to the lyophilizer to obtain the dry weight measurements that would be used to determine the degradation profile of non-drug loaded linear and tetra PEG-MI/ CS-F hydrogel. For this reason, we would suggest running a degradation assay as outlined Chapter 5.1.4. The results from this experiment would provide quantitative results as to how the hydrogel reacts in an aqueous environment. This would be separate from the swelling assay which investigates the liquid uptake capacity. This study would determine the polymer disassociation by looking at the dry weight measurements of the gels after coming out of the lyophilizer. The expected experimental design would be as follows:

Sixteen 100 µL gels using linear PEG and sixteen 100 µL gels using tetra PEG are prepared and then all gels are placed into separate 15 mL conical tubes with 5 mL of PBS. The gels are left to sit in PBS at room temperature for 2 days and then 4 conical tubes from both linear and tetra PEG samples are taken and the PBS is replaced with MilliQ water. On day 3, the 4 tubes containing the water, gels are carefully picked out and placed onto a well plate lined with aluminum foil and then frozen at –20 °C. On day 4, 4 more conical tubes from both linear and tetra PEG samples were taken and the PBS was replaced with MilliQ water. On day 5, the gels are removed from those tubes and then placed onto the well plate with the previous gels and put back into the –20 °C. On day 7, the PBS supernatant from the final 4 gels for both linear and tetra PEG is replaced with water and on day 8 the gel is removed from the tubes to be placed onto the well plate with the remaining gels. These samples in the well plate would be lyophilized for 72 h. The lyophilized gels would then be weighed on an analytical balance to obtain their dry weight measurements.

8.2.3 Hyaluronidase

Currently, the group uses PBS for swelling, degradation, and drug release studies. However, this wouldn't be an accurate representation of the tumor microenvironment. Therefore, the group suggests using Hyaluronidase, specifically 1 and 4, to mimic the tumor microenvironment. Research has shown that these two enzymes are highly active during NB and therefore would be more representative of the aqueous environment during NB than just PBS (Honda et. Al., 2012). All prior studies, such as swelling, degradation, and drug release, can therefore be done in a more accurate setting.

8.2.4 Biocompatibility Assay

The current DDS, when not loaded with chemotherapeutic agent, is comprised of components that are potentially safe for healthy cells within the body. This would be validated through running a biocompatibility assay. Cell lines would be cultured and then placed within well plates treated with the CS-F/PEG-MI hydrogels. This assay would be both qualitative and quantitative through imaging and counting. Cells would be counted prior to the plating of hydrogels within the well plate, followed by counting of both dead and live cells during specific time intervals. Microscopy imaging on these same time intervals will be done in efforts to qualitatively analyze the viability of the cells. This assay will be able to confirm or deny the biocompatibility of the hydrogel components and give insight to how the body would react to the introduction of these materials.

8.2.5 Drug Activity Assay

The team would also recommend a drug activity assay to see how the DDS is targeting NB cells. A drug activity assay would provide confirmation that the drug is being released at a rate that would be toxic to the targeted cells from the CS-F/PEG-MI hydrogels. The assay would expose neuroblastoma cells that had been cultured to the hydrogel loaded with DNR. Over specific time intervals, the live and dead cells would be counted as well as imaged. This would provide qualitative and quantitative information regarding the efficiency of the hydrogel's drug concentration as well as release over time.

8.2.6 Alternative PEGs

In all the studies done linear and tetra PEG was used. These specific PEGs have 2 attachment sites and 4 attachment sites respectively. Additionally, the PEGs used had a

molecular weight of 2.5 kDa per arm. This means that the linear PEG was 5 kDa and tetra was 10 kDa. Manipulating the molecular weights of the PEG can change the characteristics of the gel. For example, a tetra PEG that is 6 kDa (1.5 kDa per arm) could give a gel that loads more than the 2.5 kDa linear gels but has an injection force lower than the 2.5 kDa tetra gels. Additionally, the number of arms can be manipulated as well. There are PEGs that have 6 arms or 8 arms which can change the characteristics of the gels to fit constraints of the project.

8.2.7 PEG:CS Ratio

The only PEG to CS ratio that was explored in these studies was 1 to 1. By changing this ratio, one can manipulate how densely and loosely crosslinked the hydrogels are. This is another method of manipulating the gel to achieve desirable characteristics.

8.2.8 Chemotherapeutic Agents

The DDS we created uses the anthracycline DNR as the chemotherapeutic agent. DNR was chosen due to past research performed by the Coburn lab yielding results that show the drug is a viable option to deliver anticancer agents intratumorally. The interaction between CS and DNR is an electrostatic interaction- since CS is negatively charged and daunorubicin is positively charged. Through our assays, we were able to show compatibility of drug loading with our DDS. Due to this we recommend studying an alternative positively charged drug with our DDS so that it can be more generalized for clinical needs. This would be beneficial to look at so that the effect of the drug on the injection force and the release profile can be observed.

VI. References

1. Ackermann, S., Cartolano, M., Hero, B., Welte, A., Kahlert, Y., Roderwieser, A., ... & Fischer, M. (2018). A mechanistic classification of clinical phenotypes in neuroblastoma. *Science*, *362*(6419), 1165-1170.
2. Amjadi, S., Hamishehkar, H., & Ghorbani, M. (2019). A novel smart PEGylated gelatin nanoparticle for co-delivery of doxorubicin and betanin: A strategy for enhancing the therapeutic efficacy of chemotherapy. Materials Science and Engineering: C, 97, 833-841.
3. Asimakopoulou, A. P., Theocharis, A. D., Tzanakakis, G. N., & Karamanos, N. K. (2008). The biological role of chondroitin sulfate in cancer and chondroitin-based anticancer agents. *In vivo*, *22*(3), 385-389.
4. Aswathy, S. H., Narendrakumar, U., & Manjubala, I. (2020). Commercial Hydrogels for Biomedical applications. Heliyon, 6(4), e03719.
5. Akter, J., & Kamijo, T. (2021). How Do Telomere Abnormalities Regulate the Biology of Neuroblastoma? *Biomolecules*, *11*(8), 1112.
6. Allinson, L. M., Potts, A., Goodman, A., Bown, N., Bashton, M., Thompson, D., ... & Tweddle, D. A. (2022). Loss of ALK hotspot mutations in relapsed neuroblastoma. *Genes, Chromosomes and Cancer*.+
7. Alonso, J. M., Andrade del Olmo, J., Perez Gonzalez, R., & Saez-Martinez, V. (2021). Injectable hydrogels: From laboratory to industrialization. Polymers, 13(4), 650.
8. Beckett, L. E., Lewis, J. T., Tonge, T. K., & Korley, L. S. T. (2020). Enhancement of the mechanical properties of hydrogels with continuous fibrous reinforcement. ACS Biomaterials Science & Engineering, 6(10), 5453–5473.
9. Berski, S., Andrés, J., Silvi, B., & Domingo, L. R. (2003). The joint use of catastrophe theory and electron localization function to characterize molecular mechanisms. A density functional study of the diels−alder reaction between ethylene and 1,3-butadiene. *The Journal of Physical Chemistry A, 107*(31), 6014–6024.
10. Bochot, A., & Fattal, E. (2012). Liposomes for intravitreal drug delivery: a state of the art. Journal of Controlled Release, 161(2), 628-634.
11. Brodeur, G. M. (2003). Neuroblastoma: biological insights into a clinical enigma. *Nature reviews cancer*, *3*(3), 203-216.

12. Bustamante-Torres, M., Romero-Fierro, D., Arcentales-Vera, B., Palomino, K., Magaña, H., & Bucio, E. (2021). Hydrogels classification according to the physical or chemical interactions and as stimuli-sensitive materials. Gels, 7(4), 182.
13. Carvalho, C. (2022). Injectable Chondroitin Sulfate-Based Hydrogel Drug Delivery Systems A Major Qualifying Quarterly Project Report submitted to the faculty of (Doctoral dissertation, WORCESTER POLYTECHNIC INSTITUTE).
14. Chatterjee, K., Zhang, J., Honbo, N., & Karliner, J. S. (2010). Doxorubicin cardiomyopathy. Cardiology, 115(2), 155-162.
15. Chauhan, N., Saxena, K., & Jain, U. (2022). Hydrogel based materials: A Progressive approach towards advancement in biomedical applications. Materials Today Communications, 33, 104369.
16. Chen, G., Kawazoe, N., & Ito, Y. (2018). Photo-crosslinkable hydrogels for tissue engineering applications. In *Photochemistry for Biomedical Applications* (pp. 277-300). Springer, Singapore.
17. Chen, M. H., Wang, L. L., Chung, J. J., Kim, Y. H., Atluri, P., & Burdick, J. A. (2017). Methods to assess shear-thinning hydrogels for application as injectable biomaterials. ACS biomaterials science & engineering, 3(12), 3146-3160.
18. Coburn, J. M., Harris, J., Cunningham, R., Zeki, J., Kaplan, D. L., & Chiu, B. (2017). Manipulation of variables in local controlled release vincristine treatment in neuroblastoma. Journal of pediatric surgery, 52(12), 2061-2065.
19. Coburn, J. M., & Kaplan, D. L. (2015). Engineering biomaterial–drug conjugates for local and sustained chemotherapeutic delivery. Bioconjugate chemistry, 26(7), 1212-1223.
20. Coburn, J. M. Free Radical Crosslinking of a Polymer with a Methacrylate Group.
21. De Lombaerde, E., De Wever, O., & De Geest, B. G. (2021). Delivery routes matter: Safety and efficacy of intratumoral immunotherapy. Biochimica et Biophysica Acta (BBA)-Reviews on Cancer, 1875(2), 188526.
22. Di Muzio, L., Paolicelli, P., Trilli, J., Petralito, S., Carriero, V. C., Brandelli, C., ... & Casadei, M. A. (2022). Insights into the reaction of chondroitin sulfate with glycidyl methacrylate: 1D and 2D NMR investigation. *Carbohydrate Polymers*, *296*, 119916.

23. D'Este, M., Eglin, D., & Alini, M. (2014). A systematic analysis of DMTMM vs EDC/NHS for ligation of amines to hyaluronan in water. *Carbohydrate Polymers*, *108*, 239–246. https://doi.org/10.1016/j.carbpol.2014.02.070
24. El Jundi, A., Buwalda, S. J., Bakkour, Y., Garric, X., & Nottelet, B. (2020). Double hydrophilic block copolymers self-assemblies in biomedical applications. *Advances in Colloid and Interface Science*, *283*, 102213.
25. El Jundi, A., Buwalda, S. J., Bakkour, Y., Garric, X., & Nottelet, B. (2020). Double hydrophilic block copolymers self-assemblies in biomedical applications. *Advances in Colloid and Interface Science*, *283*, 102213.
26. Enas Ahmed. (2015) Hydrogel: Preparation, characterization, and applications: A review. Journal of Advanced Research, 6, 105-121
27. Fong, Y. T., Chen, C. H., & Chen, J. P. (2017). Intratumoral delivery of doxorubicin on folate-conjugated graphene oxide by in-situ forming thermo-sensitive hydrogel for breast cancer therapy. Nanomaterials, 7(11), 388.
28. Gandini, A. (2013). The furan/Maleimide Diels–Alder reaction: A versatile click–unclick tool in Macromolecular Synthesis. *Progress in Polymer Science*, *38*(1), 1–29. https://doi.org/10.1016/j.progpolymsci.2012.04.002
29. Gao, Y., Zhou, D., Lyu, J., Xu, Q., Newland, B., Matyjaszewski, K., ... & Wang, W. (2020). Complex polymer architectures through free-radical polymerization of multivinyl monomers. *Nature Reviews Chemistry*, *4*(4), 194-212.
30. Gevrek, T. N., & Sanyal, A. (2021). Furan-containing polymeric materials: Harnessing the Diels-Alder Chemistry for Biomedical Applications. *European Polymer Journal*, *153*, 110514. https://doi.org/10.1016/j.eurpolymj.2021.110514
31. Haghiri, S., Fayech, C., Mansouri, I., Dufour, C., Pasqualini, C., Bolle, S., ... & Fresneau, B. (2021). Long-term follow-up of high-risk neuroblastoma survivors treated with high-dose chemotherapy and stem cell transplantation rescue. *Bone Marrow Transplantation*, *56*(8), 1984-1997.
32. Heck, J. E., Ritz, B., Hung, R. J., Hashibe, M., & Boffetta, P. (2009). The epidemiology of neuroblastoma: a review. *Paediatric and perinatal epidemiology*, *23*(2), 125-143.
33. Hein, C. D., Liu, X.-M., & Wang, D. (2008). Click Chemistry, a powerful tool for pharmaceutical sciences. *Pharmaceutical Research*, *25*(10), 2216–2230.

34. Hermanson, G. T. (2013). The reactions of bioconjugation. *Bioconjugate Techniques*, 229–258.
35. Hermanson, G. T. (2013). Zero-length crosslinkers. *Bioconjugate Techniques*, 259–273.
36. Homayun, B., Lin, X., & Choi, H. J. (2019). Challenges and recent progress in oral drug delivery systems for biopharmaceuticals. Pharmaceutics, 11(3), 129.
37. Jain, T. K., Morales, M. A., Sahoo, S. K., Leslie-Pelecky, D. L., & Labhasetwar, V. (2005). Iron oxide nanoparticles for sustained delivery of anticancer agents. Molecular pharmaceutics, 2(3), 194-205.
38. Jin, M., Jin, G., Kang, L., Chen, L., Gao, Z., & Huang, W. (2018). Smart polymeric nanoparticles with pH-responsive and PEG-detachable properties for co-delivering paclitaxel and survivin siRNA to enhance antitumor outcomes. International journal of nanomedicine, 13, 2405.
39. Jin, X., Li, Q., Wang, Y., Zhang, W., Xu, R., Li, J., ... & Kang, Z. (2020). Optimizing the sulfation-modification system for scale preparation of chondroitin sulfate A. *Carbohydrate polymers*, *246*, 116570.
40. Keutgen, X. M., Ornell, K. J., Vogle, A., Lakiza, O., Williams, J., Miller, P., ... & Coburn, J. M. (2021). Sunitinib-Loaded Chondroitin Sulfate Hydrogels as a Novel Drug-Delivery Mechanism for the Treatment of Pancreatic Neuroendocrine Tumors. *Annals of Surgical Oncology*, *28*(13), 8532-8543.
41. Kim, E., & Koo, H. (2019). Biomedical applications of copper-free click chemistry: *in vitro*, *in vivo*, and *ex vivo*. *Chemical Science*, *10*(34), 7835–7851. https://doi.org/10.1039/c9sc03368h
42. Kraft, J. C., Freeling, J. P., Wang, Z., & Ho, R. J. (2014). Emerging research and clinical development trends of liposome and lipid nanoparticle drug delivery systems. Journal of pharmaceutical sciences, 103(1), 29-52.
43. Krayukhina, E., Fukuhara, A., & Uchiyama, S. (2020). Assessment of the injection performance of a tapered needle for use in prefilled biopharmaceutical products. Journal of pharmaceutical sciences, 109(1), 515-523.
44. Larrañeta, E., Stewart, S., Ervine, M., Al-Kasasbeh, R., & Donnelly, R. (2018). Hydrogels for hydrophobic drug delivery. classification, synthesis and applications. Journal of Functional Biomaterials, 9(1), 13.

45. Lauder, R. M. (2009). Chondroitin sulphate: a complex molecule with potential impacts on a wide range of biological systems. *Complementary therapies in medicine*, *17*(1), 56-62.
46. Li, T., Song, X., Weng, C., Wang, X., Sun, L., Gong, X., ... & Chen, C. (2018). Self-crosslinking and injectable chondroitin sulfate/pullulan hydrogel for cartilage tissue engineering. *Applied Materials Today*, *10*, 173-183.
47. Li, Q., Wang, D. A., & Elisseeff, J. H. (2003). Heterogeneous-phase reaction of glycidyl methacrylate and chondroitin sulfate: mechanism of ring-opening− transesterification competition. *Macromolecules*, *36*(7), 2556-2562.
48. Li, Q., Williams, C. G., Sun, D. D., Wang, J., Leong, K., & Elisseeff, J. H. (2004). Photocrosslinkable polysaccharides based on chondroitin sulfate. *Journal of Biomedical Materials Research Part A: An Official Journal of The Society for Biomaterials, The Japanese Society for Biomaterials, and The Australian Society for Biomaterials and the Korean Society for Biomaterials*, *68*(1), 28-33.
49. Li, W., Zhan, P., De Clercq, E., Lou, H., & Liu, X. (2013). Current drug research on pegylation with small molecular agents. Progress in Polymer Science, 38(3-4), 421–444.
50. Li, X., Xu, Q., Johnson, M., Wang, X., Lyu, J., Li, Y., ... & Wang, W. (2021). A chondroitin sulfate based injectable hydrogel for delivery of stem cells in cartilage regeneration. *Biomaterials Science*, *9*(11), 4139-4148.
51. Lin, C. C., & Anseth, K. S. (2009). PEG hydrogels for the controlled release of biomolecules in regenerative medicine. Pharmaceutical research, 26(3), 631–643.
52. Matyjaszewski, K., & Davis, T. P. (2002). *Handbook of radical polymerization* (Vol. 922). New York: Wiley-Interscience. 187-257.
53. McGowan, J. V., Chung, R., Maulik, A., Piotrowska, I., Walker, J. M., & Yellon, D. M. (2017). Anthracycline chemotherapy and Cardiotoxicity. Cardiovascular Drugs and Therapy, 31(1), 63–75.
54. Meyer, J., Meyer, L. E., & Kara, S. (2022). Enzyme immobilization in hydrogels: A perfect liaison for efficient and sustainable biocatalysis. *Engineering in Life Sciences*, *22*(3-4), 165-177.
55. Mihajlovic, M., Rikkers, M., Mihajlovic, M., Viola, M., Schuiringa, G., Ilochonwu, B. C., ... & Vermonden, T. (2022). Viscoelastic Chondroitin Sulfate and Hyaluronic Acid

Double-Network Hydrogels with Reversible Cross-Links. *Biomacromolecules*, *23*(3), 1350-1365.

56. Miyazaki, T., Yamaoka, K., Kaneko, T., Gong, J. P., & Osada, Y. (2000). Hydrogels with the ordered structures. Science and Technology of Advanced Materials, 1(4), 201–210.
57. Newman, E. A., Abdessalam, S., Aldrink, J. H., Austin, M., Heaton, T. E., Bruny, J., ... & Madonna, M. B. (2019). Update on neuroblastoma. *Journal of pediatric surgery*, *54*(3), 383-389.
58. Nimmo, C. M., Owen, S. C., & Shoichet, M. S. (2011). Diels−Alder click cross-linked hyaluronic acid hydrogels for tissue engineering. *Biomacromolecules*, *12*(3), 824–830. https://doi.org/10.1021/bm101446k
59. Ornell, K. J., Lozada, D., Phan, N. V., & Coburn, J. M. (2019). Controlling methacryloyl substitution of chondroitin sulfate: injectable hydrogels with tunable long-term drug release profiles. Journal of Materials Chemistry B, 7(13), 2151-2161.
60. Overstreet, D. J., Dutta, D., Stabenfeldt, S. E., & Vernon, B. L. (2012). Injectable hydrogels. Journal of Polymer Science Part B: Polymer Physics, 50(13), 881-903.
61. Pal, D., & Saha, S. (2019). Chondroitin: a natural biomarker with immense biomedical applications. *RSC advances*, *9*(48), 28061-28077.
62. Parhi, R. (2017). Cross-Linked Hydrogel for Pharmaceutical Applications: A Review. Advanced pharmaceutical bulletin, 7(4), 515–530.
63. Peng, Z., Ji, C., Zhou, Y., Zhao, T., & Leblanc, R. M. (2020). Polyethylene Glycol (PEG) derived carbon dots: Preparation and applications. Applied Materials Today, 20, 100677.
64. Perin, F., Mota, C., Mancini, I., Motta, A., & Maniglio, D. (2022). Photo-enzymatic dityrosine crosslinking for bioprinting. Polymer, 252, 124941.
65. Ramachandran, R., Jung, D., & Spokoyny, A. M. (2019). Cross-linking dots on metal oxides. NPG Asia Materials, 11(1).
66. Sarpong, R., Paradisi, F., & Reeves , J. (n.d.). *Click chemistry azide-alkyne cycloaddition*. Organic Chemistry. Retrieved October 13, 2022, from https://www.organic-chemistry.org/namedreactions/click-chemistry.shtm
67. Schirrmacher, V. (2019). From chemotherapy to biological therapy: A review of novel concepts to reduce the side effects of systemic cancer treatment. *International journal of oncology*, *54*(2), 407-419.

68. Schuurmans, C. C., Mihajlovic, M., Hiemstra, C., Ito, K., Hennink, W. E., & Vermonden, T. (2021). Hyaluronic acid and chondroitin sulfate (meth) acrylate-based hydrogels for tissue engineering: Synthesis, characteristics and pre-clinical evaluation. *Biomaterials*, *268*, 120602.
69. Shandilya, M., Sharma, S., Das, P. P. , & Charak, S. (2020). Molecular-Level Understanding of the Anticancer Action Mechanism of Anthracyclines. In H. Arnouk, & B. A. R. Hassan (Eds.), Advances in Precision Medicine Oncology. IntechOpen.
70. Shaul, P., Frenkel, M., Goldstein, E. B., Mittelman, L., Grunwald, A., Ebenstein, Y., Tsarfaty, I., & Fridman, M. (2013). The structure of anthracycline derivatives determines their subcellular localization and cytotoxic activity. *ACS Medicinal Chemistry Letters*, *4*(3), 323–328.
71. Shi, Y. G., Meng, Y. C., Li, J. R., Chen, J., Liu, Y. H., & Bai, X. (2014). Chondroitin sulfate: Extraction, purification, microbial and chemical synthesis. *Journal of Chemical Technology & Biotechnology*, *89*(10), 1445-1465.
72. Simental-Mendia, M., Sanchez-Garcia, A., Vilchez-Cavazos, F., Acosta-Olivo, C. A., Pena-Martinez, V. M., & Simental-Mendia, L. E. (2018). Effect of glucosamine and chondroitin sulfate in symptomatic knee osteoarthritis: a systematic review and meta-analysis of randomized placebo-controlled trials. *Rheumatology international*, *38*(8), 1413-1428.
73. Sintov, A., Di-Capua, N., & Rubinstein, A. (1995). Cross-linked chondroitin sulphate: characterization for drug delivery purposes. *Biomaterials*, *16*(6), 473-478.
74. Smith, V., & Foster, J. (2018). High-risk neuroblastoma treatment review. *Children*, *5*(9), 114.
75. Sousa, G. F., Afewerki, S., Dittz, D., Santos, F. E., Gontijo, D. O., Scalzo, S. R., Santos, A. L., Guimaraes, L. C., Pereira, E. M., Barcelos, L. S., Do Monte, S. J., Guimaraes, P. P., Marciano, F. R., & Lobo, A. O. (2022). Catalyst-free click chemistry for engineering chondroitin sulfate-multiarmed peg hydrogels for skin tissue engineering. *Journal of Functional Biomaterials*, *13*(2), 45.
76. Spencer, B., Patel, A., Cilley, R., & Grant, C. N. (2022). Surgical management in pediatric neuroblastoma diagnosis and treatment: a 20-year, single-center experience. *World Journal of Pediatrics*, *18*(2), 120-125.

77. Strehin, I., Nahas, Z., Arora, K., Nguyen, T., & Elisseeff, J. (2010). A versatile pH sensitive chondroitin sulfate–PEG tissue adhesive and hydrogel. *Biomaterials*, *31*(10), 2788-2797.
78. Tanaka, K. (1978). Physicochemical Properties of Chondroitin Sulfate: I. Ion Binding and Secondary Structure. *The Journal of biochemistry*, *83*(3), 647-653.
79. Tang, C., Holt, B. D., Wright, Z. M., Arnold, A. M., Moy, A. C., & Sydlik, S. A. (2019). Injectable amine functionalized graphene and chondroitin sulfate hydrogel with potential for cartilage regeneration. *Journal of Materials Chemistry B*, *7*(15), 2442-2453.
80. Tekade, R. K., Dutta, T., Gajbhiye, V., & Jain, N. K. (2009). Exploring dendrimer towards dual drug delivery: pH responsive simultaneous drug-release kinetics. Journal of microencapsulation, 26(4), 287-296.
81. Tessmar, J. K., & Göpferich, A. M. (2007). Customized PEG-derived copolymers for tissue-engineering applications. Macromolecular bioscience, 7(1), 23-39.
82. Thoniyot, P., Tan, M. J., Karim, A. A., Young, D. J., & Loh, X. J. (2015). Nanoparticle-Hydrogel Composites: Concept, design, and applications of these promising, multi-functional materials. Advanced Science, 2(1-2), 1400010.
83. Thorek, D. L. J., Elias, ew R., & Tsourkas, A. (2009). Comparative analysis of nanoparticle-antibody conjugations: Carbodiimide versus click chemistry. *Molecular Imaging*, *8*(4). https://doi.org/10.2310/7290.2009.00021
84. Venkatesh, P., & Kasi, A. (2022). Anthracyclines. StatPearls Publishing.
85. Verma, P., Thakur, A. S., Deshmukh, K., Jha, A. K., & Verma, S. (2010). Routes of drug administration. International Journal of Pharmaceutical Studies and Research, 1(1), 54-59.
86. Wang, H., Zhang, H., Xie, Z., Chen, K., Ma, M., Huang, Y., Li, M., Cai, Z., Wang, P., & Shen, H. (2022). Injectable hydrogels for Spinal Cord Injury Repair. Engineered Regeneration, 3(4), 407–419.
87. Wang, L. F., Shen, S. S., & Lu, S. C. (2003). Synthesis and characterization of chondroitin sulfate–methacrylate hydrogels. *Carbohydrate Polymers*, *52*(4), 389-396.
88. Westphal, M., Ram, Z., Riddle, V., Hilt, D., & Bortey, E. (2006). Gliadel® wafer in initial surgery for malignant glioma: long-term follow-up of a multicenter controlled trial. Acta neurochirurgica, 148(3), 269-275.

89. Wienke, J., Dierselhuis, M. P., Tytgat, G. A., Künkele, A., Nierkens, S., & Molenaar, J. J. (2021). The immune landscape of neuroblastoma: challenges and opportunities for novel therapeutic strategies in pediatric oncology. *European journal of cancer, 144*, 123-150.
90. Williams, A., & Ibrahim, I. T. (1981). Carbodiimide chemistry: Recent advances. *Chemical Reviews*, *81*(6), 589–636.
91. Wittes, R. E., & LeRoy, D. K. (Eds.). (1983). Laboratory Models and Clinical Cancer. In Cancer treatment reports (1st ed., Vol. 70, pp. 1–240). essay, National Cancer Institute.
92. Wolinsky, J. B., Colson, Y. L., & Grinstaff, M. W. (2012). Local drug delivery strategies for cancer treatment: gels, nanoparticles, polymeric films, rods, and wafers. Journal of controlled release, 159(1), 14-26.
93. Xin, H., & Naficy, S. (2022). Drug delivery based on stimuli-responsive injectable hydrogels for breast cancer therapy: a review. Gels, 8(1), 45.
94. Yang, J., Shen, M., Wen, H., Luo, Y., Huang, R., Rong, L., & Xie, J. (2020). Recent advance in delivery system and tissue engineering applications of chondroitin sulfate. *Carbohydrate polymers*, *230*, 115650.
95. Yang, Y., Ren, Y., Song, W., Yu, B., & Liu, H. (2022). Rational design in functional hydrogels towards Biotherapeutics. Materials & Design, 223, 111086.
96. Zeinali, M., Abbaspour-Ravasjani, S., Ghorbani, M., Babazadeh, A., Soltanfam, T., Santos, A. C., ... & Hamblin, M. R. (2020). Nanovehicles for co-delivery of anticancer agents. Drug Discovery Today, 25(8), 1416-1430.

VII. Appendix

Appendix A: Gannt Charts A – D term

A Term

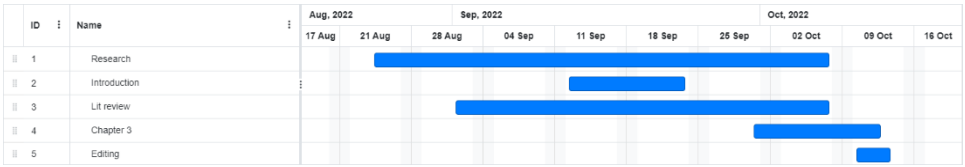

B Term

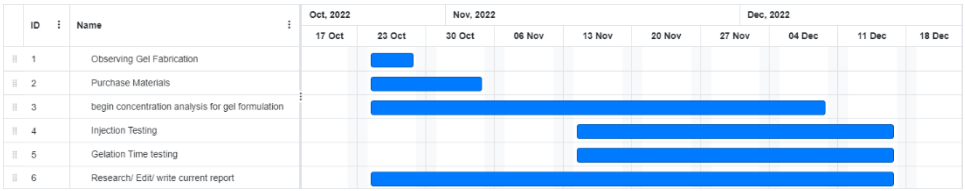

C Term

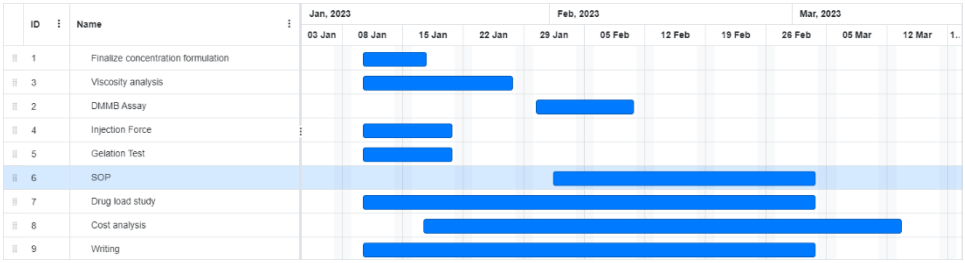

D Term

Appendix B: Protocol for PEG-MI/ CS-F Synthesis

*This protocol is set for a molar ratio of 1:2:4 (CS:Furan:DMTMM). Additional formulation ratios can be found in table below: Note: MES volume used is constant through all formulations.

Molar Ratio	Reagents		
	CS (g)	**Furan (µL)**	**DMTMM (g)**
1:2:4	0.485	188.8	1.1214
1:0.5:4	0.485	47.2	1.1214
1:0.5:2	0.485	47.2	0.5607
1:1:1	0.485	94.4	0.2804

1. Dilute MES buffer solution down from 500 mM to an 83.33 mM concentration.
2. Fully dissolve 0.485 g CS into 40 mL MES buffer in a round bottom flask on a magnetic stir plate with stirring (3 cm stir bar).
    a. Have the magnetic stir bar in the round bottom flask with MES before slowly adding the CS to minimize clumping and make dissolution easier.
3. Fully dissolve 1.1214 g DMTMM in the round bottom flask.
4. After 10 minutes of stirring, add 188.8 µL of furan dropwise to the round bottom flask.
5. Put a rubber stopper on the flask to cap it and let sit with constant stirring for 24 h.
6. Transfer the solution to dialysis tubing,
7. Dialyze for a minimum of 72 h against ultrapure water with periodic bath changes each day.
    a. Day 1: change the water baths on hour 1, 3, and 5.
    b. Day 2 and 3: change the water bath in the morning, afternoon, and evening.
8. After dialysis, transfer the solution from the tubing into 50 mL centrifuge tubes, maximum of 30 mL per tube.
9. Centrifuge at 2,500 rpm for 5 minutes.
10. Freeze the solution at a minimum of a 45° angle overnight.
11. Remove the centrifuge caps and place a Kimtech wipe over the top of the tube and secure it with a rubber band.
12. Freeze at –80 °C overnight.

13. Lyophilize minimum 72 h (light protected) (at –25 °C, 210 mTorr or on side arm 4th floor lyo).
14. Store at –20 °C after lyophilization.

Appendix C: Protocol for PEG-MI/ CS-F Hydrogels

*Depending on the number gels being made, a table below shows the corresponding reagent amount used to make various total gel solution volumes. Consider the table below to determine which ratio to use when fabricating the gels.

Ratio	Reagents				Total Gel Solution Volume (µL)
	Centrifuge tube 1		Centrifuge tube 2		
	CS-F (mg)	MES (µL)	PEG-MI (mg)	MES (µL)	
Original	18	1000	57.92	375	1375
50% scale down	9	500	28.96	187.5	687.5
75% scale down	4.5	250	14.48	93.75	343.75

Making PEG-MI/ CS-F Hydrogel Solution:

1. Calculate weight of the CS-F and PEG-MI necessary to achieve the desired concentration and volume of hydrogel.
2. Weigh out CS-F directly into a 2 mL microcentrifuge tube.
3. Add the calculated volume of MES buffer to the CS-F.
4. Vortex until thoroughly dissolved and mixed.
5. Weigh out the PEG-MI directly into a separate 2 mL microcentrifuge tube.
6. Add the calculated volume of MES buffer to the PEG-MI.
7. Vortex until thoroughly dissolved and mixed.
8. Combine the two solutions and vortex until thoroughly mixed.

Gelling of 20 µL Gels:

1. Pipette the 20 µL for each hydrogel on a glass slide lined with parafilm.
2. When the droplets are fully gelled, carefully remove them from the surface using a clean razorblade.

Gelling of 50 µL Gels:

3. Pipette the 50 µL for each hydrogel on a glass slide lined with parafilm.
4. When the droplets are fully gelled, carefully remove them from the surface using a clean razorblade.

Gelling of 100 µL Gels:

5. Pipette the 100 µL for each hydrogel on a glass slide lined with parafilm.
6. When the droplets are fully gelled, carefully remove them from the surface using a clean razorblade.

Appendix D: Protocol for Instron Testing

Adapted from:

Instron training Checklist

Compression Testing Method-Keely Nistler

Generation of Bluehill Method:

1. In Bluehill start by creating a testing method and choose the compression test option.
2. Within the General tab select SI for units.
3. In the Calculations tab select Peak Max/Min.
4. To designate the collection data for testing select the following in the Test tab:
    a. Start by using the start button.
    b. Test: 4 mm/min rate
    c. Data: Take data every 250 ms
5. In the Console tab select the following:
    a. Set Live Display to Extension and Load
6. For the Workspace tab select the following:
    a. Results 1: Max Load, and Specimen Label
    b. Graph 1: Extension v. Load
    c. Raw Data, Time, Extension, and load
    d. Layout: Graph and Result table
7. To select the information being exported use the Export tab to select the following:
    a. File settings: Set the location where the file should be saved to
    b. Export results
    c. Export raw data (and include the specimen label and test rate)

Testing Hydrogels for Injection force:

(*Remember to always take proper safety precautions and wear proper PPE or goggles)

1. Upon entering, check that the Instron is on. If not, turn it on to warm up for 15 minutes.
2. Before entering the Instron room to test, preload the syringes with the hydrogels to test for the day.

3. Once the Instron has warmed up, follow these steps (taken from the Instron Training Checklist).
4. Make sure the Instron is in Vertical position for Instron testing.
5. Start the Instron Console software.
6. Make sure to select proper commissioning files for the orientation of the Instron.
    a. Click the double arrow in the bottom left of the Console bar.
    b. Click the wrench.
    c. Click yes, you are sure you want to continue.
    d. Click the Pink Electro pulse tab.
    e. Select the commissioning tab on the left side bar.
    f. Select vertical commissioning, next, and okay.
7. Attach the 2 kN load cell (attached to machine, place the data cable in the head in the proper position).
8. Calibrate the load cell by going to “Load” in the console, selecting “Calibration”, “Calibration Wizard”.
    a. Keep all default values and move through the menu.
    b. Select “Auto Calibrate and press start”.
    c. Following calibration make sure you “Lock Calibration” and “Save Calibration” with a file name with the appropriate inputs as follows “date.load cell.initials”.
9. On the Instron, move the actuator into position (make sure to place into I mode), to the bottom black line.
10. Open Bluehill and select the MQP Compression Test Protocol from the team flash drive.
    a. If messages come up, select “no” to move forward.
11. Measure the height of the gel before loading in the box and input into the extension measurement control in the Protocol pink tab.
12. Load the sample into the syringe testing box as follows:
    a. If on the Instron, remove the bottoms silver plate with an Alen wrench so the dark grey platform is left.
    b. Place the syringe (28 G, 0.5 mL, 0.5 in) into the hole in the top of the syringe box.
    c. Place the finger holds of the syringe underneath the washers on the top of the box and tighten the bolts to hold the syringe in place.

13. On the Instron, attach the Syringe Compression hold with a pin and safety lock.
14. Place the syringe box on the Instron and lower the actuator into position so the plunger is placed in the hole of the syringe compression hold.
    a. Move the body of the Instron if necessary, with the black switch on the controls box.
15. Once in place, zero the extension and balance the load cell.
16. Input proper specimen labels and run the tests necessary.
17. Remove the sample and box from the Instron when finished **(Before Exporting Data, Closing Bluehill, and Closing the console).**
18. In a new folder on the flash drive make sure to save the protocol before finishing the test.
19. Select finish test and select "no" for running more samples.
20. Check the flash drive and make sure the data from the test was saved.
    a. If needed, look through the computer to find the exported files.
21. Close the Instron Console.

Notes:

- If you need to stop the machine in an emergency, hit the red button on the actuator. To start it again after this, you will need to turn the button to release it.
- Do not store your results on the computer. Copy them on to an external device and delete them off of the computer and empty the recycling bin.
- All accessories for the Instron must remain in the Instron room – be careful not to walk away with any pieces.
- Always clean up after yourself, wipe down all surfaces with 70% ethanol and put items back in their place.
- If you experience any problems with the Instron, report them IMMEDIATELY.

Appendix E: Protocol for DNR Loading and Release Studies

Drug loading

1. Retrieve DNR powder from the fridge and let it warm up at room temperature for a minimum of 1 to 2 minutes to avoid condensation.
2. Place prepared 20 µL hydrogel into a 2 mL microcentrifuge tube. Label accordingly (dependent on PEG used).
3. Create a stock solution of 200 µg/mL (e.g. for 1 mL of solution add 980 µL of MilliQ water and 20 µL of 10 µg/mL stock DNR.)
4. For each microcentrifuge tube add 1 mL of new stock solution
5. Let gel for 48 h.
    a. The drug is loaded when the gel appears orange/red.
6. Following the loading of the gel, remove the supernatant and run it through a UV/Vis Spectrophotometer.
7. The drug concentration was determined using a standard curve of DNR.

Drug Release

1. Prior to beginning the drug release study, a serial dilution was performed accordingly, as shown below:

Dilutions with MilliQ Water

Start With:	Dilution Process
200 µg/mL	20 µL of 10 mg/ul stock concentration of DNR + 980 µL MilliQ water
100 µg/mL	250 µL previous dilution + 250 MilliQ water
50 µg/mL	250 µL previous dilution + 250 MilliQ water
25 µg/mL	250 µL previous dilution + 250 MilliQ water
12.5 µg/mL	250 µL previous dilution + 250 MilliQ water
6.25 µg/mL	250 µL previous dilution + 250 MilliQ water
3.125 µg/mL	250 µL previous dilution + 250 MilliQ water
1.56 µg/mL	250 µL previous dilution + 250 MilliQ water

0.78 µg/mL	250 µL previous dilution + 250 MilliQ water

2. Using a 96-well plate, transfer 200 µL from each microcentrifuge tube into the plate. Perform this in duplicate.
3. Prepare the plate as shown below.

	1	2	3	4	5	6	7	8	9	10	11	12
A	200	100	50	25	12.5	6.25	3.125	1.56	0.78			
B	PBS	PBS	PBS	PBS	PBS	PBS	PBS	PBS	PBS			
C												
D												
E												
F												
G												
H												

4. To read the amount of drug released, press the drawer button on the plate reader, remove the purple guard and insert the loaded plate into the tray. Press drawer again to close.
5. Open SoftMax Pro software on the computer adjust settings accordingly:
    a. Click plate 1.
    b. Click ABS mode à end point read.
    c. Set wavelength to 485 nanometers.
    d. Highlight the wells on the plate area map to correspond with wells filled with solution (highlight).
6. Once the settings have been adjusted, click read. This may take a few seconds to return the data.
7. Save and export the data.
8. When done using the machine, remove the plate and close the drawer and exit the software before turning the machine off.
    a. Clean the plate used in the release study by using a 1 mL pipette to transfer the solution to the waste bottle. Pipette 1 mL of MilliQ water into each well, remove

the liquid and transfer to waste bottle. Rinse the plate 2 times using MilliQ water. Place the well plate upside down in the oven for a maximum of 24 h to dry out.